# THE PRODUCTION OF AZ31 ALLOYS BY GAS ATOMISATION METHOD AND ITS CHARACTERISTICS

**2019**

**DOCTORAL THESIS**

**MANUFACTURING ENGINEERING**

**Kamal AKRA**

# THE PRODUCTION OF AZ31 ALLOYS BY GAS ATOMISATION METHOD AND ITS CHARACTERISTICS

**A THESIS SUBMITTED TO**
**THE GRADUATE SCHOOL OF NATURAL AND APPLIED SCIENCES OF KARABUK UNIVERSITY**

**BY**

**KAMAL AKRA**

**IN PARTIAL FULFILLMENT OF THE REQUIREMENTS FOR**
**THE DEGREE OF DOCTOR OF PHILOSOPHY IN**
**DEPARTMENT OF**
**MANUFACTURING ENGINEERING**

**June 2019**

I certify that in my opinion the thesis submitted by Kamal AKRA titled "THE PRODUCTION OF AZ31 ALLOYS BY GAS ATOMISATION METHOD AND ITS CHARACTERISTICS" is fully adequate in scope and in quality as a thesis for the degree of Master of Science.

Prof. Dr. Mustafa BOZ ……

Thesis Advisor, Department of Manufacturing Engineering

This thesis is accepted by the examining committee with a unanimous vote in the Department of Manufacturing Engineering as a PhD thesis. 12/06/2019

| Examining Committee Members (Institutions) | Signature |
|---|---|
| Chairman: Prof. Dr. Süleyman GÜNDÜZ (KBÜ) | …… |
| Member : Prof. Dr. Mustafa BOZ (KBÜ) | …… |
| Member : Assoc. Prof. Dr. Serkan ISLAK (KÜ) | …… |
| Member : Assoc. Prof. Dr. Yunus TÜREN (KBÜ) | …… |
| Member : Asst. Prof. Dr. Mehmet AKKAŞ (KÜ) | …… |

….. / ….. / 2019

The degree of Doctor of Philosophy by the thesis submitted is approved by the Administrative Board of the Graduate School of Natural and Applied Sciences, Karabük University.

Prof. Dr. Filiz ERSÖZ ……

Head of Graduate School of Natural and Applied Sciences

*"I declare that all the information within this thesis has been gathered and presented in accordance with academic regulations and ethical principles and I have according to the requirements of these regulations and principles cited all those which do not originate in this work as well."*

Kamal AKRA

## ABSTRACT

**Ph. D. Thesis**

**THE PRODUCTION OF AZ31 ALLOYS BY GAS ATOMISATION METHOD AND ITS CHARACTERISTICS**

**Kamal AKRA**

**Karabük University**
**Graduate School of Natural and Applied Sciences**
**The Department of Manufacturing Engineering**

**Thesis Advisor:**
**Prof. Dr. Mustafa BOZ**
**June 2019, 127 pages**

The aim of this study is to investigate AZ31 alloy powder production and characterization processes experimentally by gas atomization method. For this purpose, firstly, the design and production of gas atomization unit were done at Karabük University Faculty of Technology Department of Manufacturing Engineering. In this gas atomization unit, the manufacturability of AZ31 powder from magnesium alloys was investigated by gas atomization method which is one of the production methods by powder metallurgy. The parameters and the literature used in the production of materials similar to the AZ31 alloy are taken into account as producibility parameters. In the gas atomization method parameters such as nozzle diameter, gas pressure and temperature must be controlled in order to produce the desired properties in metal powder production. The diameter of the nozzle is crucial because it affects the gas pressure and temperature, the size of the powder and the shape of the powders. Experimental studies were carried out using 3 different

temperatures (790-820-850 ºC), 4 different nozzle diameters (2-3-4-5 mm) and 4 different gas pressures (5-15-25-35 bar). In the process of atomization of molten metal and in the process of forming protective gas atmosphere, argon gas is preferred. Scanning electron microscopy (SEM) was used to determine the shape of the AZ31 powders produced, XRD, XRF and SEM-EDX analyzes were used to determine the phases in the internals of the produced powders and percentages of these phases, and laser measurement devices were used for powder size analysis hardness tests and tree-point bending tests were performed to determine the mechanical properties of the produced powders. The powders produced were pressed into masses at 4 different pressing pressures (300, 400, 500 and 600 MPa). TGA-DTA analyzes were performed to determine the best sinterability values of the bulked powders and sintering process was performed at 3 different temperatures (500-550-600 °C). Density measurements were made after pressing and sintering of the powders. As a result of the experimental studies, it was found that the powder size decreased with the increase of the gas pressure but the nozzle diameter, and the powder shape changed to the dripping and the spherical in the ligament and complex form. It has been observed that the temperature has no significant effect on the powder size and shape.

**Key Words :** Gas atomization, AZ31 alloy, magnesium, powder metallurgy.
**Science Code :** 915.1.195

# ÖZET

**Doktora Tezi**

## GAZ ATOMİZASYON YÖNTEMİYLE AZ31 TOZU ÜRETİMİ VE KARAKTERİZASYONU

**Kamal AKRA**

**Karabük Üniversitesi**
**Fen Bilimleri Enstitüsü**
**İmalat Mühendisliği Anabilim Dalı**

**Tez Danışmanı:**
**Prof. Dr. Mustafa BOZ**
**Haziran 2019, 127 sayfa**

Bu çalışmanın amacı, gaz atomizasyon yöntemiyle AZ31 alaşım tozu üretimi ve karakterizasyonu işlemlerinin deneysel olarak araştırılmasıdır. Bu amaç doğrultusunda öncelikle Karabük Üniversitesi Teknoloji Fakültesi İmalat Mühendisliği Bölümünde gaz atomizasyon ünitesi tasarımı ve imalatı yapılmıştır. Kurulan bu gaz atomizasyonu ünitesinde, toz metalürjisi ile üretim yöntemlerinden biri olan gaz atomizasyon yöntemi ile magnezyum alaşımları sınıfından AZ31 tozunun üretilebilirliği araştırılmıştır. Üretilebilirlik parametreleri olarak AZ31 alaşımına benzerlik gösteren malzemelerin üretiminde kullanılan parametreler ve literatür göz önünde bulundurulmuştur. Gaz atomizasyonu yönteminde metal tozu üretiminde istenilen özelliklerde tozun üretilebilmesi için nozul çapı, gaz basıncı ve sıcaklık gibi parametreler kontrol edilmek zorundadır. Nozul çapı, gaz basıncı ve sıcaklık, toz boyutunu ve tozların şeklini etkilediği için son derece önemlidir.

Deneysel çalışmalar 3 farklı sıcaklık (790-820-850 ºC), 4 farklı nozul çapı (2-3-4-5 mm) ve 4 farklı gaz basıncı (5-15-25-35 bar) uygulanarak yapılmıştır. Ergimiş metalin atomizasyon işleminde ve koruyucu gaz atmosferi oluşturulması işlemlerinde argon gazı tercih edilmiştir. Üretilen AZ31 tozlarının şeklini belirleyebilmek için taramalı elektron mikroskobu (SEM), üretilen tozların iç yapılarında oluşan fazları ve bu fazların yüzde oranlarını belirleyebilmek için XRD, XRF ve SEM-EDX analizi, toz boyut analizi için ise lazer ölçüm cihazı kullanılmıştır. Üretilen tozların mekanik özelliklerini belirleyebilmek için sertlik testleri ve 3 nokta eğme testleri yapılmıştır. Üretilen tozlar 4 farklı presleme basınçlarında 600 MPa preslenerek kütle haline getirilmiştir. Kütle haline getirilen tozların en iyi sinterlenebilirlik değerlerini belirleyebilmek için TGA-DTA analizleri yapılmış ve 3 farklı sıcaklıkta (500-550-600 °C) sinterleme işlemi gerçekleştirilmiştir. Tozların presleme ve sinterleme işlemleri sonrasında yoğunluk ölçümleri yapılmıştır. Deneysel çalışmaların sonucu olarak, gaz basıncının artması ve nozul çapının küçülmesi ile toz boyutunun küçüldüğü ve toz şeklinin ligament ve karmaşık şekilden, damlaması ve küresele doğru değiştiği tespit edilmiştir. Sıcaklığın toz boyutunda ve şeklinde önemli bir etkisinin olmadığı görülmüştür.

**Anahtar Kelimeler** **:** Gaz atomizasyon, AZ31 alaşımı, magnezyum, toz metalürjisi.
**Bilim Kodu** **:** 915.1.195

## ACKNOWLEDGMENT

First of all, I would like to express my gratitude to Allah'u Teala, who has given me these days, always protects me, gives me strength and makes me successful.

I would like to thank Prof. Dr. Mustafa BOZ whom I have benefited from his extensive knowledge and experience in the planning, research, execution and formation of this thesis.

In addition, I would like to express my thanks to the dear colleagues, whom I shared the exchange of ideas at every stage of my thesis, that allowed me to look with a different perspective to the problems I encountered dear colleagues, Karabük University, Faculty of Technology Manufacturing Engineering Department Member Research Assistant Atakan Oğuz OCAK, Kastamonu University, Faculty of Engineering and Architecture Mechanical Engineering Department Member Assistant Professor Dr. Mehmet Akkaş and Dr. Tayfun Çetin.

Finally, I thank my dear family for their patience, self-sacrifice and support, and for all physical and spiritual assistance with my whole heart.

The project was supported by Karabük University with KBÜBAP-DR-201 project number I want to present my thanks to Karabük University.

## CONTENTS

**Page**

**Page**

**Page**

**Page**

## LIST OF FIGURES

**Page**

**Page**

**Page**

**Page**

## LIST OF TABLES

**Page**

## SYMBOLS AND ABBREVITIONS INDEX

### SYMBOLS

Mg : magnesium
Al : aluminum
Cu : copper
Ti : titanium
Zn : zinc
Fe : iron
Mn : manganese
Y : yttrium
Sn : stannum
Si : silicon
Ba : barium
Pb : plumbum
Sb : stibium
Ca : calcium
Sr : strontium
Bi : bismuthum
Be : beryllium
K : potassium
Ag : argentum
Li : lithium
Zr : zirconium
Ce : cerium
Na : sodium
Ln : lanthanide
Nd : neodymium

**ABBREVITIONS**

SEM : Scanning Electron Microscope

EDS : Energy Dispersice Spectrometry

ASTM : International American Society of Tests and Materials

XRD : X-Ray Diffraction

XRF : X-ray fluorescence

EDX : Energy Dispersive X-Ray

DV : Dimensions Values

HV : Hardness Values

# PART 1

## INTRODUCTION

Magnesium alloys have an importance at the defense industry and the transport industry due to their density of 1.74 gr / $cm^3$ and light weight and high specific strength properties [1-6]. Since it has low strength and toughness values without alloying, it is generally used by forming alloy with other elements. Magnesium also has properties like high thermal conductivity, good electromagnetic protection, high dimensional stability, good absorbing, easy recycling and good workability [7-10]. With these properties Mg alloys are used in many industries such as automotive, aerospace, computer, sports equipment, mobile phones. It is also used as an implant material due to its low weight and metabolism compatibility [11-16].

For the last 20 years, metal powder production with gas atomization have been widely used due to properties such as chemical homogeneity and uniform microstructure [17].

Atomization is the process of solidifying the liquid metal with a gas such as air, nitrogen, argon or helium and forming the solidified droplets into powders. In gas atomization, there are processing parameters such as gas pressure, nozzle diameter and temperature affecting the powder grain size and distribution. In this study, the effects of atomization variables such as gas pressure, nozzle diameter and metal melting temperature on powder particle size and distribution, powder form and microstructure were investigated [18].

As a result of the literature research, any studies related to the production of AZ31 magnesium alloy powder by gas atomization method could not be found. For this purpose, AZ31 magnesium alloy powder production was studied in order to fill this gap in literature. I the present experimental work, powder size distribution of AZ31, powdered grain shape, the phases of the powders and the concentration of these

phases, the elemental and chemical composition of the powders and the mechanical strength values of the produced pieces were determined.

## PART 2

## LITERATURE REVIEW

Ibrahim USLAN and Serdar KUCUKARSLAN used closely matched Mannesmann type nozzle in tin powder production studies. They used air as atomization gas. The tin was heated to a casting temperature of 400 ºC. Gas parameters were used between 5 and 30 bar pressures. At the distances between 2 and 8 mm, tin was atomized. The average size of the finest powders produced is 68,50 μm. As a production parameter of these powders, a pressure of 10 bar was selected with a liquid metal flow pipe having an internal diameter of 3 mm at projection distances of 8 mm. Generally, the powders obtained were observed to be complex shaped. Powders of less than 10 μm are very uniform and smooth. It is concluded that the powders above 100 μm have a generally rod-shaped structure and cellular structure [19].

Bülent BOSTAN and his colleagues produced powders from pre-alloyed AA 2014 by gas atomization method. The closely matched nozzle used as the nozzle type and argon gas is used as the atomization gas. Gas parameters have been chosen between 5 and 30 bar and the temperature of liquid metal as 750-810. The resulting powders are classified by sieve analysis method. The average powder size was measured as 90,66 μm. As a result of the SEM and optical microscopy studies, it is concluded that the powders are transformed from spherical shapes to rod and droplet shapes with increasing temperature. By the EDS analyzes, it was concluded that powder size and distribution are based on the solidification direction of the powder grains. The formation of satellites formed by the adherence of small powder grains to large grains of powder was observed. Powders were slightly oxidized [20].

Mehmet AYDIN and Rahmi ÜNAL performed a study at Dumlupınar University Gas Atomization Unit, tin was superheated to 430 °C and atomized at different

pressures. A closely matched nozzle is used as the nozzle selection. Nitrogen was used as atomization gas. The average powder size value of the finest powders was measured as 11.39 μm and these powders were produced at a pressure of 1.47 MPa. Global powder distribution was observed in general. More than 20 μm powder was observed in cellular surface structure. Satellite formation with small grains clinging to large grains was observed [21].

A. Rudajevová and colleagues have worked to determine the thermal diffusivity and thermal conductivity of Mg-Al alloys. The thermal diffusivity and thermal conductivity of magnesium-aluminum alloys AZ31, AZ91 and AM60 were investigated in the temperature range of 20 to 300 °C. The thermal diffusivity of the AM20 increased with increasing temperature up to 160 °C. It has been concluded that the change in the slope of the temperature graph of the heat dissipation is probably due to the reduction of the $Mg_{17}Al_{12}$ phase. The thermal conductivity values of the thermal diffusivity and the solid solution were found to be lower than the values obtained when the alloys contained two phases [22].

Fa-he CAO et al. investigated the environmental friendly plasma electrolytic oxidation and corrosion resistance of AZ31 magnesium alloy. Plasma electrolytic oxidation of Mg-based AZ31 alloys was investigated using a 50 Hz AC anodized (aluminum surface treatment) technique in a new organic type alkaline borate solution. The anodic film is composed of MgO, $MgAl_2O_4$ and $MgSiO_3$ and is emphasized to be relatively smooth with some micropores and cracks. The electrochemical behavior of the anodic film was investigated by electrochemical impedance spectroscopy and potentiodynamic polarization. Polarization results showed that PEO (Poly ethylene oxide) treatment can reduce the corrosion current by 3-4 times more than the pure AM60 alloy. It has been concluded that the salt spray test based on ASTM B117 for the AM60 magnesium alloy offers a good level of corrosion protection over 272 hours [23].

Yong-qang Li et al. studied atmospheric corrosion of AZ31 Mg alloys in industrial city environment. In this study, they investigated the atmospheric corrosion behavior of ingot shaped and rolled AZ31 Mg alloys in a dirty city. It was observed that the

corrosion rate of the ingot samples was higher than the corrosion rate of the extruded samples and that the size of the powder particle conglomerates (gravel) adsorbed on the sample surfaces were related to the pit dimensions. The main corrosion products of both alloys contain MgSO46H2O and MgSO36H2O. The extruded samples have more homogenous structures and less secondary phase content than ingot samples. As a result, it was concluded that the corrosion films formed in the rolled samples had better protective effects than the corrosion films formed in ingot samples [24].

Katsuyoshi Kondoh et al. investigated the effect of powder metallurgy on the microstructure and mechanical properties in the mass production of non-combustible rolled magnesium alloy. One of the fast solidification processes, water atomization and powder production, fine α-Mg grains and $Al_2Ca$ intermetallic compound consisting of 1-4 mm long rough granular non-combustible magnesium alloy powder aimed to produce. Since this method has a very high solidification rate compared to the conventional atomization process, it has been reported to be economical and safe to produce very good micro structures and coarse-grained Mg alloy powder in the mass production process. The AMX602 (Mg-6% Al- 0.5% Mn-2% Ca) powders were compressed at room temperature. The microstructure and mechanical properties of compressed AMX602 alloys were evaluated. It has been observed that these microstructures have an excellent effect on the mechanical properties of rolled alloys. As a result, the AMX602 alloys rolled at 573 K, 447 MPa yield strength, 425 MPa yield strength and 9.6% elongation [25].

Lagutkin et al. worked on the atomization process for metal powder. In this study, they developed a new atomization process that combines pressure and gas atomization. The melt flows through the nozzle through a hole in the form of a thin film cone. After the pre-film step, the melt is atomized by a gas stream sent by a ring nozzle. The aim of this research is to obtain a narrow size distribution and low specific gas consumption compared to conventional gas atomization techniques. Tin and some alloys are successfully atomized by this technique [26].

Neikov et al. have studied water atomization of aluminum alloy powders. A new rapid solidification process based on high pressure water atomization of the melt for

the manufacture of advanced aluminum alloys was carried out in an experimental apparatus. They observed that the ratio of powder-water interaction related to pH value. While the rate of room temperature reactions was very slow at pH 3.0-4.0, it was concluded that increasing the pH to 6.0 resulted in intensive powder oxidation [27].

Liu et al. studied the production of Fe-Si-Al-Ni-Ti soft magnetic alloy powder by inert-gas atomization. They produced Fe - 3% Si - 0.5% Al - 2% Ni - 2% Ti soft magnetic alloy powders with inert gas atomization. They produced the powder composition, phase structure, size distribution, surface morphology and cross-sectional microstructural analysis by the X-ray diffractometer, laser scattering particle size distribution analyzer and electron probe micro analyzer. They investigated the effects of gas atomization pressure and temperature on powder size and morphology. They reported that the gas atomization pressure of 5,5 MPa and 1550 °C was obtained with a rough surface and low spherical powders with a diameter of 54.38 μm. When the gas atomization temperature was fixed at 1550 °C and the gas atomization pressure was increased from 5.5 to 6.5 MPa, the powder size decreased from 54.38 to 35.51 μm and the level of saturation on the surface increased. When the gas atomization pressure was fixed to 5.5 MPa and the gas atomization temperature was increased from 1550 to 1650 36, the powder size decreased from 54.38 to 36.63 μm and they determined that the powders had a smooth surface and high sphericity. The phase structure of the powder is the single α-Fe phase and the solidification structure in the powder has been reported to be predominantly equal to the axis of dendrites as well as a small amount of dendrites [28].

Kim and Chae have investigated the consolidation of gas atomized Mg alloy powders. In this study, the extrusion behavior of MgZn4.3Y0.7 alloy powders produced by gas atomization was investigated. They combined the effect of the composition and the process to change the weak mechanical properties of Mg alloys. As the extrusion ratio increased from 10: 1 to 15: 1, the powders were plastic deformed better and the mechanical properties such as tensile strength and elongation were increased. MgZn4.3Y0.7 alloy powders atomized using an industrial scale gas

atomizer provided nearly spherical morphology and the average powder size was found to be approximately 55 μm in diameter. The magnesium oxide layer formed on the Mg alloy surface has a thickness of about 48 μm. They observed that both strength and elongation improved with the increase of plastic deformation and increased extrusion rate [29].

Karagöz et al. examined the parametric relations in terms of metallic powder processing technology and processing stages. In this study, they examined the production methods of the powders and the related powder size and powder size distribution, powder shape, surface quality of powder and shaping pressure, sintering temperature and time for production. In this study, titanium and iron based alloy powders produced by atomization method were examined. They used powders produced by rotating electrode method. They pressed the powder produced and then sintered and microstructure images were examined. In general, it has been reported that global powders are desired in powder metallurgy. The most important reason for the global powder demand is that the powder-powder contact must be homogeneous and versatile in the pressing and sintering stages. Since powder size distribution is an important parameter in powder metallurgy, it has been emphasized that it is an important criterion for determination of fluidity, compressibility, atomic bond formation and mechanical properties [30].

Öztürk et al. carried out studies on the effects of AA 2014 Aluminum alloy powders on cooling rate by water-cooled rotary disk atomization method. In this study, they produced aluminum alloy powders using rotary disk atomization. Copper and stainless steel disc material, speed of these discs, metal heating rate, the degree of cooling water, the effects of these parameters on the microstructure and cooling speed of the produced powders were investigated. It has been observed that the ratio of ligament, droplet and spherical powders increased with the reduction of the powder size. In this study, with the increase of the temperature of the cooling water, the size of the powder size is reduced, and the speed of the disk with the increase in the size of the powder size is emphasized [31].

Bao et al. Investigated the structural characterization of Al and Ni powders produced by gas atomization. The purpose of this study is to examine the structure and to identify the existing phases in the volume of the grains. When the weight fractions are changed, the three main phases are obtained; $Al_3Ni_2$, $Al_3Ni$ and Al. They observed that in any of the powder studied, there was no B2 AlNi phase. They found one or more additional metastable phases with decreasing size in grains with diameters less than about 200 μm [32].

Zdujic and Uskokovic studied on the atomization of metal and alloy powders using the rotating electrode method. In this study, they used centrifugal atomization method. With this method, they reported that the refractory metals (molybdenum, tungsten) could be atomized and that the powders produced could be pure and fine-grained. In the study, they produced iron, nickel and titanium powders. They used argon and helium gases in the cooling process. They changed the average size and size distribution of the particles easily and accurately by changing the speed and diameter of the rotating electrode. They have expanded the particle size range by increasing the melting speed in any material. Centrifugal atomized powders have reported that they can be characterized by a spherical particle shape and high purity in the production of reactive metals and alloys in powder formation [33].

Dr. Rahmi Ünal examined the effect of pressure formation at the end of the molten conduction pipe on the tin powder size and the gas / melt rate in the gas atomization method. He used a newly designed near-matched nozzle system to produce tin powder by studying the effect of the melting tube on the pressure formation at the molten end of the projection length. The results obtained from this study reported that the observed metal flow rate did not behave as previously assumed, ie the deeper absorption metal flow rate increased. The melt reduced the flow rate by increasing the atomizing gas pressure. He observed that for the same projection length, the gas increased the melt mass flow rate, which increased the fine powder particle size. For the protrusion lengths of 5 and 15 mm, 1.0-3.5 MPa stressed that at the end of the spray gas pressure, there was always negative pressure at the end of the melt delivery tube. On the other hand, he stated that there is pressure fluctuation at the tip of the melt pipe between positive and negative values in the pressure range 1.0-2.0 MPa for

10 mm protrusion length. The atomization process has determined that the protrusion lengths of 5 mm and 10 mm are more stable for a protrusion length of 15 mm [34].
Alper Sofuoğlu, carried out experimental and numerical studies on the production parameters of gas atomized aluminum and tin powders. In this study, production parameters of gas atomization are investigate, the effect of atomization parameters on powder particle sizes of gas atomized aluminum and tin powders were also investigated. Gas pressure, nozzle exit zone, protrusion length, melt distribution tube (nozzle) diameter and super temperature temperature are selected as atomization parameters. It has been emphasized that atomization nozzles are divided into two basic types as free fall and closely related to the position of atomization gas and molten metal. Gas pressure and super heat temperature have been found to significantly affect the average size of the powder particle. When the gas pressure and super heat temperature increased, the powder particle size decreased. Increased protrusion length and gas pressure reported that the tin powder caused a reduction in particle size. The molten distribution diameter, the projection length, and the nozzle outlet have reported little impact on the powder particle average [35].

Özgür DUYGULU et al. have done research on the production and development of magnesium sheet alloys. In the study, they produced AZ31, AZ61, AZ91, AM50 and AM60 magnesium alloys with plates of 4-8 mm thickness and 1500 mm width with twin roll continuous casting technique. Then, these alloys were homogenized and heat treated. After the heat treatment, they made optical microscopy, scanning electron microscopy and conducting electron microscopy. In order to determine the mechanical properties of the alloys, tensile test and hardness tests were applied to the alloys. Magnesium reported that it was the lightest of all structural metals with a density of 1.74 gr / cm3 and magnesium was 1.5 times more than aluminum, 3 times more than titanium and 4 times more intense than iron. Magnesium alloys have high specific strength, high specific hardness, good pourability and workability, heat content per volume unit, high damping capacity and good electromagnetic imaging capability. They stated that magnesium can be easily welded, resistant to impact forces. Magnesium is the sixth most abundant metal and eighth element on the earth's surface, and moreover, magnesium is readily recyclable, and magnesium alloys have reported an effective heat distribution [36].

Legan Hou et al. investigated the high temperature microstructure and mechanical properties of Mg-Al-Ni alloys prepared with powder metallurgy. Mg-Al-Ni alloys prepared with powder metallurgy and their microstructures and high temperature mechanical properties were investigated. The results showed that, in addition to the α-Mg matrix, Mg-Al-Ni alloys contained coarse Al3Ni2 particles and fine AlNi nanoparticles. The strength at 150 °C was improved with an increase in Ni content. The Mg-18.3Al-8Ni alloy had a compressive strength of 234.7 MPa and a yield strength of 146.5 MPa. Plasticity at low concentration was also improved with Ni. The Mg-11.3Al-2Ni alloy has been reported to have a compression ratio of 17.3%. Al3Ni2 and AlNi phases in alloys have been observed to block the movement of grain boundaries and displacements during high temperature deformation. The presence of the AlNi phase has provided a non-basal shift system, which has been reported to cause plasticity to heal [37].

A. Vahidgolpayegani et al. Conducted research on the production methods and characterization of porous Mg and Mg alloys for biomedical applications. Magnesium and some alloys have a good biocompatibility and have a higher strength / weight ratio than other metallic polymeric and ceramic biomaterials, and have functional properties in the human body and similar mechanical properties associated with bone tissues. It has been concluded that it attracts increasing interest. Porous Mg and Mg alloys can be used instead of bones with similar characteristics to bone structure. Because the structures in the bone tissue and porous Mg materials are similar, existing bone cells grow up to the pores of an Mg skeleton and form new bone tissue. Moreover, it is concluded that the porous Mg and Mg alloys are gradually biodegraded after the implantation, then the Mg ions are absorbed in the body, Mg skeletons are made more convenient than other porous metal biomaterials and the need for removal of the implant with the next surgical procedure is eliminated. In the manufacture of porous Mg and Mg alloys, it has been observed that different production methods have been developed which can be divided into two categories as the melting process method and the solid processing method according to the state of the materials being processed. Examples of casting, metal with gas eutectic solidification, infiltration, and negative salt-casting processes can be the introduction of a blowing agent into the molten metal, followed by mixing or

introducing a gas or a vacuum into the Mg melt before infiltration of the beds of hollow spheres or solidification. Powder metallurgy can be considered as a solid processing method with a gap holder or a blowing tool. There are also other methods in which a porous structure is formed in both the melt and the solid processing methods using Mg alloys, strips or fibers. Some porous Mg and Mg alloys have been reported to be formed by a combination of metallurgical and mechanical processes. Technological advances have led to the development of understanding of porous structures and properties, and the use of many methods to produce porous structures. However, some methods are not economically feasible. The final product forms a porous structure for implant applications that are not biocompatible due to inappropriate pore size and porosity. For this reason, it is concluded that it is very important to choose a suitable production method to produce porous Mg and Mg alloys by controlling the pore size, shape and porosity compatible with medical applications [38].

Oğuz et al. have studied the effect of gas pressure on powder size and shape in tin powder production by gas atomization method. In the study, they first produced gas atomization unit. They reported that the gas atomization unit consisted of four main sections as induction furnace, nozzle, atomization tower and powder collection unit. They used graphite crucible for melting. They used a closely matched and circular slotted nozzle as the nozzle. The tests used argon at a temperature of 500 º C, a diameter of 3 mm nozzle and a protective gas. In this study; Since the aim is to investigate the effect of gas pressure on the powder size, gas pressure is used as 2, 4, 6, 8, 11 bar. In the experiments, they determined that the size of the powder decreased with the increase of gas pressure. They reported that almost all of the powders were spherical, especially at pressures of 8 and 11 bar [39].

Fahri Öztürk and İlyas Kaçar have done research on the investigation of magnesium alloys and their usage areas. In this study, the production methods of magnesium and its alloys, formability, corrosion resistance, environmental impacts and their use have been investigated. They reported that the use of magnesium in the aerospace and automotive industries in general is increasing day by day. They found that magnesium and its alloys are not widely used and that industrialists prefer materials

such as iron and steel instead of magnesium and its alloys. This is due to the fact that magnesium alloys are expensive. They emphasized that Al, Mg and Ti alloys are the most suitable materials to replace steel and cast iron [40].

# PART 3

## POWDER METALLURGY

Powder metallurgy (P/M) is the process of mixing metal powders in certain proportions and compressing them to molds at certain pressing pressures and sintering.

Powder metallurgy consists of mixing, packaging and sintering of powders. Figure 3.1 shows the steps of powder metallurgy in detail. Today, the P/M method is widely used and an alternative to the production methods known [41]. As an advanced manufacturing method, P/M is a method which is very suitable for the production of technological materials and provides a large number of small parts and economical production [42-44]. Powder metallurgy production method consists of; Metal and non-metal powders are produced and blended by mixing these powders and then pressed in a mold to obtain the desired geometry and then sintering process is performed by applying a method [39,45].

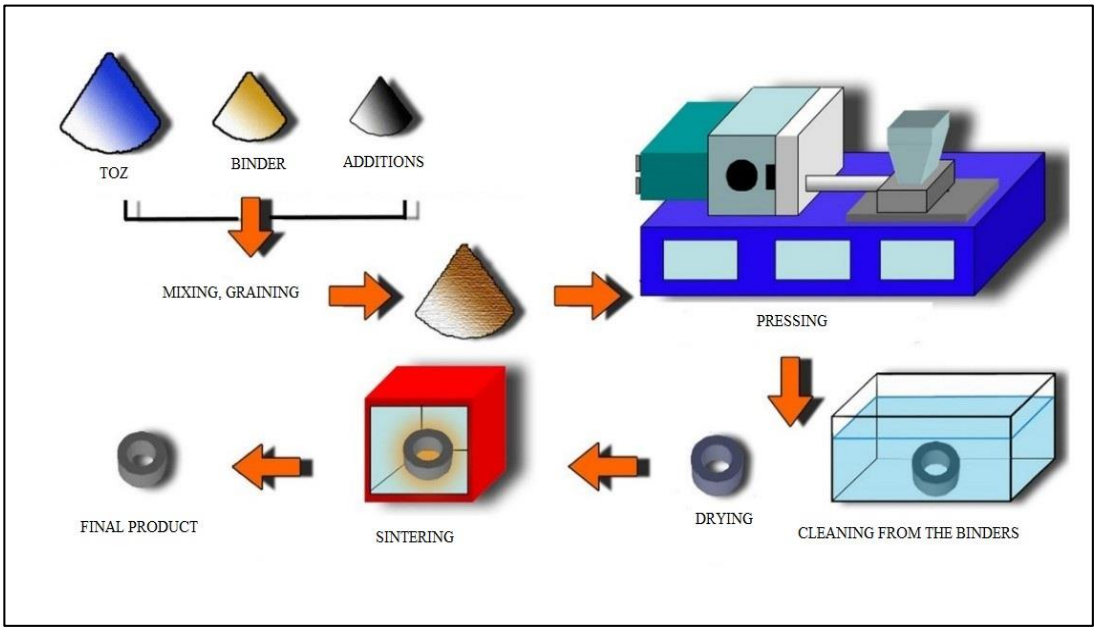


Figure 3.1. Powder metallurgy production stages [46].

This process consists of specific stages, including powder production, mixing of the powders produced, pressing powders, sintering of powders [47]. Very fine characteristic solid particles having a size of less than 1 mm can be characterized as powder [48]. The powders are generally metallic and the most important property of a powder is that the volume value is low relative to the surface area value [47]. The specific properties of the powder produced depend on the powder production methods and production parameters.

### 3.1. POWDER PRODUCTION METHODS

The production of metal powders is carried out by many techniques. The aim here is to keep the shape and size values of the powder in the desired range and to ensure that the chemical structure of the powder does not change. Powder characterization is important for other production parameters. It is inevitable for a controlled start to produce parts of the desired quality [49].

There are four basic mechanisms for the production of metal powders [50]. These are;

1. Mechanical method
2. Chemical method
3. Electrolysis method
4. Atomisation method

Generally, each material can be powdered. The powdering process is formed by 3 different methods. These; atomization, chemical and electrolytic. Atomization is the process of smelting molten metal in a vertical or horizontal way by spraying with gas or water [50,51].

Metallic powder production by chemical method is the process of metal reduction into elemental powder. The electrolysis method is the process of dissolving metal by using electric current and thus becoming powder. Powders are transported from the

anode to the cathode by means of electricity and adhered on a thin film. The powder adhered to this film is dried to produce the desired powders [50,52].

The ability of a powder production method to be selected among the others depends on the economics of the method, the properties of the powders obtained, and the extent to which these properties can meet the needs of the place of use. The geometric shape of the powder can be in many different ways from the sphere to the dendritic forms depending on the production method. Similarly, the surface condition of the powder, ie smooth or porous, also varies according to the method of production [53].

### 3.1.1. Mechanical Method

Mechanical methods can be examined in three groups: machining, grinding and mechanical alloying [54].

#### 3.1.1.1. Machining

With this method, it is possible to produce very large and complex powders using machining techniques such as turning, milling and grinding. Powders produced can be ground to a fine powder form. Difficulties in controlling powder properties may be contamination problems by mixing with oxidation, lubrication, dirt retention and other materials. High-carbon steel powders are produced by this method [54].

#### 3.1.1.2. Grinding

Although it is a powder production technique by mechanical methods, this method, which is used to break the powders produced by other techniques, is mostly made in ball mills (Figure 3.2). In this method, where the production of powders of brittle materials is made, the basic principle is to cause a blow between the material to be broken and a hard object. Iron alloys, iron-chromium, iron-silicon etc. brittle materials are ground in ball mills [54].

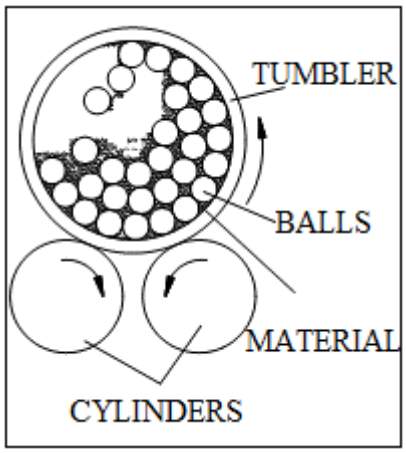


Figure 3.2. Ball grinding [54].

### 3.1.1.3. Mechanical Alloying

Mechanical alloying is used to weld metal powders to each other and to re-break these welds and to produce high strength materials with a fine and homogeneous microstructure (Figure 3.3) [54].

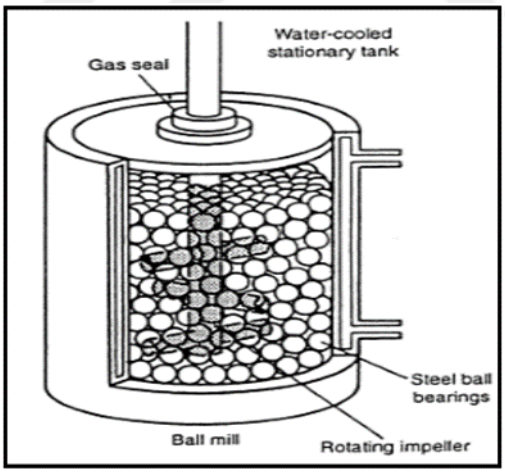


Figure 3.3. Mechanical Alloying [54].

### 3.1.2. Chemical Method

Chemical production of metal powders is based on the principle of chemical reduction of metal oxides (iron, copper, tungsten, molybdenum, nickel and cobalt) from their oxides by reducing gases such as CO or hydrogen [55].

The production of iron powder by chemical method is an important example of this method [56]. The iron ore is mixed with the coke, the mixture is continuously passed through the furnace by reducing the production and the production of cake-shaped sponge iron. The representation of the production of iron powder is given in Figure 3.4. With the completion of the reduction sponge iron is obtained. The produced sponge iron material can be brought to the desired particle size by grinding process because it is made up of powdered powders in about 1260 $^{o}$ C [57].

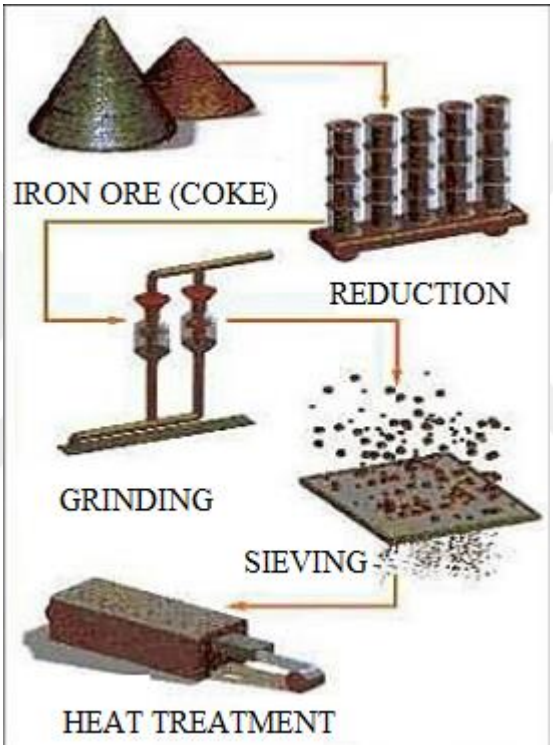


Figure 3.4. Iron powder production by chemical method [58].

### 3.1.3. Electrolysis Method

Electrolysis is generally used in the production of metal powders with high conductivity. Electrolysis is the transfer of a cell from the anode to the cathode using the electric current, followed by a precipitation of the metal powders (Figure 3.5). One of the most important metal powders produced by electrolysis method is copper powder. This method is also suitable for the production of iron, cobalt, tin, zinc, lead powders. The purity of the powders produced by this method is high. In electrolysis process, basic variables such as density of metal ions in the environment,

conductivity of the electrode, temperature, voltage value, current density, liquid bath and particle addition are available.

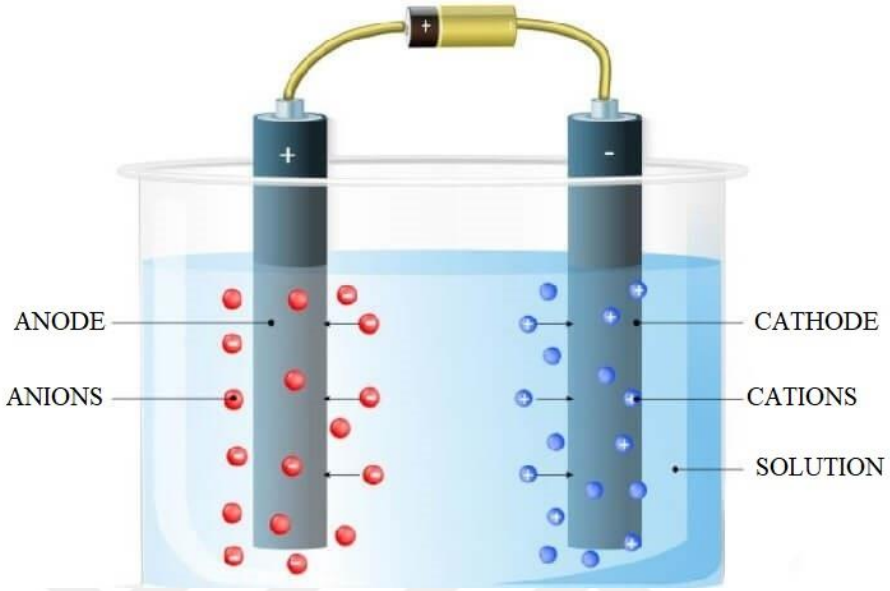


Figure 3.5. Electrolysis method [59].

### 3.1.4. Atomisation Techniques

In general, all kinds of metals that can be melted in the atomization technique can be powdered. The liquidation of the liquid metal with a high-speed gas such as nitrogen, argon or helium is called as atomization by solidifying the water droplets suddenly and excessively. The vertical gas atomization system is given in Figure 3.6. The most commonly used techniques; Water, gas, centrifuge, rotary electrode and vacuum atomization method. The most important feature of this method is that the shape and shape of the powders can be controlled. Water or gas atomization is generally preferred to produce high capacity and economical powder. According to the production methods, the powder shapes may vary. These differences are shown in Figure 3.7 [60,61].

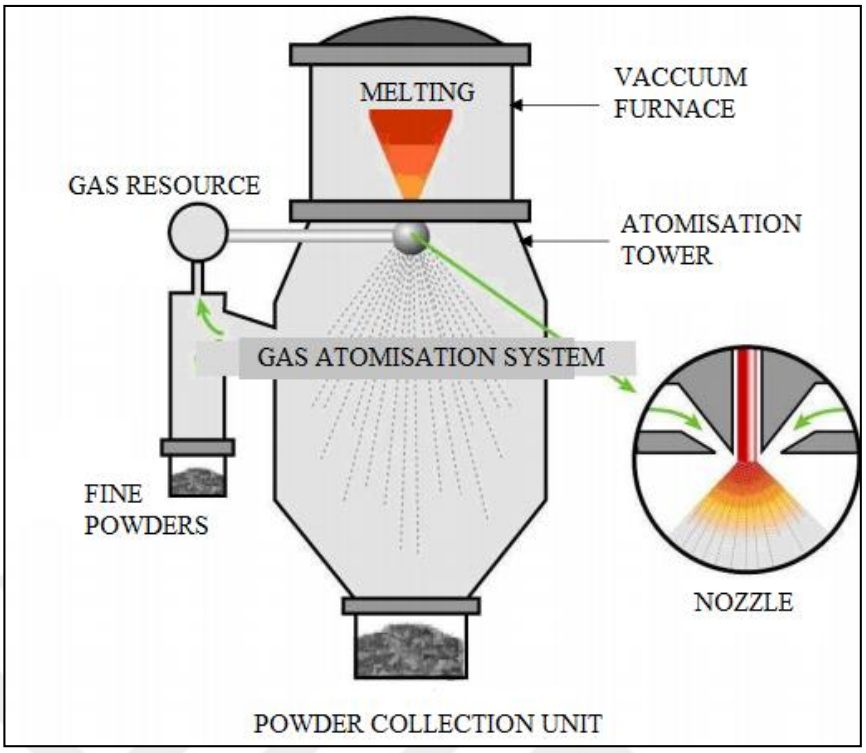


Figure 3.6. Gas atomisation system [52].

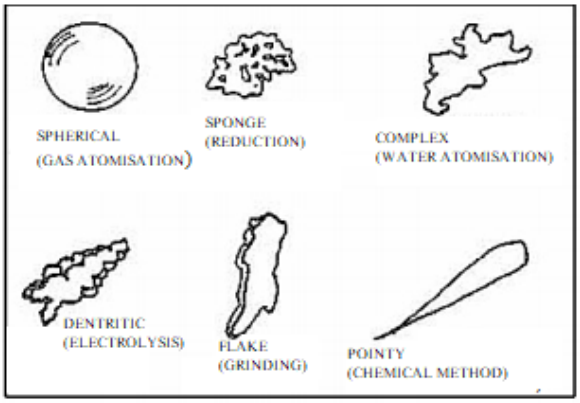


Figure 3.7. Powder shapes of the production methods [62].

## PART 4

## GAS ATOMISATION AND ITS IMPORTANCE

Atomization is based on the principle of melting liquid and liquid to droplets. The droplets become cold by cooling rapidly. Atomization is an attractive method because it can be applied to different types of materials thanks to controllable process parameters [63]. Atomized powders have the properties and advantages that cannot be achieved by other production methods. In this process, the molten metal is broken down into very small droplets and cooled without contact with each other or with solid surfaces. The basic principle is that the molten metal is flushed into a very thin strip and, in this way, it becomes solidified by a water or gas jet into very small particles. Air, carbon dioxide, helium, nitrogen and argon are frequently used as gases [53,64]. As global powders are generally desirable, inert gases are preferred. [65].

Gas has three different tasks in gas atomization. First, to transfer the kinetic energy required to cut and smelt the melted liquid metal material into the droplets and then to determine the speed and direction of the droplets formed within the atomization tower. In addition, in the formation of powder, it causes the powders in the system to cool [66].

The general properties of powders produced by gas atomization are as follows [67];

1. Smooth surface spherical powder shape
2. Rapid solidification in small diameter powders
3. Allow mass production
4. Chemical composition of melted metal does not change

Due to the mentioned properties, powder production by gas atomization method is preferred for many applications and production.

## 4.1. GAS ATOMISATION SYSTEMS

Gas atomisation units can vary in terms of the metal feed mechanisms, melting and the structure of the powder collection sections. The basic principle in all units is to produce powder by transferring energy to the liquid metal bundle. For metal with a low melting temperature, gas atomisation units generally designed horizontally are preferred [68].

In the system seen in Figure 4.1, the melt moves towards the gas expansion zone by the siphon effect of the high-speed gas passing through the metal nozzle. Here, the droplets caused by the spraying of the metal under the influence of gas, energy loss to the powder collecting units, and they lose their energy with a free fall motion [55].

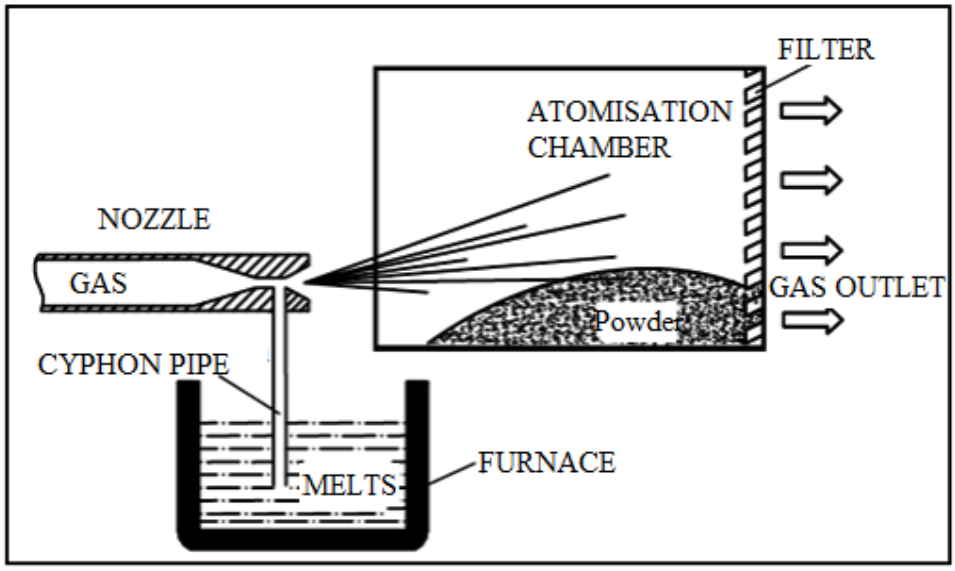


Figure 4.1. Horizontal gas atomization system [68].

In horizontal systems, atomized powders have a better structure and a broader powder distribution range than the powders produced in the vertical atomization system [69].

In the atomization of metals with a high melting temperature, vertical gas atomization units with a closed silo filled with inert gas are used and thus the oxidation of the powders is avoided. In this system, the metal is heated to a temperature above the melting temperature by the induction furnace or by the heating system (casting temperature) and the melt is passed through the metal nozzle into the silo.

The atomization tower should be designed to allow the droplets to solidify without hitting the tower walls. Towers are made of stainless steel. Stainless steel is preferred to prevent powders from adhering to the tower walls. Evacuation of the gas used in the atomization process through the gas atomization tower is an important stage. Cyclone systems are used for this purpose. Cyclones are also used in the handling of fine powders (Figure 4.2) [68].

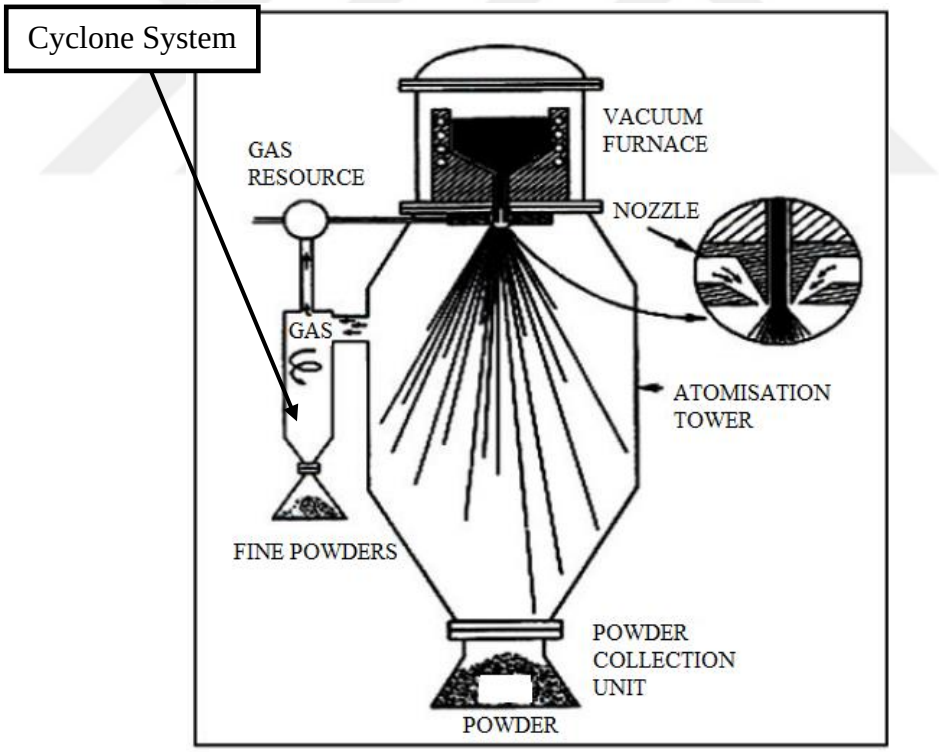


Figure 4.2. Gas atomization system designed vertically [68].

In gas atomization systems, gases such as argon, air, helium, argon, carbon dioxide are used to break down molten metal. In these systems, reactive metals such as noble gases, superalloys and titanium are used in atomization processes or when the

amount of oxygen is desired to be low and global powders are obtained. In atomization processes where air is used, powders are usually complex. The global powder form is a preferred feature in terms of grouping and mixing ease in commercial powder metallurgy applications [69].

## 4.2. OPERATING PRINCIPLE OF THE ATOMIZATION SYSTEM

The molten metal from a nozzle to the atmosphere can take the form of a cylindrical, flat or conical surface, depending on the nozzle design of the gas surrounding it. These droplet forming mechanisms consist of three stages. These; [70,71].

1. The onset of rapidly increasing amplitude sine wave,
2. The formation of a rod (ligament) structure with the growth of the sine wave,
3. The formation of spherical droplets by dividing the ligament structure.

The powders are spherical, ligamentous or dendritic in shape, resulting in their flight in the atomization tower.

Dombrowski and Johns developed a physical model of droplet formation from the flat sheet. The physical model of atomization mechanisms developed by Dombrowski and Johns is shown in Figure 4.3 [72].

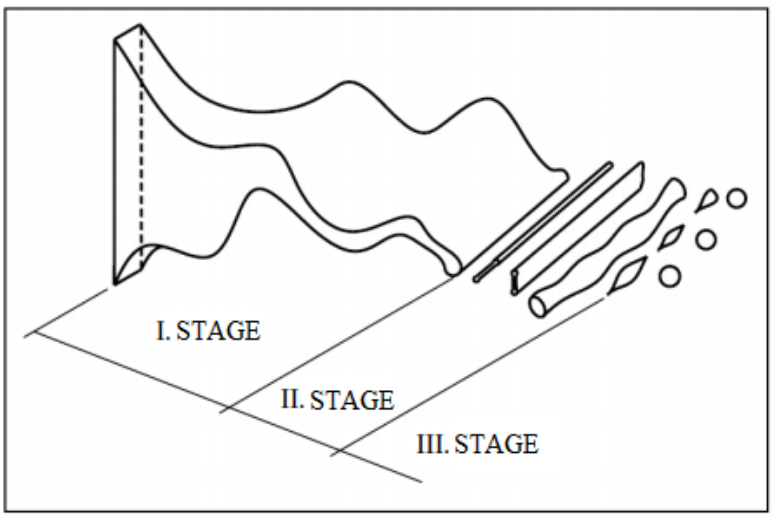


Figure 4.3. Droplet formation from flat sheet [72].

See and Johnston found three conditions for gas atomization of melt metals as a result of their studies on modeling:

1. First stage
2. Second stage
3. Solidification

These stages (conditions) are shown in Figure 4.4.

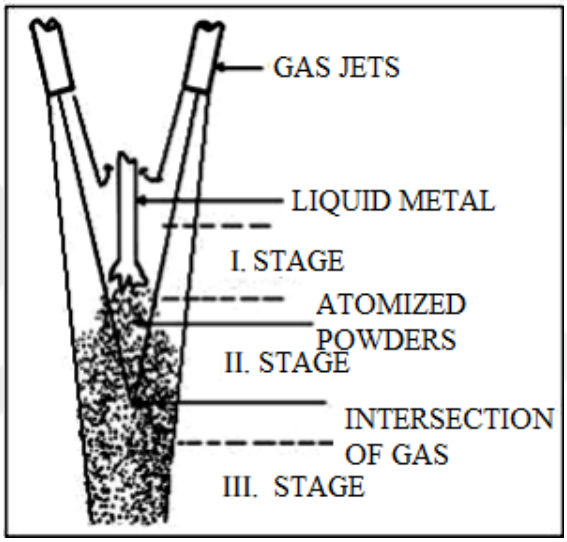


Figure 4.4. Demonstration of three conditions in gas atomization [73].

In the first stage, the molten liquid metal enters the high-speed gas flow region where the pressure changes. Increased pressure leads to breakage of the liquid metal bundle. If the pressure exceeds the restructuring energy due to the surface energy, the second situation occurs. In the third stage, spherical metal particles begin to form depending on the solidification and time. German [55] clearly demonstrated the gas atomization and the occurrence of metal powder by See and Johnston (Figure 4.5). The melt is first seen in a conical manner and then in a ligament and in a spherical shape due to the suction pressure in the expansion zone of the gas.

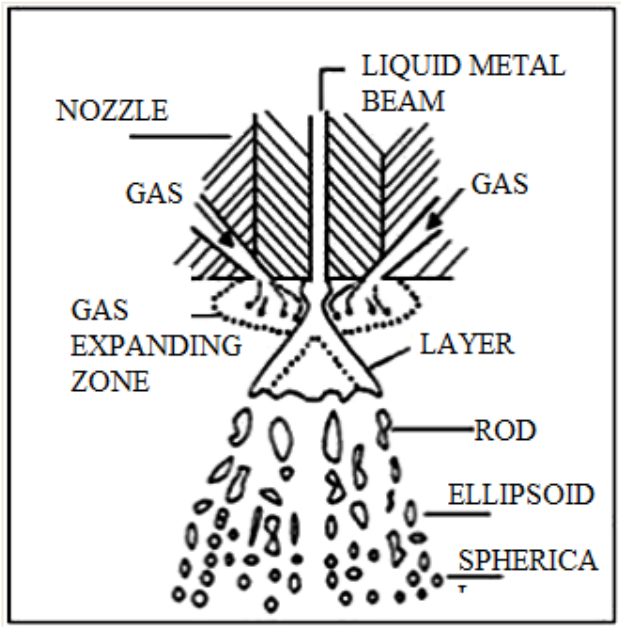


Figure 4.5. The formation stages of metal powder shapes [72].

As can be seen from the studies, the gas atomization process occurs in a few stages and in the first stage the liquid metal is converted into a layer or barbed structure, followed by the second stage. In the latter stage, it is described as the solidification of the droplets. The cooling and solidification of the powders occurs while flying in the atomization tower. The solidification rate of liquid metal droplets is important. Because the rate of solidification determines the shape of the powders.

### 4.3. NOZZLE SYSTEMS

Nozzle systems have 2 types as closely matched and free fall. In free fall systems, the liquid metal flows freely until it meets the pulverizing gas. After it contacts with the gas for a certain period of time under the influence of gravity. Most closely matched nozzle systems are used in combination with circular slot gas jets. In these systems, the liquid metal comes into contact with the gas from the nozzle and the atomization process is carried out [72]. Figure 4.6 shows a schematic representation of nozzle systems.

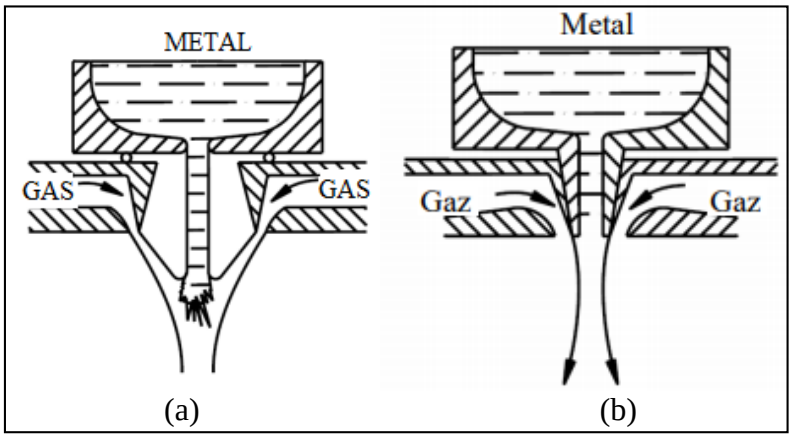


Figure 4.6. Nozzle systems. a) Free fall, b) Closely matched [74].

In free fall systems, it is generally not preferred to produce fine sizes of powder because they are expensive and not economical. Because of the transfer of energy from the gas jet to liquid metal can be a problem. The large gas jet angle leads to an inefficient and unstable atomization process. At the same time, the optimum gas pressure value cannot be achieved and the instability of the gas occurs when working at high gas pressures. [74].

Closely matched systems work with high efficiency, but this system has some difficulties. The most important of these difficulties is the pressure at the tip of the nozzle. This pressure can be negative or positive. The stability of the liquid metal flow at high pressures can be overcome by designing the negative pressure at the nozzle end. Another problem is the solidification of the liquid metal at the nozzle end without further gas jet. After this solidification process, the liquid metal flow will not continue and the atomization process is ended. Therefore, the metal is heated to a temperature above 100-150 °C of its melting temperature. In closely matched systems, the splitting of the liquid metal is more easily divided than the free fall system and spherical powders can be produced with finer, fluidity and compressive capacity. [72].

## 4.4. NOZZLE TYPES

The task of the nozzle in the atomization units is to collide the liquid metal with the gas and separate it into particles. In other words, the nozzle has a geometric structure to control the flow directions of the gas jets and to produce the desired properties of the powder. Nozzle types affect the size and shape of the powders and their geometries are important. The nozzle types are divided into circular split and circular holes according to their gas output geometries (Figure 4.7) [69].

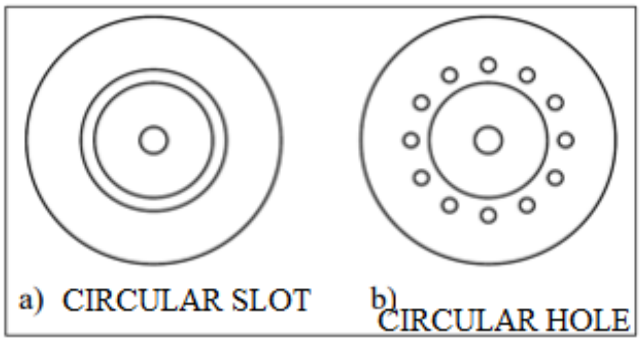


Figure 4.7. Nozzle types [75].

In the gas atomization systems, the nozzle is an important part of the atomization system as it provides the interaction between the liquid metal and gas. Nozzle is a constant part of the atomization system because there is no change in the geometry of the atomization systems. [75].

Nozzles have 2 types according to their geometric structure (Figure 4.8):

1. Sonic nozzles (narrowing angle)
2. Supersonic nozzles (narrowing-expanding angle)

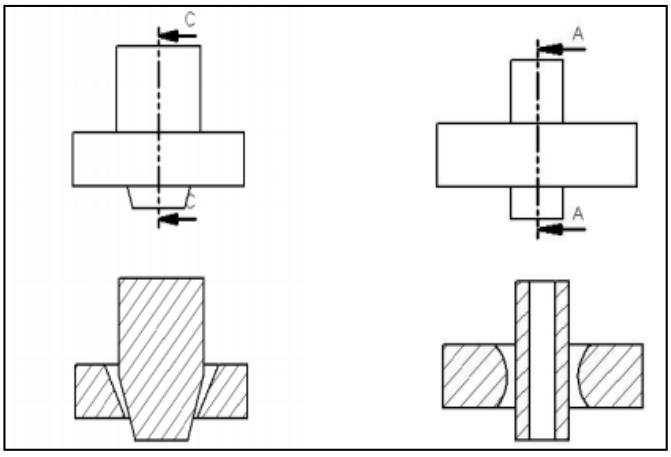


(a) (b)

Figure 4.8. Nozzle geometries. a) Sonic geometry, b) Supersonic geometry [75].

It is very important to choose a nozzle that can work in suitable conditions for a high efficiency atomization system. Therefore, the performance of the nozzle should be well investigated. Gas flow zones are examined as a result of sending gas to nozzle to examine nozzle performance. The gas flow region is shown schematically in the sonic and supersonic nozzle types (Figure 4.9 and Figure 4.10) [75].

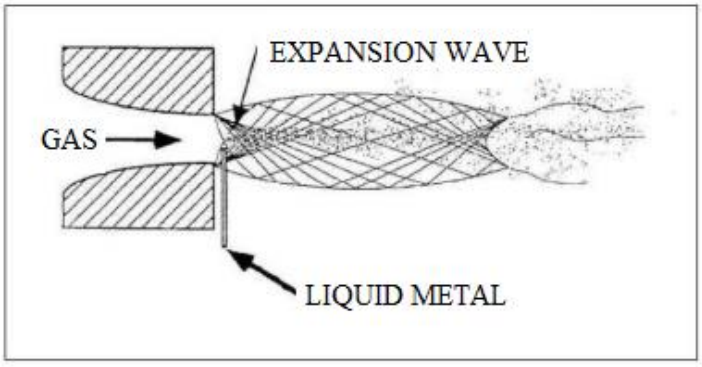


Figure 4.9. Development of high-speed gas jet in sonic nozzles [69].

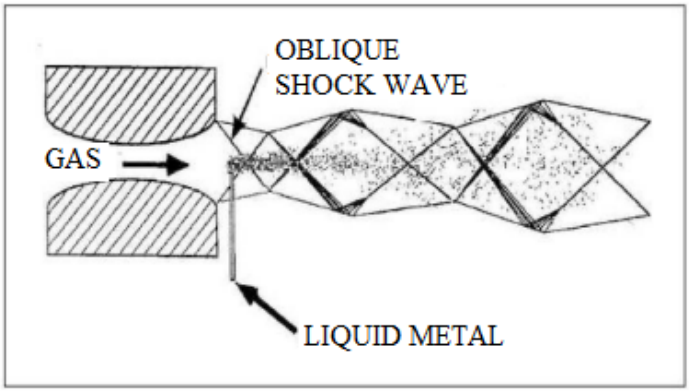


Figure 4.10. Development of high-speed gas jet in supersonic nozzles [69].

The rate at which the atomization gas exits from the nozzle may be in the form of a narrowing-expanding design (Figure 4.10), which allows the gas velocity to reach velocities (M> 1) above the constrictive design (Figure 4.9) or sound velocity (M> 1), which limits the velocities below the velocity of sound (M <1) (Figure 4.11) [76].

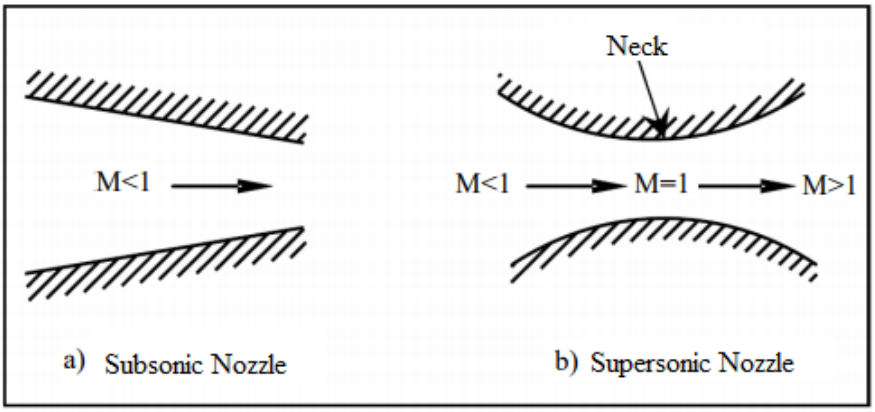


Figure 4.11. Nozzle types according to lower and upper flow values [77].

Since liquid metal has a high surface tension, supersonic nozzles are generally preferred in atomization processes. In sonic nozzles, high gas pressures reach supersonic speeds, while supersonic nozzles achieve supersonic velocity peaks at low gas pressures. [76].

The nozzles in the shrinking-expanding geometry are known as the Laval nozzle (Figure 4.12). Gas outlet, concentric ring-shaped nozzles with narrowing geometry are called Mannessmann nozzle (Figure 4.12).

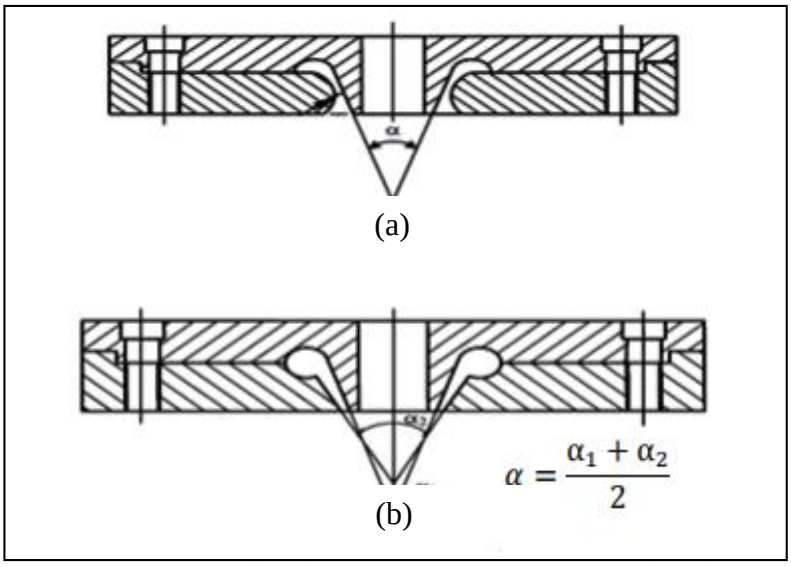


Figure 4.12. Nozzle geometry types a) Laval, b) Mannesmann [77].

## 4.5. NEGATIVE AND POSITIVE PRESSURE

At the point where the liquid metal comes out of the nozzle, there may be negative or positive pressure at the nozzle end according to the dynamics of the gas. In the case of negative pressure, the liquid metal is forced to flow through the metal flow pipe into the atomization tower, and in the case of positive pressure, the liquid metal is forced back into the melting pot without being discharged from the metal flow tube and is rebounded. Therefore, a negative pressure condition in powder metallurgy is desirable [78]. The negative pressure at the metal flow pipe end is the sum of the gas flow forces in the circulation zone acting on the liquid metal. In the literature studies, it was observed that supersonic nozzles produced a stronger negative pressure than the sonic nozzles. [79].

The most important factor affecting the negative pressure formation is the position of the metal flow pipe relative to the nozzle gas outlet. It has generally been found that a stronger negative pressure is produced by the increase of the projection of the liquid metal flow pipe. However, the elongation of this protrusion causes the liquid metal to freeze in the metal flow pipe. In their research, Le and Henein found that maximum negative pressure was generated in the position where the metal flow pipe was 10 mm below the nozzle outlet (Figure 4.13). [80].

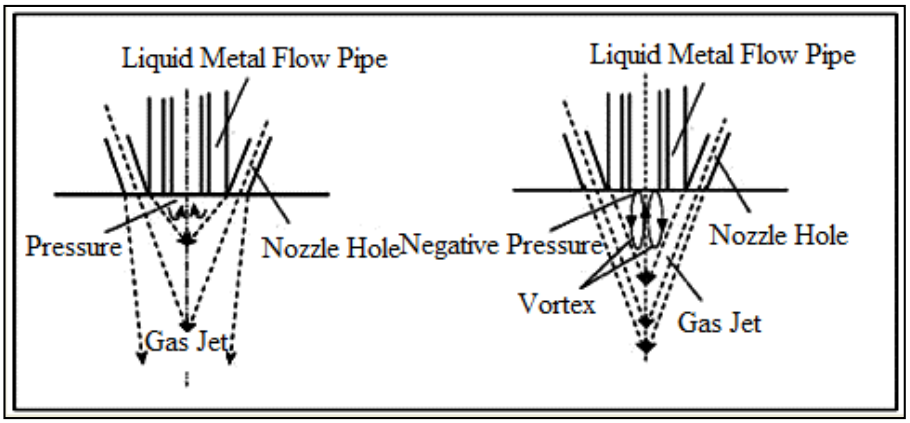


Figure 4.13. Negative and positive pressure formation at the end of metal flow pipes [77].

# PART 5

# POWDER CHARACTERIZATION

The raw materials of the products produced by powder metallurgy are powders. Powder selection is important to ensure that the product to be obtained has the desired properties and strength. Knowing the methods by which a powder is produced provides a preliminary information on the particle size, size distribution, physical and chemical properties of the powder.

The powder properties can be listed as follows.

1. Powder shape
2. Powder size and distribution
3. Compressibility
4. Specific surface area
5. Fluency
6. Apparent and vibrant density
7. Impurity

## 5.1. POWDER SHAPE

According to the production method, the powder shapes may be different (Figure 5.1). The shapes of the powders play an important role in their fluency and packaging. The flux of spherical powders is much better than that of dendritic or complex shaped powders. In addition, the powder shape also affects the properties of the powders such as apparent density, compressibility, raw density and sinterability. The apparent density of complex shaped powders has a lower value than that of spherical powders. Pressing of the powders of the spherical structure is easy and pressing of complex and porous powders is difficult. [81].

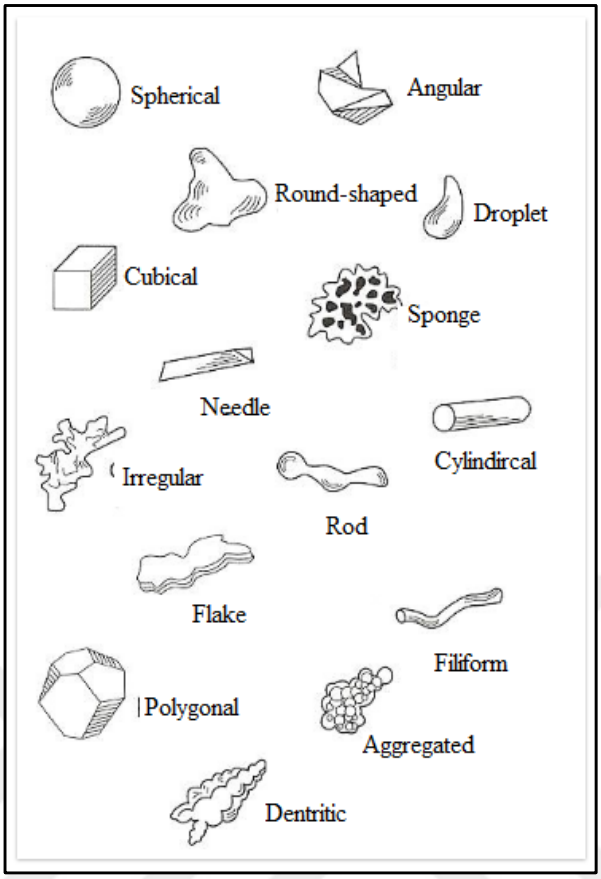


Figure 5.1. Powder shapes [63].

## 5.2. POWDER SIZE AND DISTRUBITION

Powder size is one of the most important factors of powder metallurgy. It cannot be said that the powders produced by powder metallurgy are at the same size, but the average grain size can be considered. As the shape of the powder particles becomes complex, the powder size measurement techniques also change. Generally; while for spherical powders only diameter measurement is sufficient; In the form of pulses, both the thickness and the length of the neck should be measured. Therefore; As the shape of the powder particles progresses towards the complex, several dimensions need to be measured. The grain size of very complex shaped powders can be found from the surface area [82].

## 5.3. COMPRESSEBILITY

Compression is a common way of shaping powders. The resistance of powders to compression is an important feature of the powders. Compressibility is to measure the condensation of powders under a given pressure. Usually, cylindrical and rectangular geometries are used for this process. The powders are filled into the mold at an apparent density and the density value is measured after pressing. This density value is called raw density. Raw density is used to express compressibility [55].

## 5.4. SPECIFICAL SURFACE AREA

The surface area is an average measure of the outer surface of a large number of powders. Such a chemical parameter is useful since it is linked to chemical reactivity, packaging, catalytic behavior, adsorption, contamination and even briquetting and sintering. However, the surface area of a powder cannot say much about the distribution in the properties and the powder structure. Therefore, the surface area of the powder is combined with other parameters for detailed identification of the powder. Specific surface area is explained as area per unit mass ($m^2$ / g) [55].

Surface area per unit weight is given by: S=A/w, in this context;

S = 6 / PM.D
S: Specifical surface area
D: Average grain size
PM: Theoretical material density
w: Weight of the grain

## 5.5. POWDER FLUIDITY

It is a method used to determine the flow ability of powders. In principle, it is a measure of how long the powders taken at a constant weight (50g) pass through a Hall funnel (Figure 5.2) under gravity and this is considered to be the fluidity of the powder. The fluidity of the powder depends on the grain size of the powder, the

specific surface area and the shape of the powder grain. As the powder grain size decreases, the fluidity of the powder decreases. The shape of powdered grain decreases as it moves away from spherical geometry [63].

Figure 5.2. Hall funnel [83].

## 5.6. APPERANT AND VIBRANT DENSITY

The apparent density is the loose (uncompressed) density of the powder. The density of the free-flowing powders (apparent density) is greatly increased by the vibrating of the mold prior to pressing. The increased density with vibration is related to the shape and powder distribution. In complex shaped powders, this increase is much higher than that of spherical and smooth surfaces. The reason this; The relative densities of the spherical shaped powders are due to the high density, low density and low density of the powders having a small powder size distribution. The viscosity and viscosity of the powders are very important in terms of the manufacturing process. The flow rates of the powders in the spherical structure and the packaging properties in the mold are better than the other complex shaped powders. In other words; the spherical powders fill the mold faster than the complex shaped powders and have a higher visible and vibrating density before pressing [84].

## 5.7. IMPURITY

The purity of the powders is also important for powder metallurgy. Constructive substances in the powders also affect the pressing. The fact that the powders have a thin oxide layer does not affect the pressing. During pressing, the oxide layer can easily be torn off due to friction between the powders. Reduction of this oxide layer during sintering, however, is important for component strength (Figure 5.3). [85].

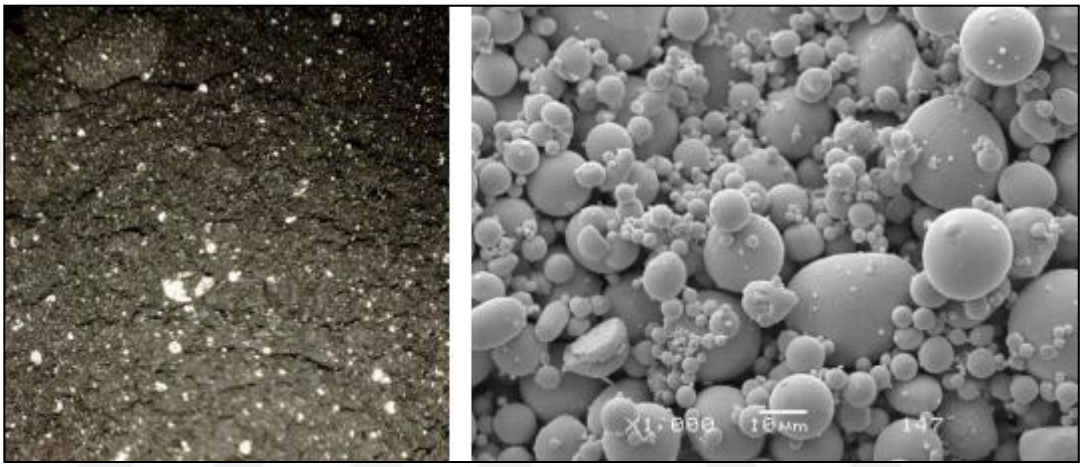

(a) (b)

Figure 5.3. a) Oxidized powder surface, b) Clean powder surface [86].

# PART 6

# PARTS PRODUCTION WITH POWDER METALLURGY

## 6.1. MIXING AND BLENDING

Mixing and blending are often used before compression. In both processes, the powder becomes a homogenous mass. Blending is the mixing of different sized powders of the same chemical composition, and mixing is the process applied to powders of different chemical composition. The reason for blending powders is to control particle size distribution.

The best mixing occurs when the volume of the powder is between 50% and 60% of the mixer volume. As the mixing time, usually 5 to 30 min. are enough for a succesful mixture [82,87]. The mixing of metal powders is usually carried out by means of V or Y type mixers in double-pipe and double-cone mixers (Figure 6.1). Keeping the mixing time long causes the powder particles to be broken and spherical and plastic deformation. Such reasons reduce the compressibility of the powder. The most important part of the mixture is to provide homogeneity in each compartment of the powder by adjusting the composition well [88].

Figure 6.1. Powder mixing turbula [89].

## 6.2. FORMING OF POWDERS

In the forming process of the powders, the density of the powders is considered to be approximately equal to the apparent density. By increasing the pressure applied to the powders, the point contact between the grains of the powder is disrupted and the amount of porosity decreases due to the increase of the pressure. Plastic deformation and density also increase due to increased pressure [90]. The forming of the powders into pieces is usually done by extrusion, rolling and pressing.

### 6.2.1. Extrusion

This manufacturing method is usually applied to light metals (such as Al, Cu, Mg). The powder mixture is put into a receiving sleeve and the powder mixture is pressed by means of a press. The powder mixture is forced through the mold we call the matrix. Thus, powder forming process is performed by extrusion. And also; powder mixes can be processed by injection molding in different shapes and molds (Figure 6.2) [91].

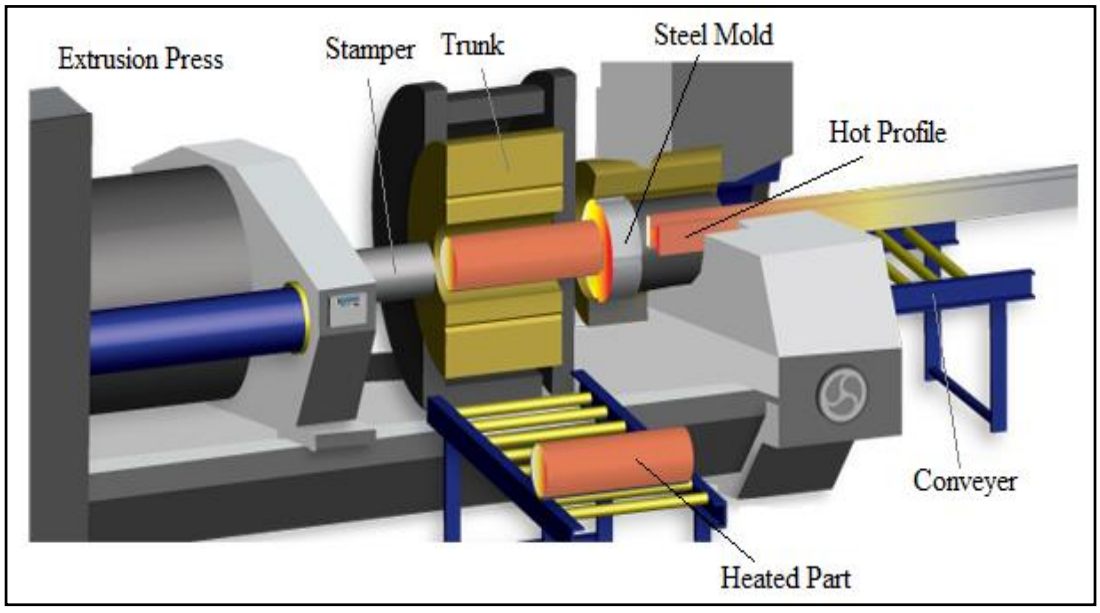


Figure 6.2. Schematic representation of extrusion process [92].

### 6.2.2. Rolling

The process of plastic forming by passing between two rolls rotating around the axes of the material is called rolling. (Figure 6.3). The rollers rotate at the same speed and in the opposite direction. At the material; deformation is provided by the compressive force providing compression and the surface shear stress caused by friction between the material and the rollers. In addition, the friction force also allows the material to advance [63].

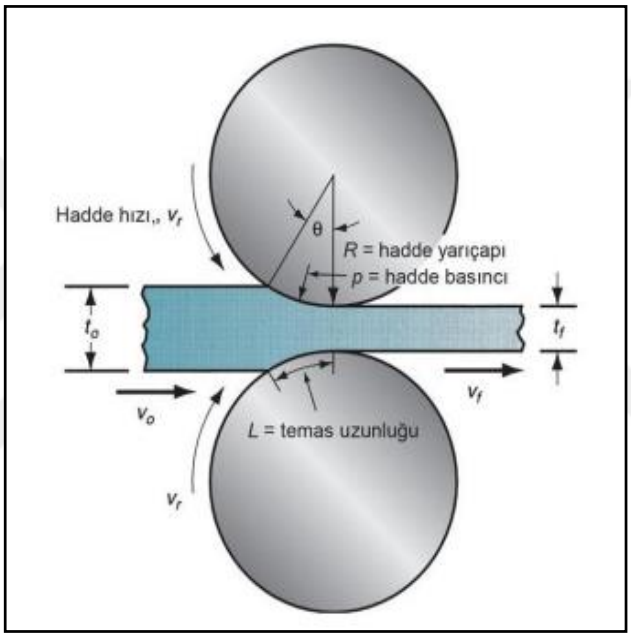


Figure 6.3. Rolling system [63].

### 6.2.3. Pressing

Pressing process in general is defined by; The powder placed between the two staples applying high pressure on two axes. Pressing is commonly used in serial manufacturing of simple parts. The pressure obtained by applying pressure is called bulk. The term Bulk means that it is not yet sufficiently compressed. The strength of the bulk material is very low, but the strength of the final product after sintering is very high. In some pressing applications, sintering process is carried out by applying heat to the powders together with the pressing process. In such applications, both the

pressing and the sintering process has been done, so the final product is manufactured at one time [63].

#### 6.2.3.1. One-way Pressing

In the one-way pressing process, with the commencement of the deformation process, it causes an irregularity in the distribution of friction force formed between the powder itself and inside the powder mold. This irregularity significantly affects the distribution of the applied pressure. The density of the powder is high in the areas where the stapler is in the region of the stapler while the staple is low. Density distribution in unidirectional pressing is distributed as seen in Figure 6.4. This reduction in the amount of density depends on the length / diameter ratio of the manufactured part. In the unidirectional pressing, the ratio of the powder height to the mold diameter before the pressing operation significantly affects the density distribution after the pressing process. Because of these reasons; height / diameter ≤ 4 is recommended [93].

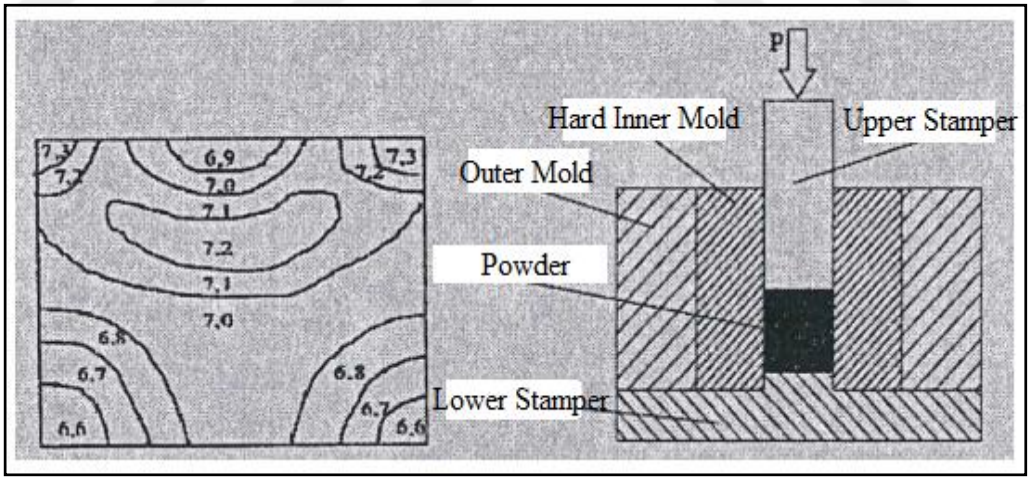


Figure 6.4. Density distribution in one-way pressing and schematic representation of one-way die [93,94].

#### 6.2.3.2. Bidirectional Pressing

It is the process of pressing the powder at the same time by two punches which are mutually working from the bottom and top at both sides (Figure 6.5). An equal

amount of pressure is applied in both directions. By means of bi-directional pressing, a regular compression occurs in the mold. Density distribution is more homogenous than the density distribution of the parts produced by one-way pressing. [93].

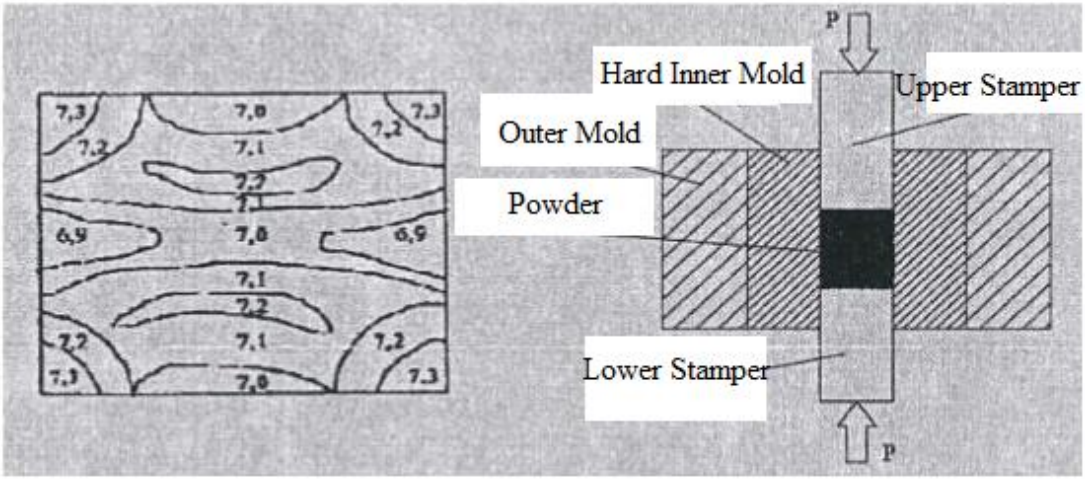


Figure 6.5. Densty distribution in bidirectional pressing and schematic representation of bidirectional die [93,94].

### 6.2.3.3. Cold Isostatic Pressing

It is a method whereby the pressures applied during the pressing of the powder are applied equally in all directions (Figure 6.6). Cold isostatic pressing is generally applied to parts with complex grading, length and diameter ratio. The powder is placed in a sealed elastic container used as a mold and sealed. Because the air inside the mold will come out during pressing, it is emptied from the mold in advance. After unloading, the mold is placed in a pressure vessel in a liquid bath. High pressure is applied into the liquid and the mold is subjected to hydrostatic pressure. The mold is removed from the liquid bath and the soft mold on the part is removed. By this method, a homogeneous density distribution is obtained in the pressed parts [95].

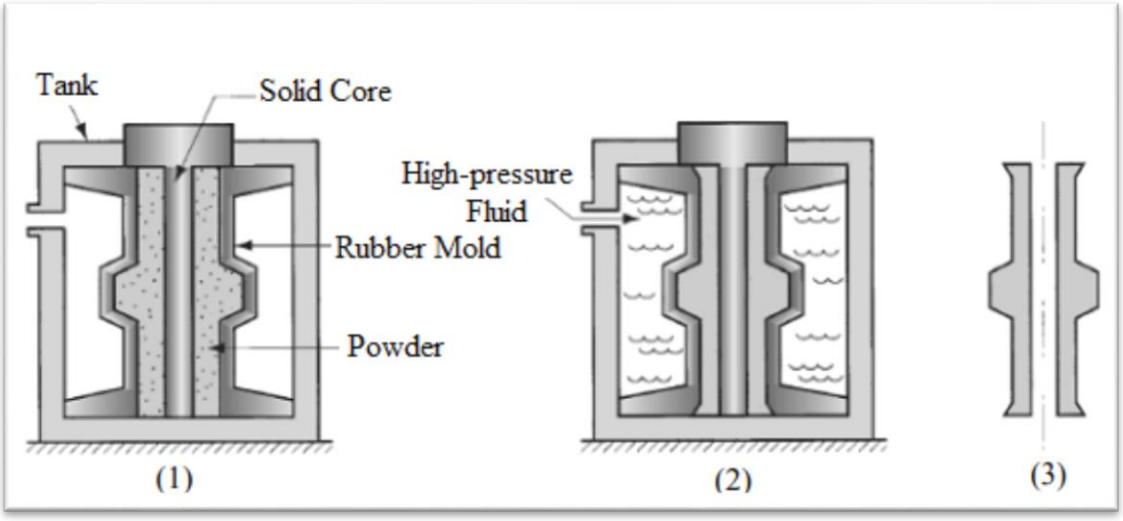


Figure 6.6. Schematic representation of cold isostatic pressing [93].

#### 6.2.3.4. Hot Isostatic Pressing

Hot isostatic pressing is a method in which pressure is applied in all respects and flexible molds are used compared to the hot-pressing method where only axial pressure is applied (Figure 6.7). In this method, the sintering process is carried out while the pressure is applied by gas from the three axes coaxially in the mold where the powders are located. The only difference between this method and the cold isostatic press is the heating of the pressure applied by an additional system. Argon or helium gas is used in order to avoid any negative reaction when applying pressure at high temperatures. In hot isostatic pressing, the process temperature can be reached up to 2000 °C, while the pressure varies between 30 and 400 MPa. The most important advantage of the hot isostatic press is that high density materials can be produced without grain growth. With this method, the microstructure is difficult to control for the desired properties, but the component shape consistency is high [95].

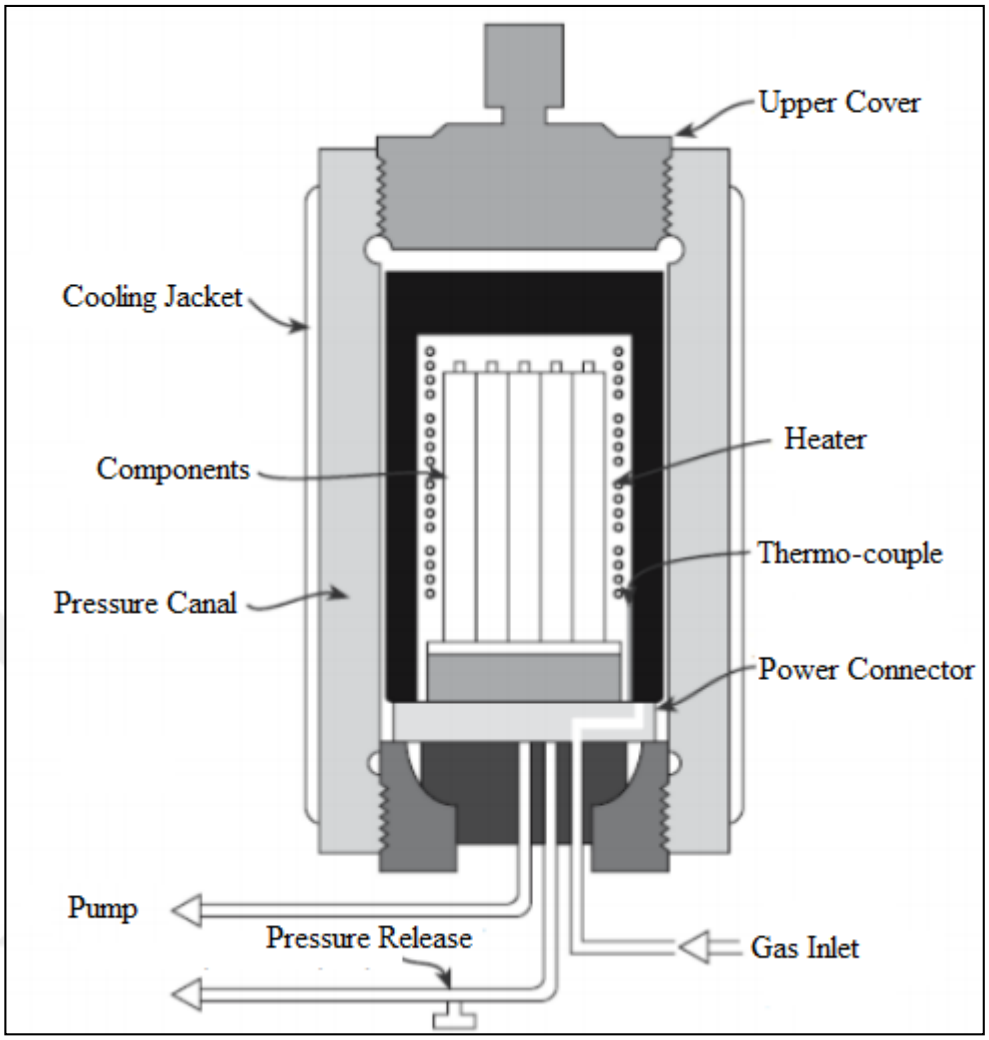


Figure 6.7. Schematic representation of hot isostatic pressing [94].

## 6.3. SINTERING

Sintering is a kind of heating process which enables the bonded powdered metal parts to connect to each other and provides significant strength increase and improvement of the properties. For sintering to be effective, the most important factor is the contact of the powders with each other. In this context, sintering is applied to pressed or molded powders [96].

Sintering is the heat treatment of the pressed parts in order to obtain the desired properties in a controlled atmosphere and at high temperature. In the case of sintering temperature; 70% to 80% of the melting temperatures of the metals are taken, while the sintering temperature in some refractory materials reaches up to 90% of the

melting temperature. The sintering temperature can be mixed with more than one material and the pressed parts can be above the melting temperature of some components. In such cases, materials with a low melting temperature melt and fill the gaps between powders with high melting temperatures.

The sintering process usually occurs in 3 stages (Figure 6.8). These;

1. Burning or cleaning zone
2. High temperature zone
3. Cooling zone

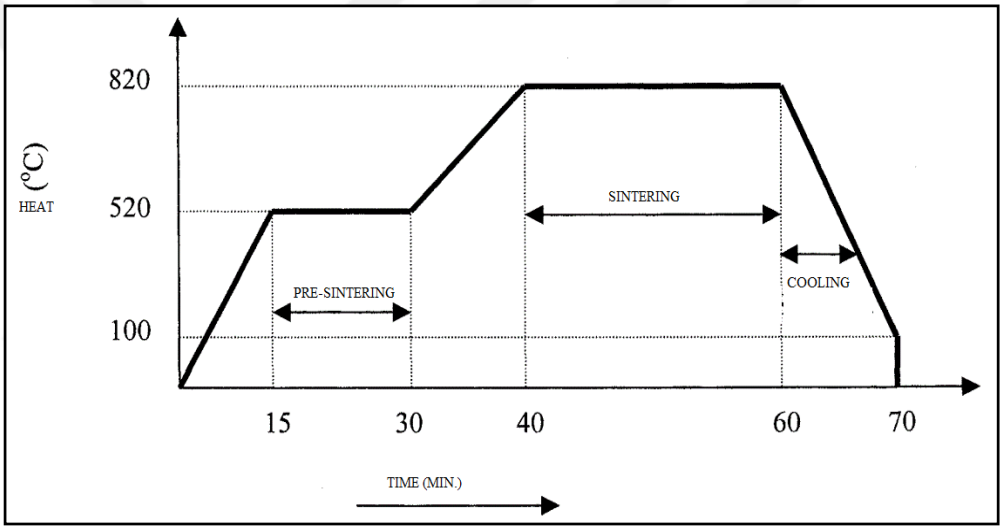


Figure 6.8. Stages of sintering [97].

The first combustion and cleaning zone is the area where oil and binders are removed by air burning. Cleaning of lubricants and binders in the material occurs at low heating speeds. At high heating speeds; The binder and air, which usually burn in the pores, cause internal fragmentation by causing internal pressure. Bonds begin to form between the particles in the high temperature zone. This process occurs by solid state diffusion. The formation of intermetallic phases and solid solutions occurs by means of solid-state diffusion. At the high temperature, a bond is formed between the contacting parts and this bond is strengthened by the mutual transfer of atoms. The waiting time in this region varies according to the desired density and characteristics. Waiting time is usually 10 min. between several hours. Oxidation is prevented as the

cooling zone is made under atmospheric control. Since fine powder particles do not provide full contact before sintering and contain residual porosity, atmosphere control must be present in these 3 steps [63].

Another measure of sintering is determined as the ratio of neck diameter to sphere diameter. (X/D) and the neck diameter as determined by Figure 6.9. The region indicated by P in the figure is called the radius of the neck circular profile. In addition to the actual neck growth, a sintered mass is shrunk (ie, the pores are ejected), concentrated and increased in strength.

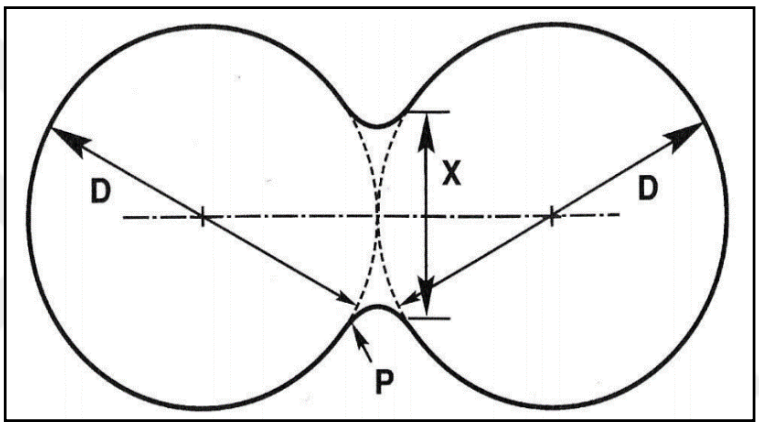


Figure 6.9. Sintering profile of two grains [84].

When two of the assemblies in Figure 6.10 are considered, there is a plurality of mating zones in the compressed powder pile. The bonds between the particles in contact with the progress of the sintering process expands and join. Each boundary grows one limit. As shown in Figure 6.10, the two particles are completely joined together as a result of a long sintering, resulting in a single sphere of 1.26 times the starting diameter.

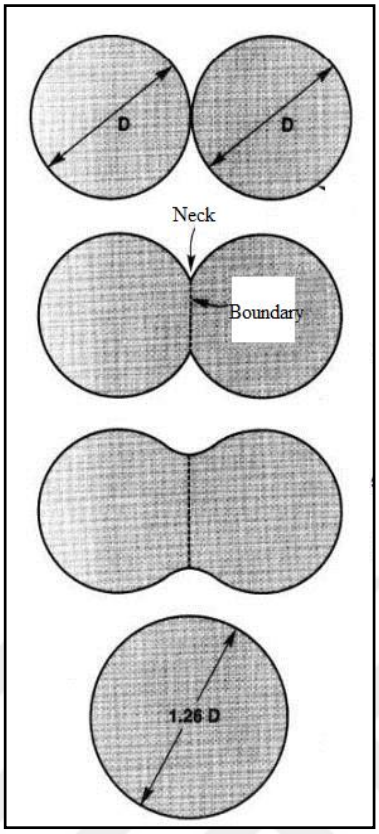


Figure 6.10. Sintering model of two grains [98].

As shown in Figure 6.11, a schematic diagram showing the change of the pore structure during sintering starting with the point contact of the particles is given. The space volume gradually decreases and gaps become more spherical. Clearly, it is clear that gaps are replaced by grain boundaries as globalization of space is formed.

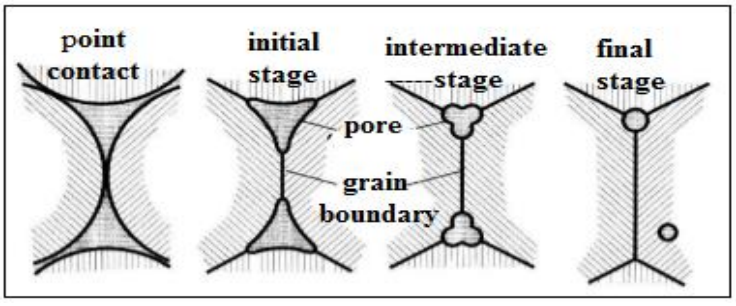


Figure 6.11. Schematic illustration of the change of the pore structure during sintering [98].

### 6.3.1. Solid Phase Sintering

The solid phase sintering process is the result of intense condensation of the powder particles to the sintering temperature. The solid phase sintering process is shown in the diagram in Figure 6.12. In the diagram, solid-state sintering occurs in the X1 composition between A and B at temperature T1.

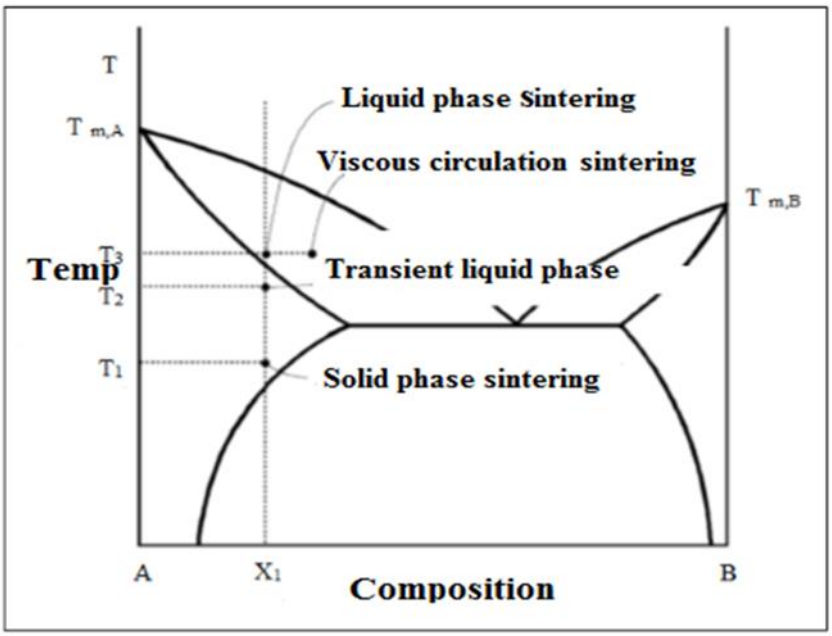


Figure 6.12. Sintering phase diagram [99].

### 6.3.2. Liquid Phase Sintering

The liquid phase sintering is sintered at the temperature at which the liquid phase is formed. A sudden shrinkage occurs by the formation of the liquid phase. During this shrinkage, the solid particles enter a new order in the liquid phase. Liquid phase sintering occurs when a liquid phase is formed in the powder during sintering. The diagram showing the liquid phase sintering is given in Figure 6.12. In the diagram, liquid phase sintering occurs in composition X1 at temperature T3. In liquid phase sintering, the amount of liquid phase cannot exceed 20 percent. In liquid phase sintering, ceramic powders can be sintered at low temperature and in short time.

However, parts produced by liquid phase sintering are not suitable for use at high temperatures [99].

While the main powder remains solid during the sintering, the additive powder provides the liquid phase formation. Figure 6.13 consists of 4 parts. In the first part, the powders appear to be crude. In the second part, liquid phase propagation occurs. In the third section, the precipitation process occurs in the melt. Finally, in the fourth section, the liquid phase sintering process is finished and the solid skeleton of the material appears.

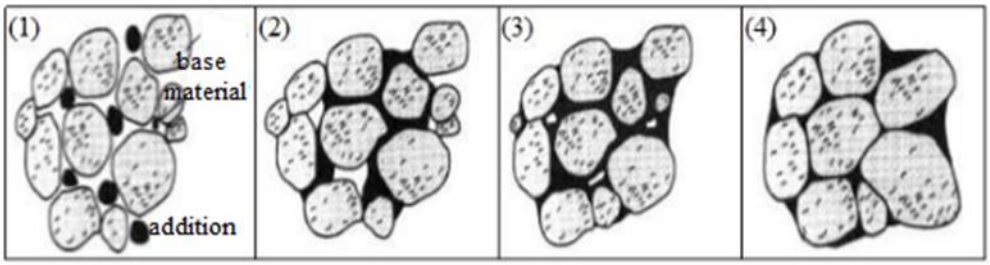


Figure 6.13. Stages of liquid phase sintering using two powder mixtures [99].

In Figure 6.14, grain growth occurs by re-precipitation of solids formed by the precipitation of small size grains on large grains. In addition to grain growth, the sintering process also gives the grain shape adjustment process. Thus, the solid is better packed and any remaining pore is thought to be better filled with liquid.

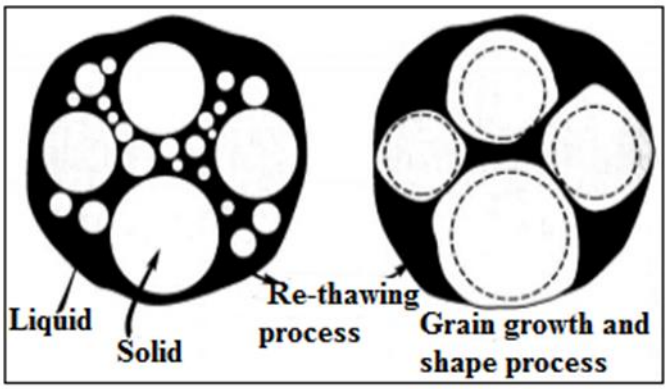


Figure 6.14. Precipitation and grain growth in liquid phase sintering process [99].

## PART 7

## MAGNESIUM ALLOYS

In recent years, with the increasing use of lightweight materials in engineering applications where weight savings are important in performance development, the importance of magnesium and its alloys has increased in the automotive, aerospace, communication and communication industries.

With the increasing demand for the use of magnesium alloys, there is a large increase in the demand for composite materials produced by powder metallurgy. Compared to metals such as Al, Ti, Zn and Fe, magnesium with a very low density of 1.74 g / cm3 is approximately 35% lighter than aluminum alloys and 65% lighter than titanium alloys [100,101]. Magnesium is more advantageous than materials such as aluminum and titanium with high strength - density and high elastic modulus - density ratio at room temperature. In addition, it has advantages such as excellent castability, weldability and high thermal conductivity. However, the magnesium crystal causes a tight package with hexagonal (hcp) lattice structure, limited ductility and toughness with only 3 shear systems. Cold forming in magnesium is difficult to perform and therefore the forming processes need to be carried out at high temperatures [102,103].

Magnesium has a low melting temperature and is therefore very difficult to use at high temperatures. Creates a creep resistance of approx. 100 - 200 °C. In addition, the oxidation resistance decreases at high temperatures and the resulting oxide layer accelerates oxidation [104, 105]. However, the mechanical properties of magnesium alloys have been improved in order to increase the creep and oxidation resistance at room temperature and at high temperatures. Magnesium-based composite materials products, with many advantages and uses are increasing. Magnesium and magnesium alloys of commercial purity have higher mechanical properties and are more useful at

high temperatures. Therefore, the use of magnesium and magnesium based composite materials in engineering applications is increasing day by day [106].

## 7.1. PHYSICAL PROPERTIES OF MAGNESIUM

Magnesium has a hexagonal close packed (HCP) crystal structure and has a length of a = 0.320 nm, c = 0.520 nm c / a = 1.624 nm. Magnesium is the lightest of all engineering materials since it has a density of 1.74 g / $cm^3$. In Table 7.1, the properties of pure magnesium are given. Approximately (2.7 g / $cm^3$) of aluminum is two times lighter than steel (7.86 g / $cm^3$) four times lighter [107, 108].

Table 7.1. Physical Properties of Magnesium [109].

| | |
|---|---|
| **Atomic no** | 12 |
| **Atomic mass** | 24.31 g/g.mol |
| **Color** | Silvery gray metal |
| **Density** | At 20 °C, 1.738 g.cm-3<br>At 650 °C, 1.58 g.cm-3 |
| **Melting point** | 650 °C |
| **Boiling point** | 1103 °C |
| **Crystal structure** | Hexagonal close packed |
| **Combustion heat** | 25020 kJ.kg-1 |
| **Flash point** | 2800 °C |
| **Evaporation heat** | 5272 kJ.kg-1 |
| **Specific heat** | At 20 °C, 1025 J.K-1.kg |
| **Vapor pressure** | At 527 °C, 20 Pa |
| | At 650 °C, 360 Pa |
| | At 1727 °C, 400 Pa |
| **Viscosity** | 650 °C'de 1.25 cp |
| **Thermal conductivity** | At 27 °C, 156 W/m K |
| | At 527 °C, 146 W/ m K |

Since magnesium is a reactive metal, it is not found metallic in nature. In nature, calcium compounds are present as oxide, silicate or carbonate. Because magnesium has high reactivity, high energy is needed during production. Therefor magnesium is

not a cheap metal [110,111]. The advantages of magnesium and its alloys are given below;

1. Lightest in all engineering materials,
2. Having a good electromagnetic shield
3. High strength / density ratio,
4. Vibration and impact damping capability,
5. Excellent castability,
6. Grinding at high speeds,
7. Being able to weld in atmosphere controlled environment,
8. Good corrosion resistance in the use of high purity magnesium.

Compared with polymer materials;

1. Better mechanical properties,
2. Better aging time,
3. High thermal electrical conductivity,
4. High recyclability.

Magnesium has properties that limit its use due to some weaknesses [112]. These features are given below;

1. Low modulus of elasticity,
2. Limited cold deformation ability and toughness,
3. Low creep resistance at high temperatures,
4. High shrinkage ratio during solidification,
5. High chemical reactivity,
6. Low corrosion resistance.

Magnesium alloys having a low melting temperature (650 °C) are another disadvantage of limiting the usage area. Alloying magnesium with elements such as aluminum, zinc, manganese, rare earth elements, thorium and zirconium provide creep resistance at high temperatures, strength, weight reduction and reduction of

inertial forces [113,114]. Due to this alloying property, steel has replaced copper-based alloys, cast iron and even aluminum alloys [110]. Magnesium and magnesium alloys include automotive, industrial, material transport, commercial and space equipment as structural applications. It is used in organic chemistry in non-structural applications [115]. In recent years, magnesium, double, triple and multi-magnesium based alloys have been worked and different alloy systems have been obtained. These alloy systems are considered because of their high strength / weight ratio compared to other alloy systems. Magnesium is a metal usable in many sectors due to its low density, high specific heat capacity, high sound absorption and thermal conductivity [116].

## 7.2. MECHANICAL PROPERTIES OF MAGNESIUM AND ITS ALLOYS

Magnesium alloys are a metal with mechanical properties such as 160-300 N / $mm^2$ tensile strength, 80-190 N / $mm^2$ 0.2% yield strength and 2-15% elongation at break. However, the increase in temperature decreases the strength of magnesium alloys and low ductility at room temperature. The difference between yield and tensile strength decreases at high temperatures. Magnet with hexagonal crystal lattice structure and 3 slip plane numbers is harder to form cold compared to aluminum having a surface centered cubic structure and 12 sliding planes. As the number of sliding systems in a crystal increases, the deformation of the material becomes easier, ie the ductility increases. In magnesium at temperatures above 210 °C, ineffective sliding planes are activated, so the ductility of the magnesium increases as the temperature increases [117].

## 7.3. CLASSIFICATION OF MAGNESIUM ALLOYS

Mg alloys were determined by ASTM (A275) standard system. The method covers two numbers with two letters. The first letter represents the element that has the highest structure in the composition after Mg and the second letter represents the 2nd highest element in the alloy. In the figure, the first figure is the % slice of the metal most found in the structure after Mg, and the second symbol represents the % of the

second most common element in the structure. In Table 7.2 commonly used alloy elements are listed in a single letter.

Table 7.2. Alloy elements and abbreviations [118-122].

| **Letter** | A | C | E | H | J | K | L | M | Q | S | W | X | Z |
|---|---|---|---|---|---|---|---|---|---|---|---|---|---|
| **Element** | Al | Cu | Re | Tr | Sr | Zr | Li | Mn | Ag | Si | Yi | Ca | Zn |

For example; The description of the AZ31 alloy is given below

A→ Represents aluminum.

Z→ Represents zinc.

3→ Represents % amount of approximate aluminum.

1→ Represents % amount of approximate zinc.

More is represented in Table 7.3.

Table 7.3. Mg alloys standards and compositions (ASTM B 93 / B 93M and ASTM B94) [120,123].

| rest ALLOY ELEMENT | MG ALAŞIMLARI | | | | | | | | | |
|---|---|---|---|---|---|---|---|---|---|---|
| | **AM50** | **AM60** | **AS21** | **AS41** | **AZ31** | **AZ61** | **AZ80** | **AZ91** | **ZE10** | **ZK60** |
| **Al** | 4,5-5,3 | ***5,6-6,4*** | 1,9-2,5 | 3,7-4,8 | 2,5-3,5 | 6,5 | 7,8-9,2 | 8,5-9,5 | 0,05 max | 0,05 max |
| **Zn** | 0,20 max. | ***0,20 max.*** | 0,15-0,25 | 0,10 max. | 0,7-1,3 | 1,0 | 0,2-0,8 | 0,45-0,90 | 1,0-1,5 | 4,8-6,2 |
| **Mn** | 0,28-0,50 | ***0,26-0,50*** | 0,20 min. | 0,35-0,60 | 0,20 min. | 0,15 | 0,15-0,5 | 0,17-0,40 | 0,1 max. | 0,1 max. |
| **Si** | 0,05max. | ***0,05max.*** | 0,70-1,2 | 0,60-1,4 | 0,05 max. | 0,20 max. | 0,10 max. | 0,05 max. | 0,05 max. | 0,05 max. |
| **Fe (max)** | 0,004 | ***0,004*** | 0,004 | 0,0035 | 0,005 | - | 0,05 | 0,004 | 0,03 | 0,03 |
| **Cu (max)** | 0,008 | ***0,008*** | 0,008 | 0,015 | 0,05 | 0,08 | 0,05 | 0,025 | 0,02 | 0,05 |
| **Ni (max)** | 0,001 | ***0,001*** | 0,001 | 0,001 | 0,005 | 0,010 | 0,005 | 0,001 | 0,005 | 0,005 |
| **Be** | - | - | - | - | - | - | 0,002 | - | 0,002 | 0,002 |
| **Ce** | - | - | - | - | - | - | - | - | 0,12-0,25 | - |
| **Zr** | - | - | - | - | - | - | - | - | - | 0,3-0,9 |
| **Diğer** | 0,01 | ***0,01*** | 0,01 | 0,01 | - | - | - | 0,01 | - | - |
| **Mg** | rest | rest | rest | rest | rest | rest | rest | rest | rest | rest |

### 7.3.1. Properties of AZ31 Magnesium Alloys

AZ alloys from Mg alloys are especially used in the construction of steering, wheel, automobile seat frames in terms of their high toughness and energy absorption

properties [124]. AZ31 alloys have good elongation and impact resistance. They also have good castability, good mechanical properties and corrosion resistance. However, these alloys have low creep resistance at temperatures above 120 °C. The microstructure of AZ31 alloys generally consists of α-Mg and $Mg_{17}Al_{12}$ phases [125].

Magnesium, especially Al, Zn and Mn, alkaline earth metals and very small amounts of Si, Sn, Pb, Y, Ba, Sb, Ca, Sr and Bi elements such as alloying, mechanical properties are improved and the improvement performance and uses day by day. AZ31 (Mg-Al-Mn) alloys are generally used in the production of automobile parts and this alloy has a good pourability [126]. The use of magnesium alloys in wide automobile plates, such as doors, hoods and tailgate, which require high bending resistance, provides 50% weight advantage compared to steel and 20% weight compared to aluminum. Mg-Al-Mn alloys from magnesium alloys are industrially important because of their strength, lightness and partly good corrosion resistance.

In Mg alloys, Al facilitates the solid precipitate strength of Mg, the pourability of the melt and reduces the micropores in the casting process. The presence of Alloy, in Mg alloys increases the solidification time of the alloy and the hardness values. But it decreases ductility. $Mg_{17}Al_{12}$ intermetallic is formed in the structure (< 120 $^{o}$ C) and increases the strength of the structure. It is known that the alloy is present in a large amount of alloys and causes micro-pore formation in the structure [119,120,127,128].

The presence of Mn in the alloy increases the corrosion and friction resistance of the structure. However, the strength of Mg alloys has little effect on Mn [119,120,128,129]. Mn can form a solid solution depending on the temperature up to 3.4% in Mg.

The mechanical properties, physical properties and the chemical composition of AZ31 can be seen in Table 7.4, 7.5 and 7.6.

Table 7.4. AZ31 Mechanical Properties [109].

| | |
|---|---|
| Tensile | 220 Mpa |
| Yielding Strength (Pulling) | 130 Mpa |
| Yielding Strength (Pressure) | 130 Mpa |
| Brinell Hardness | 60 |
| Absorption Ability | %52 |
| Elasticity | 45 Gpa |
| Poisson's Ratio | 0.35 |
| Elongation | %8 - %15 |
| Notched Impact Strength | 3.2 Joule |
| Fatigue Strength | 60 Mpa |

Table 7.5. AZ31 Physical Properties [109].

| | |
|---|---|
| Density | 1.79 gr/cm$^3$ |
| Conductivity | 61 W/m$^o$ K |
| Thermal Expansion | 25.6 um/m$^o$ K |
| Corrosion Resistance 3 days, %5 NaCl | 0.05 mg/cm$^2$/d |
| Casting Temperature | 650 - 695 $^o$C |

Table 7.6. AZ31 Chemical Composition [130].

| **Element** | Al | Mn | Si | Zn | Fe | Cu | Ni | other | Mg |
|---|---|---|---|---|---|---|---|---|---|
| **%** | 2.5-3.5 | 0.45 | 0.22 | 1.62 | 0.005 | 0.010 | 0.002 | 0.003 | Remaining |

In order to make the desired properties of the mechanical properties of Mg alloys, new products are obtained by means of powder metallurgy by adding alloying elements to magnesia (126). Magnesium, which has a hexagonal tight package (HSP) lattice structure, can produce solid solubility with a large number of elements. Magnesium is mainly alloyed with basic elements such as Al, Zn, Mn, Be, Si, Ca, Cu, Fe, Ag, Sn and Zr by adding earth elements such as K, Na, Li alkali and Y, Ce, Ln, Nd. When magnesium is alloyed with one or more of these elements, the alloys usually increase the high strength / weight ratio [126].

## 7.4. THE EFFECT OF ELEMENTS ON MAGNESIUM ALLOYS

In order to give strength to the magnesium alloys, different melting and precipitation hardening is applied with different alloying elements. Mostly, the aluminum element increases the tensile strength and stiffness, improves pourability but increases the tendency to porosity. Calcium improves creep resistance, thinning the grain structure, and also negatively affects pourability, such as adhesion and hot tearing. Manganese increases the tensile strength, provides grain thinning, increases the weldability [99, 131]. It develops properties such as rare earth elements, creep resistance, corrosion resistance and high temperature strength, but it increases the cost with these positive properties. Silicon affects pourability negatively, but increases creep resistance. Zinc improves tensile strength and pourability, but increases micro-porosity and tendency to hot tear. Finally, zirconium increases the tensile strength and is very effective for grain refining, but is not preferred in alloys containing aluminum or silicon [116].

### 7.4.1. Effect of Aluminum

Aluminum is one of the most effective elements in alloying elements. The addition of aluminum to the magnesium increases the hardness and the tensile strength of the alloy, as well as the solidification range. Heat treatment can be applied when over 6% of aluminum is added to the alloy, but aluminum in industrial alloys is kept below 10% by weight. The optimum strength and ductility properties are seen in magnesium alloys containing 6% by weight of aluminum [116,132]. The maximum solubility of aluminum at eutectic temperature (437 °C) is approximately 33% by weight, as seen in the Mg - Al equilibrium phase diagram in Figure 7.1.

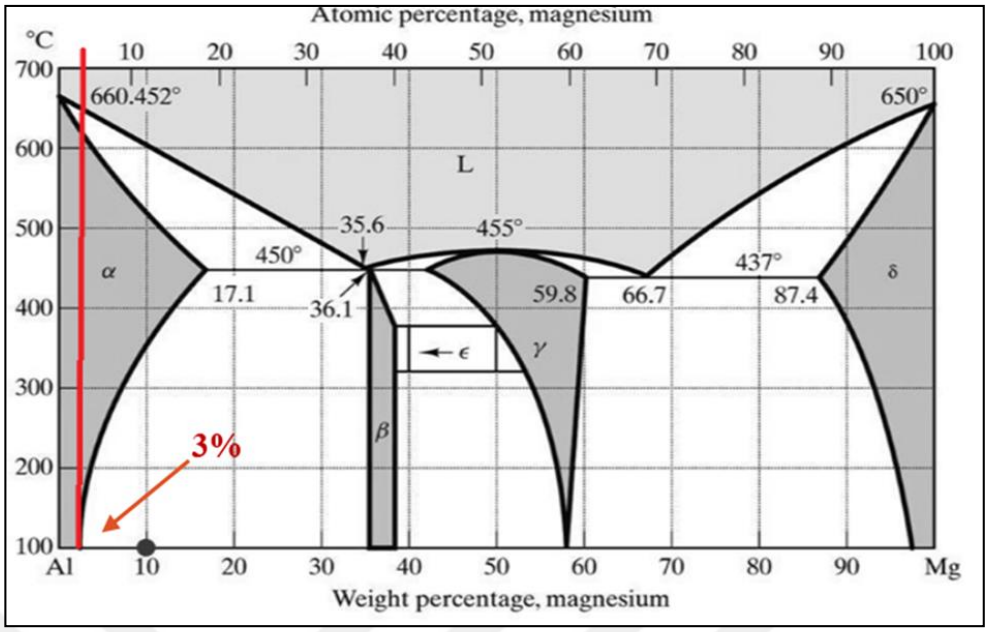


Figure 7.1. Mg-Al phase diagram [133].

In alloys containing more than 2% by weight aluminum, a number of eutectic phases are usually formed depending on the cooling rates. Therefore, a significant amount of eutectic phase formation is observed in magnesium alloys such as AZ31, AM50, AM60 and AZ91. The eutectic six magnesium-aluminum alloys have a wide range depending on the composition and cooling rate. [134].

### 7.4.2. Effect of Iron

The presence of small amounts of magnesium alloys is one of the elements that significantly reduce corrosion resistance. In commercially important magnesium alloys, the iron content should generally be in the range of 0.01 to 0.03 wt%. For best corrosion resistance, the upper limit of iron content in the alloy should be 0.005% [126].

### 7.4.3. Effect of Manganese

Manganese has a significant effect on the tensile strength of magnesium alloys and increases the yield strength. The most important feature of manganese in the alloy is the formation of second phase particles such as Al and Fe and AlMnFe, reducing the

iron content and increasing the corrosion resistance due to this reduction. Commercially important magnesium alloys rarely contain more than 1.5% by weight of manganese. The solubility of manganese in Mg-Al alloys can be as low as 0.3% by weight. [132].

### 7.4.4. Effect of Zinc

When magnesium is used as alloying element with aluminum in zinc alloys, its effect is high. Zinc, when used in conjunction with aluminum at low temperatures (room temperature) provides increased strength. In addition, the use of zinc with aluminum is also used to increase strength without reduction in ductility. Adding more than 1% by weight of zinc to magnesium alloys containing from 7 to 10% by weight of aluminum increases the tensile strength at high temperatures. Zinc is also used for the purpose of preventing the harmful corrosion effect of nickel and iron impurities [133].

### 7.4.5. The Effect of Zirconium

Because the lattice parameter of magnesium (a = 0.320 nm, c = 0.520 nm) is very close to the lattice parameter (a = 0.323 nm, c = 0.514 nm) of zirconium, there is a significant grain refinement effect in the magnesium alloys of zirconium. During the beginning of the solidification, the rich zirconium solid particles provide heterogeneous nucleation during the solidification of the magnesium grains. In aluminum or manganese-containing alloys, zirconium is generally not used because the zirconium solid moves away from the melt and forms a stable compound with these elements. [134].

### 7.4.6. Effect of Copper

In magnesium alloys, when the copper is added more than 0.05% by weight, the corrosion resistance is negatively affected. Copper has a limited solubility in magnesium. The copper added to the magnesium was observed to increase its

strength at room temperature and at high temperatures, but the ductility property was compromised. [126].

### 7.4.7. Effect of Nickel

Nickel is one of the impurities in magnesium alloys that significantly reduces the corrosion resistance. However, up to 0.005 wt% of nickel elements are allowed to provide the best resistance to corrosion in magnesium alloys. [135].

### 7.4.8. The Effect of Rare Earth Elements

Magnesium alloys, rare earth elements with creep and corrosion resistance are added to increase the strength at high temperatures. However, these elements are generally used for advanced technology alloys because they are as expensive as possible. The presence of these elements in the alloy accelerates the solidification of the alloy, resulting in less porous structure and prevents welding cracking [133].

## 7.5. APPLICATIONS OF MAGNESIUM AND ITS ALLOYS

### 7.5.1. Automotive Industry

The aim of the automotive industry worldwide is to produce light, environmentally friendly, safe and cheap vehicles. Vehicle manufacturers aim to reduce vehicle weights by taking into account user requests and decisions made for environmental health and to reduce harmful exhaust gases from vehicles. As it is known, the fuel consumption increases as the vehicle weight increases, as the fuel consumption increases and the CO2 emission of the vehicles increases. High-strength steels, aluminum alloys and composite materials are used by automotive companies to reduce vehicle weight, but there is no targeted reduction in vehicle weight with such materials. Therefore, there has been a significant increase in the use of magnesium, especially in recent years due to its low density in the automotive industry. On the other hand, low fatigue resistance, creep resistance, flammability, low corrosion resistance and poor wear resistance affect the widespread use of magnesium [103].

Many researches have been carried out in the automotive industry on magnesium alloys. For example, Volkswagen used 22 kg of magnesium and its alloys in the Beetle model vehicle [136]. In 1928, Porsche used magnesium and its alloys in engine construction [132]. The lightest six-cylinder engine, weighing 161 kg, used Mg-Al alloy in the BMW R6 model. Mg-Al alloy Al material provided 24% light weight and low fuel consumption compared to used engine. Using the magnesium in the V8 Quattro model of the Audi V8, the weight of the other 8-cylinder engines is 5 kg [137]. Figure 7.2 shows the display panel, AZ31 12 kg if made of magnesium alloy and 18 kg if made of steel [138]. Figure 7.3 shows some car parts made from AZ31 alloy.

Figure 7.2. Examples of magnesium used doors [117].


Figure 7.3. Land Rover Dashboard and steering wheel produced from magnesium alloy [117].

### 7.5.2. Aerospace Industry

Magnesium has been used in aerospace industry, aircraft construction since the 1900s and has become widespread in 1950s. After 1950, a significant amount of

magnesium was used in the construction of military aircraft and aircraft. The Sikorsky S-56 model made by Westland Aircraft in 1950 used 115 kg of magnesium. 8600 kg of magnesium was used by the European aircraft industry in the construction of the Convair B-36 Peacemaker model. The use of magnesium in the aircraft industry has decreased since the 1990s, but the helicopter industry continues to use parts such as gearboxes and gearboxes [134]. Furthermore, the Technical Data Package (TVP) was prepared with the design of the ATAK helicopter's upper body (Figure 7.4) and the design parameters of the magnesium casting process and domestic design [137].

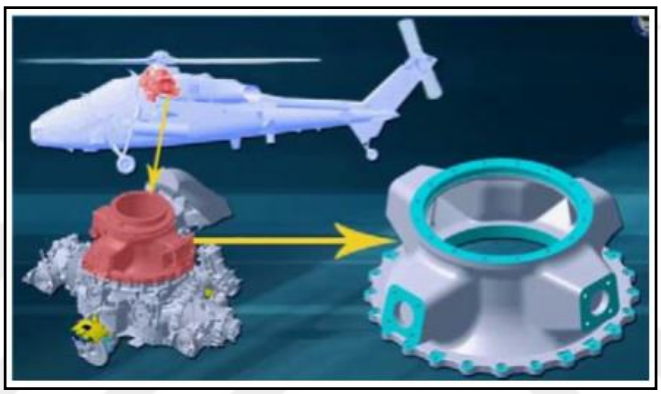

Figure 7.4. Upper body of ATAK helicopter gear box [137].

To summarize the use of magnesium in the aerospace industry: strength, low density, high shock and vibration resistance are the advantages of magnesium, but low temperatures and low corrosion resistance are the disadvantages of magnesium. Disadvantages of magnesium limit the use area, but the alloying with other metals and composite materials can be significantly increased when the composite material is made. [139].

### 7.5.3. Biomaterials Industry

Materials used to perform or support the functions of organs or tissues in the human body are called biomaterials. Metals, ceramics, polymers and composites are divided into 4 groups. The human body is a highly corrosive environment for materials used as biomaterials. Stainless steels, titanium and its alloys and chromium and cobalt

alloys are metallic biomaterials used today. These materials may be toxic ion or particles from corrosion or abrasion, leaking into the tissue and damaging the cells, which can lead to tissue loss. In addition, the compatibility of metallic biomaterials with the body structure shows that the elastic modules are not fully compatible with bone tissue. This incompatibility affects the speed of formation of new bone tissue and the stability of the implant. Furthermore, since the metallic materials such as plates, screws and nails used in the body are permanent and the tissue is healed, the removal of metals from the body by another operation increases the health expenses [139]. In addition to the low density of magnesium, it has a higher fracture toughness than other ceramic biomaterials (Table 7.7).

Table 7.7. Comparison of physical and mechanical properties of different biomaterials with natural bone [139].

| **Property** | **Bone** | **Magnesium** | **Titanium Alloys** | **Cr-Co Alloys** | **Stainless Steels** | **Synthetic Hydroxyapatite** |
|---|---|---|---|---|---|---|
| Density gr/cm3 | 1.8-2.1 | 1.74-2.0 | 4.4-4.5 | 8.3-9.2 | 7.9-8.1 | 3.1 |
| Elastisity, GPa | 3-20 | 41-45 | 110-117 | 230 | 189-205 | 73-117 |
| Yielding Strength, MPa | 130-180 | 65-100 | 758-1117 | 45-1000 | 170-310 | 600 |
| Fracture toughness, $MPam^{1/2}$ | 3-6 | 15-40 | 55-115 | - | 50-200 | 0.7 |

The yield strength and elasticity module is closer to the bone than other metallic materials. In addition, magnesium is the fourth most common action in the human body. An adult individual has approximately 30 g of magnesium in his body, the majority of which are located in the muscles and bones [139].

The magnesium element is non-toxic in the body and is easily soluble, and the soluble magnesium is spontaneously excreted from the body. In addition, the interface showing the compatibility of magnesium with bio-environment is shown in Figure 7.5. In addition, magnesium accelerates bone development. As a result,

magnesium and its alloys help the formation of new tissue within 20-90 days after implantation and after the formation of tissue, magnesium is dissolved in the body without any further surgery. The major disadvantage of using magnesium as a biomaterial is its low corrosion resistance. But in order to increase the corrosion resistance, the protective surface coating is made and can be used as a suitable biomaterial in the body [52].

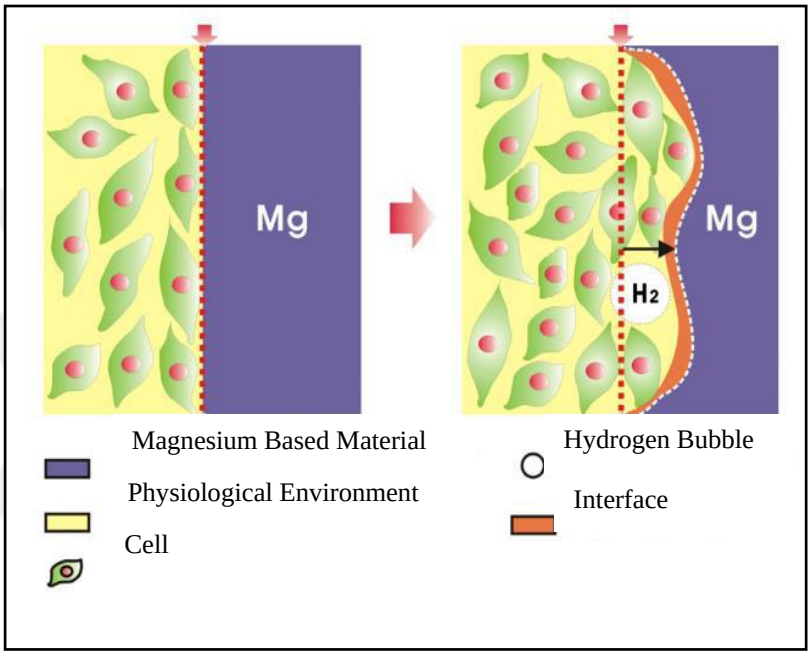


Figure 7.5. Dynamic interface between Mg-based materials and bio-environment during surface degradation [140].

# PART 8

## EXPERIMENTAL STUDIES

In this study, firstly, gas atomization unit was designed and manufactured in Karabük University Technology Faculty Manufacturing Engineering Department. In this gas atomization unit, production of AZ31 powder, which is magnesium alloy by gas atomization method from metal powder production methods, was chosen. The parameters used in the materials, which have similarity to AZ31 alloy as production parameters, are taken into consideration. Experimental studies were performed with three different temperatures (790, 820 and 850 °C), 4 different nozzle diameters (2, 3, 4 and 5 mm) and four different gas pressures (5, 15, 25 and 35 bar). Argon gas was used to atomize the liquid metal melt and create a protective gas atmosphere. In order to determine the shape of the AZ31 powders produced, the scanning electron microscope (SEM) was used, in addition, to determine the phases formed in the internal structures of the powders XRD, XRF and SEM-EDX analysis techniques were used and to determine the percentages of these phases, and the laser measurement device for powder size analysis method was used.

In order to determine the mechanical properties of the produced powders, hardness test and three-point bending test were performed. In addition, in order to determine the usability of the powders produced, rectangle shaped of 32 mm length, 13 mm width and 7 mm thickness samples were manufactured. For this purpose, samples prepared at 600 MPa pressing pressure in one-way press were subjected to be sintered at different temperatures (500, 550 and 600 °C). Pre and post sintering densities of the prepared samples were determined and the percentage of the pores in samples were determined approximately.

## 8.1. GAS ATOMIZATION UNIT

Experimental studies were carried out at the Gas Atomization Unit at Karabük University, Manufacturing Engineering Department of Technology Faculty. The Gas Atomization Unit shown in Figure 8.1. consists of seven basic parts:

1. Melting furnace
2. Atomization tower
3. Nozzle and nozzle holder
4. Powder collection unit
5. Gas system
6. Cyclones
7. Control panel

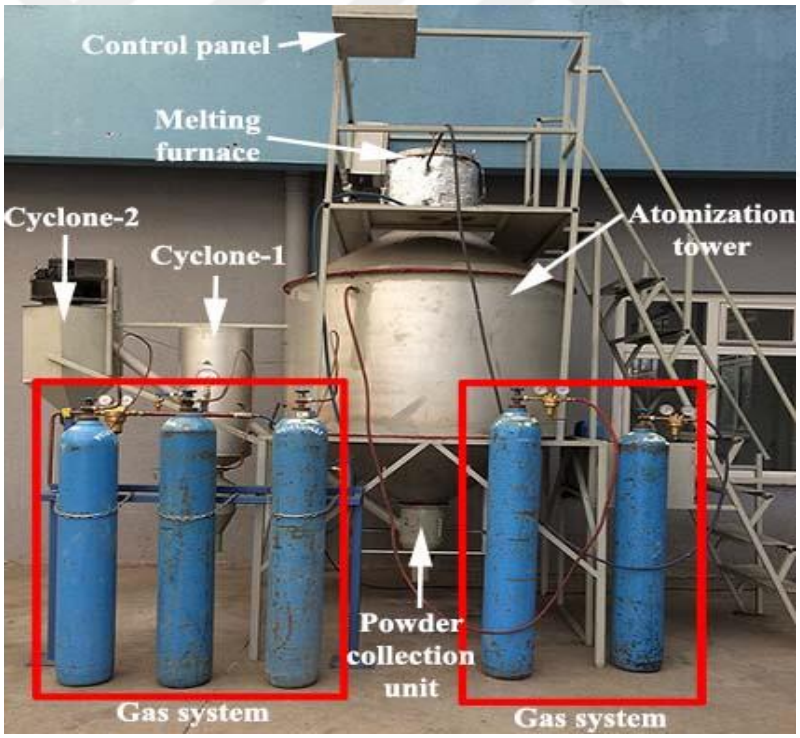


Figure 8.1. Gas atomization unit

The melting furnace is designed and manufactured to operate continuously at approximately 1200 °C. During the melting, gas inlet and outlet units are placed on the side of the melting furnace in order to form a protective gas to prevent the

formation of oxide while and after the atomization. In order to control the flow of the melted metal in the ladle (Figure 8.2b), the worm screw system and the graphite stopper were used. The melting furnace is shown in Figure 8.2.a.

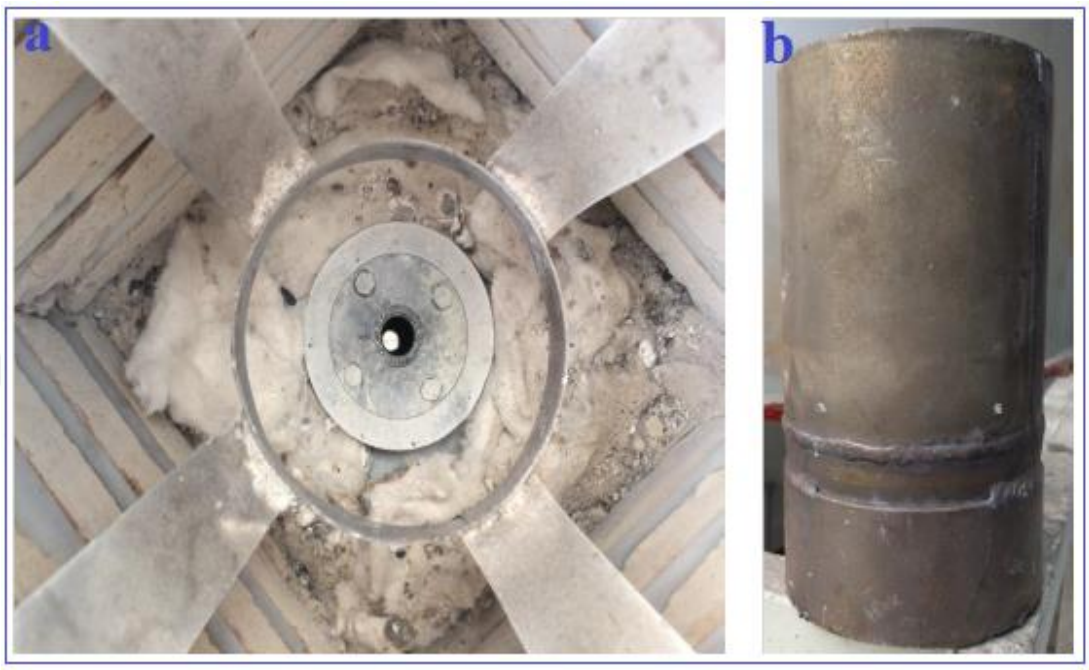


Figure 8.2. (a) Image of the interior of the melting furnace, (b) Melting pot.

Magnesium alloy AZ31 has a melting temperature of 620 °C. The casting temperature of the materials ranges between 150 and 200 °C above of melting temperature. For this reason, a minimum of 790 °C, a maximum of 850 °C and an average values of temperatures are taken as 820 °C. The liquid metal was heated for one hour after reaching the required temperature, and the graphite plug with the helical screw system was manually turned up and the metal flow was ensured. During the metal melting process, argon gas was released at low pressure (about 2 bar) in the furnace to protect the dissolved metal against the occurance of oxidation and combustion reaction.

The atomization tower of the Gas Atomization Unit is shown in Figure 8.3. The produced powders are collected in the powder collector located at the bottom of the atomization tower.

Figure 8.3. Atomization tower.

In order to atomize the liquid metal, a closely coupled supersonic nozzle holder with a circular hole is used which is shown in Figure 8.4a. Nozzle holder and nozzles are made of stainless steel.

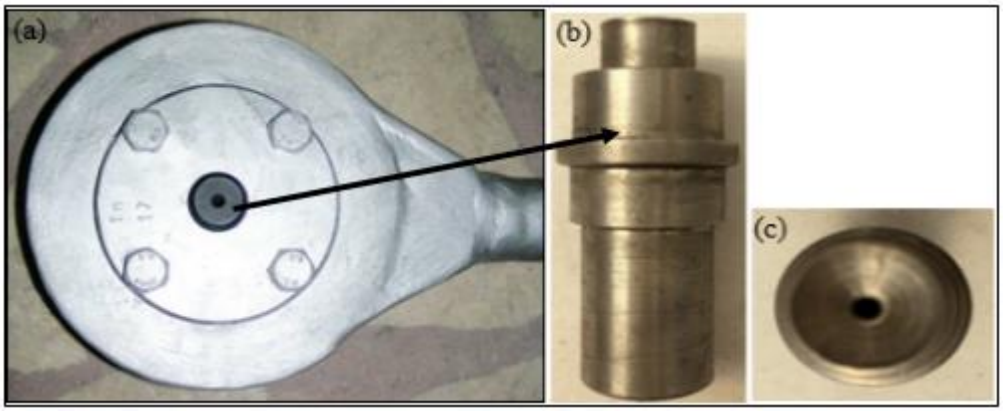


Figure 8.4. (a) Nozzle holder and Nozzle, (b) Front view, (c) Top view.

The nozzle (Figure 8.4. a and b) is placed on the nozzle holder in the furnace. Four different nozzles with diameters of 2, 3, 4 and 5 mm were used. In closely matched systems, the heating of the nozzle is extremely important. If the nozzle is not heated sufficiently, the temperature of the melt metal at the nozzle end will decrease and the flow of liquid metal flow will slow down [60]. Therefore, the nozzle holder and nozzle used in this study were placed inside of the melting furnace and the solidification of the liquid metal in the nozzle was prevented.

The produced powders are collected in the lower part of the atomization tower and in the lower part of the two cyclones connected in parallel to the powder collection unit (Figure 8.5).

Figure 8.5. Powder collection unit.

The powder collector and cyclones are made of stainless steel. The powder collector is cylindrical, 400 mm high and 300 mm in diameter. And the cyclones are made of with a cylindrical height of 800 mm and a diameter of 400 mm. After each experiment, the inside of the atomizing device and the cyclones were cleaned. The produced powders were stored in desiccators to prevent oxidation.

In the experiment, an argon pressure tube having an operating pressure of 200 bar was used as the atomizing gas. Three argon tubes are connected to the gas ramp to prevent gas pressure fluctuations when the gas pressure in the tube drops during the atomization process (Figure 8.6). After the atomization process begins, the pressure reading in the gauge is considered to be the gas pressure. Figure 8.7 shows the pressure gauge used during the atomization process. Argon gas is used as the atomizing gas. The tests were carried out at 5, 15, 25 and 35 bar pressures.

Figure 8.6. Argon gas system.

Figure 8.7. Manometer.

Two cyclones connected in parallel with each other were used to evacuate the gas used in the atomization tower and to maintain fine powder. The image of the cyclones is shown in Figure 8.8. In addition, a powder removal fan is used to remove fine powder. The power of the powder removal fan is 2500 rpm. The first production which is called the roughest powders fall into the powder collector. Second, the

average size of powder falls to the center. Finally, the finest powders fall through the powder fan to the last cyclone.

Figure 8.8. Cyclones.

## 8.2. ATOMIZATION PROCESS

Gas-atomized AZ31 powder was produced using a closely matched circular perforated supersonic nozzle system during operation in a gas atomization device. During the atomization work, the liquid was superheated at AZ31 melting temperature (620 °C). The operations performed during the atomization work are listed below.

1. First, nozzle holder for the test was placed at the bottom of the furnace.
2. The nozzle used in the experiment was placed in the nozzle holder to provide flow between the pot and the nozzle holder.
3. The stainless-steel pot was placed on the nozzle in the furnace.
4. The furnace top cover is closed. A graphite plug having a stainless-steel annular thread system that controls the flow of molten metal when the lid is closed is mounted in a manner to provide a seal for the center of the pot in the furnace.
5. During the metal melting process, argon gas is flown into the furnace at a low pressure (about 2 bar) to protect the molten metal from the onset of oxidation and combustion reactions.

6. About 50 g of AZ31 material in the form of ingot was used for each test, the AZ31 material was heated to 790 for one hour. The temperature of the melted material was measured by means of two thermocouples which were immersed into the stainless pot and were located outside the pot.
7. Argon gas was given at low pressures within the atomization tower for 15 minutes before the atomization process to prevent the produced powders from reacting with air.
8. The atomization gas pressure was adjusted to the desired pressure with manometer and gas was sent to the nozzle.
9. It is ensured that the molten AZ31 alloy is flowing and atomized by argon gas by turning up the graphite plug with worm screw system. After the metal flow was completed, the gas flow was stopped and the atomization process was completed.
10. Powder collected in powder collector and cyclones are stocked in desiccators. The powder collector, cyclones and atomization tower were cleaned for the next test.

The installation of the unit was repeated, and the above listed procedures were repeated for a new test. The basic principle of gas atomization and powder production is given in Figure 8.9.

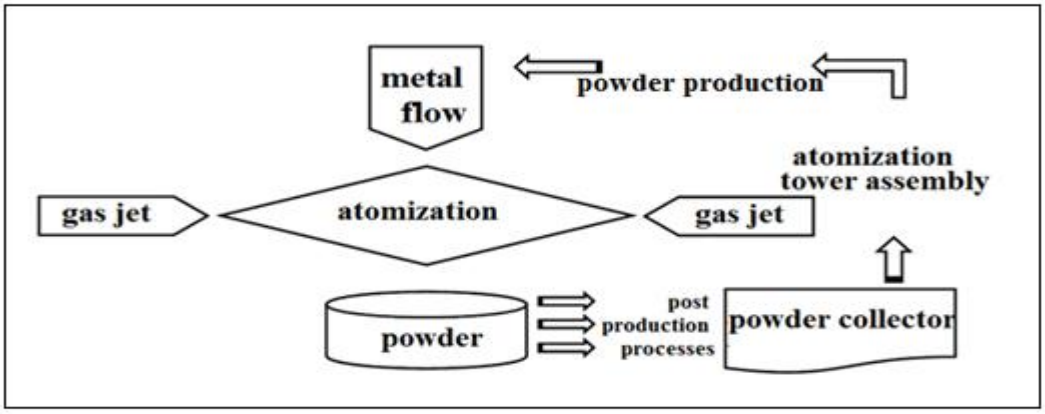


Figure 8.9. Gas atomization flow chart.

The atomization parameters of the AZ31 powders produced by the gas atomization method are given in Table 8.1.

Table 8.1. Powder production parameters.

| Sample No | Melting metal temperature Cº | Nozzle diameter mm | Gas pressure bar |
|---|---|---|---|
| 1 | 790 | 2 | 5 |
| 2 | | | 15 |
| 3 | | | 25 |
| 4 | | | 35 |
| 5 | | 3 | 5 |
| 6 | | | 15 |
| 7 | | | 25 |
| 8 | | | 35 |
| 9 | | 4 | 5 |
| 10 | | | 15 |
| 11 | | | 25 |
| 12 | | | 35 |
| 13 | | 5 | 5 |
| 14 | | | 15 |
| 15 | | | 25 |
| 16 | | | 35 |
| 17 | 820 | 2 | 5 |
| 18 | | | 15 |
| 19 | | | 25 |
| 20 | | | 35 |
| 21 | | 3 | 5 |
| 22 | | | 15 |
| 23 | | | 25 |
| 24 | | | 35 |
| 25 | | 4 | 5 |
| 26 | | | 15 |
| 27 | | | 25 |
| 28 | | | 35 |
| 29 | | 5 | 5 |
| 30 | | | 15 |
| 31 | | | 25 |
| 32 | | | 35 |
| 33 | 850 | 2 | 5 |
| 34 | | | 15 |
| 35 | | | 25 |
| 36 | | | 35 |
| 37 | | 3 | 5 |
| 38 | | | 15 |
| 39 | | | 25 |
| 40 | | | 35 |
| 41 | | 4 | 5 |
| 42 | | | 15 |
| 43 | | | 25 |
| 44 | | | 35 |
| 45 | | 5 | 5 |
| 46 | | | 15 |
| 47 | | | 25 |
| 48 | | | 35 |

Number of samples were 4*4*3=48 samples

4 = variable of nozzle → (2, 3, 4, 5) mm

4= variable of pressure → (5, 15, 25, 35) bar

3 = variable of temperature → (790, 820, 850) ºC

As in production of powder alloys with the changing of nozzle diameter and different gas pressure with different temperature, then powder particle size distributions were made by sieve method which is the easiest and most widely used analysis method. The size analysis of the powders was done by vibratory sieve analyzer. The sieve analyzer is given in Figure 8.10. The device can measure powder sizes between 45-1000 μm. The size of AZ31 alloy powders were determined by using sieves in 8 hole in sizes of 45 μm, 63 μm, 90 μm, 125 μm, 250 μm, 500 μm, 710 μm and 1000 μm, respectively.

Figure 8.10. Sieve Analyzer

The particle size distribution of the powders was determined with the sieve analyzer located in Manufacturing Engineering Laboratory of Karabuk University.

## 8.3. ANALYSIS OF ATOMIZED POWDER

Powder size analyzes were performed with the Mastersizer 3000 model device in Bartın University Central Research Laboratory. The principle of operation of the device is the red and blue laser light on the sample. The laser light reflected from the sample and broken rays are examined by detectors. The angle and intensity of the scattered light determine the particle size distribution of the sample. Pure water was used as a vector medium during measurements. The scattering angle of the laser light passing through the particle depends on the size of the particle. With low particle size, the scattering angle increases logarithmically. The dispersion angles of the large particles are low, the intensity of the scattered laser light is high. In small particles, the dispersion angle is high and the intensity of the scattered laser light is low.

The SEM images and the EDX analysis of the AZ31 alloy powder were obtained from the Carl Zeiss Ultra Plus Gemini Fesem SEM (Figure 8.11) at the Iron and Steel Research Institute of Karabuk University. For the SEM images, the powders were placed on "carbon tape" and covered with gold


Figure 8.11. SEM analysis device.

The XRD measurements of the powders were performed with the RIGAKU - Ultima IV model device as seen in Figure 8.12. XRF measurements were taken with the help of RIGAKU ZSX Primus II model device (Figure 8.13). The measurements were carried out at the Karabük University Iron and Steel Research Laboratories. X-ray diffraction (XRD) is a method used to study the crystalline atomic and molecular structure. X-ray Fluorescence (XRF) spectroscopy provides the opportunity to determine the elemental composition.


Figure 8.12. RIGAKU - Ultima IV XRD analyzer.


Figure 8.13. RIGAKU ZSX Primus II XRF analyzer.

## 8.4. PRODUCTION OF THE BULK MATERIALS

### 8.4.1. Mixing Powders

The powders produced by the gas atomization method are mixed for 60 minutes. The powders produced by the gas atomization method were sieved and the powders below 100 μm were selected. An overview of the powders mixed in three-dimensional turbula for 60 minutes is given in Figure 8.14.

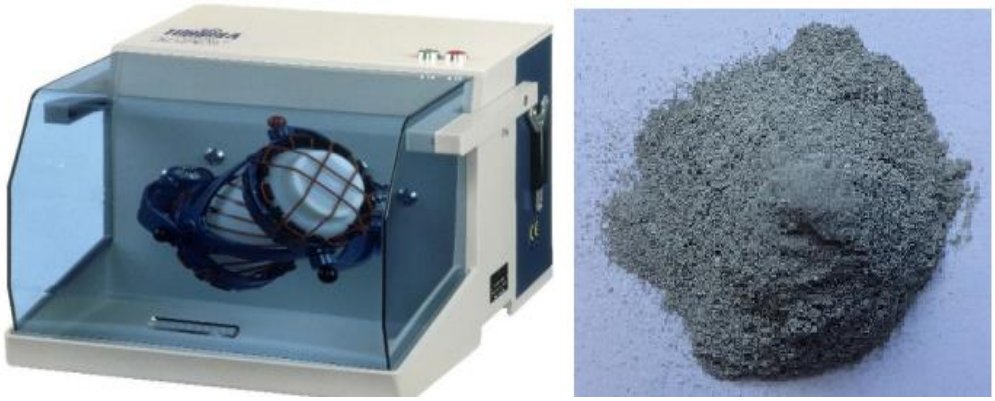

Figure 8.14. General views of three-dimensional turbula AZ31 powders.

### 8.4.2. Powders Pressing

The powders produced in different parameters and then mixed in the turbulent were subjected to pressing. The pressing process was carried out with HALIM USTA HIDROLIKSAN brand in Karabuk University Central Research Laboratory (Figure 8.15). In the pressing process, a triangle mold with a dimension of 30*13*7 mm was used as a die. Approximately 4.7 grams of powder was applied to each sample and pressed. 600 MPa were applied as the pressing pressure. Figure 8.16 shows the appearance of the raw material which is converted to raw mass at different pressures.


Figure 8.15. The pressing machine that is HALIM USTA HIDROLIKSAN branded.

Figure 8.16. General view of pressed powders.

### 8.4.3. Sintering of Powders

The sintering process of the powders were carried out with an atmosphere-controlled heat treatment furnace (PTF 16/80/610) (Figure 8.17) at the Karabuk University Iron and Steel Institute Research Laboratories.

Figure 8.17. Atmosphere controlled heat treatment furnace (PTF 16/80/610).

The powders were pressed and massed at pressures 600 MPa and sintered under atmosphere controlled furnace at three different temperatures (500, 550 and 600 °C)

for two hours. The sintering process was completed in a total of 180 minutes. In order to expel the wastes, temperature were raised to 500, 550 and 600 °C. Sintering temperatures were kept at a constant temperature for 120 minutes, the cooling to room temperature up to 180 minutes were carried out under atmospheric control.

### 8.4.4. Density Measurement

Sintered and post-sintered densities were measured to determine the optimum compressibility and sinterability of samples which are pressed at 600 MPa and sintered at different temperatures (500, 550 and 600 C). Pre-sintering and post-sintering density values were measured separately for each sample. The densities was calculated by the ratio of the weight (m) to the volume (v) of the sample produced (m/v). After these processes, the relative densities (% density) of the samples were determined. Relative densities are calculated by the ratio of the produced sample's density to the original density.

### 8.4.5. Hardness Measurement

The hardness measurements of AZ31 alloy produced after sintering at 600 MPa and different temperature (500,550,600) °C were made using the SHIMADZU brand HMV-G21 model micro hardness measuring device under HV0,5 (Figure 8.18). The purpose of obtaining hardness from produced samples is to compare the effect of temperature on the hardness of the samples.

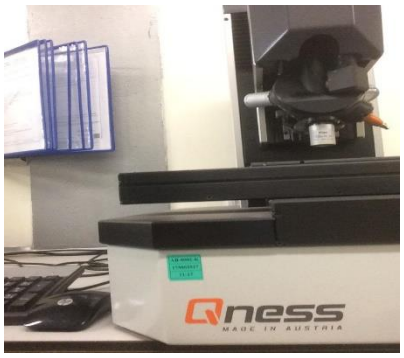


Figure 8.18. Qness model microhardness measuring device.

### 8.4.6. Three Point Bend Test

To determine the impurity toughness three-point bending test was performed in the universal traction device with a capacity of KN at ASTM B528-83a standard at a crosshead speed of 1 mm/min. 32mm×13mm×7mm specimens were used for point bending test. Figure 8.19 shows a three point bending test device.


Figure 8.19 ASTM B528-83a standard three point bending test device.

# PART 9

# EXPERIMENTAL RESULTS AND DISCUSSION

In this chapter; different temperature, different nozzle diameter and different gas pressures, powder size and shape, density, hardness, bending, microstructure, compressibility and sinterability properties of AZ31 powders are discussed.

## 9.1. POWDER SIZE ANALYSIS

The results of the analysis obtained from the Mastersizer 3000 laser size analyzer include Dv (10), Dv (50) Dv (90), specific surface area, D [3; 2], D [4; 3] cumulative percentage values of the produced powders. In addition, powder size distribution (frequency) and cumulative percentage curves are given.

Dv (10), Dv (50) and Dv (90) dimensions and specific surface areas, changes in atomization temperature, atomization gas pressure and nozzle diameter (as obtained from atomization unit) of powders produced at different temperatures (7790, 820 and 850 ° C are given in Table 9.1.According to the results given in Table 9.1, it is seen that powder size decreases with increasing gas pressure and powder size increases with increasing nozzle diameter. It is understood that an increase in atomization temperature from 790 °C to 850 °C resulted in an increase in powder size. In addition, powder dimensional changes of powders produced at 820 °C temperature, 2 mm nozzle diameter and 5, 15, 25 and 35 bar gas pressure are shown in Figure 9.1. as an example of the study.

Table 9.1. Particle size of AZ31 powders.

| Atomisation Temperature °C | Nozzle Diameter (mm) | Gas Pressure bar | $D_v$ (10) µm | $D_v$ (50) µm | $D_v$ (90) µm | Specific Surface Area m²/kg |
|---|---|---|---|---|---|---|
| 790 | 2 | 5 | 174 | 433 | 878 | 18.46 |
| | | 15 | 73.9 | 126 | 441 | 43.19 |
| | | 25 | 36 | 86.6 | 267 | 84.58 |
| | | 35 | 18.1 | 46 | 99.2 | 186.7 |
| | 3 | 5 | 136 | 388 | 847 | 22.09 |
| | | 15 | 53.9 | 140 | 367 | 58.98 |
| | | 25 | 44.7 | 118 | 330 | 68.51 |
| | | 35 | 28.1 | 66.1 | 146 | 117.8 |
| | 4 | 5 | 173 | 433 | 870 | 19.05 |
| | | 15 | 52.2 | 119 | 256 | 64.67 |
| | | 25 | 26.5 | 62.6 | 131 | 124.7 |
| | | 35 | 35.4 | 80.2 | 235 | 90.38 |
| | 5 | 5 | 227 | 519 | 1070 | 14.73 |
| | | 15 | 56.6 | 145 | 427 | 54.73 |
| | | 25 | 54 | 144 | 402 | 57.31 |
| | | 35 | 28.3 | 92.0 | 203 | 113.1 |
| 820 | 2 | 5 | 176 | 461 | 1050 | 17.82 |
| | | 15 | 41.8 | 133 | 287 | 70.73 |
| | | 25 | 25.9 | 98 | 211 | 119.5 |
| | | 35 | 31.2 | 79.1 | 201 | 101.6 |
| | 3 | 5 | 212 | 448 | 926 | 15.95 |
| | | 15 | 47.3 | 123 | 353 | 65.24 |
| | | 25 | 19.7 | 86.6 | 223 | 151.7 |
| | | 35 | 24.2 | 72.8 | 195 | 143.7 |
| | 4 | 5 | 93.3 | 400 | 1050 | 27.95 |
| | | 15 | 67.9 | 202 | 586 | 43.01 |
| | | 25 | 45.3 | 90.1 | 392 | 64.17 |
| | | 35 | 44.2 | 78 | 484 | 62.71 |
| | 5 | 5 | 65.1 | 401 | 773 | 41.97 |
| | | 15 | 68.6 | 194 | 526 | 44.05 |
| | | 25 | 24.5 | 93.8 | 263 | 127.8 |
| | | 35 | 32 | 92.8 | 255 | 94.98 |
| 850 | 2 | 5 | 167 | 327 | 906 | 19.15 |
| | | 15 | 57.5 | 166 | 450 | 52.53 |
| | | 25 | 22 | 104 | 378 | 169.2 |
| | | 35 | 21.6 | 84.6 | 252 | 143.7 |
| | 3 | 5 | 79.2 | 359 | 911 | 32.52 |
| | | 15 | 39.8 | 178 | 302 | 72.88 |
| | | 25 | 65.8 | 169 | 453 | 47.38 |
| | | 35 | 35 | 90.3 | 231 | 93.56 |
| | 4 | 5 | 100 | 383 | 984 | 27.89 |
| | | 15 | 56.9 | 176 | 367 | 56.51 |
| | | 25 | 25.8 | 150 | 230 | 124.6 |
| | | 35 | 26.7 | 78.8 | 232 | 124.5 |
| | 5 | 5 | 160 | 489 | 864 | 20.04 |
| | | 15 | 67.6 | 180 | 441 | 46.75 |
| | | 25 | 40.9 | 130 | 416 | 72.65 |
| | | 35 | 19.3 | 75.6 | 177 | 167.9 |

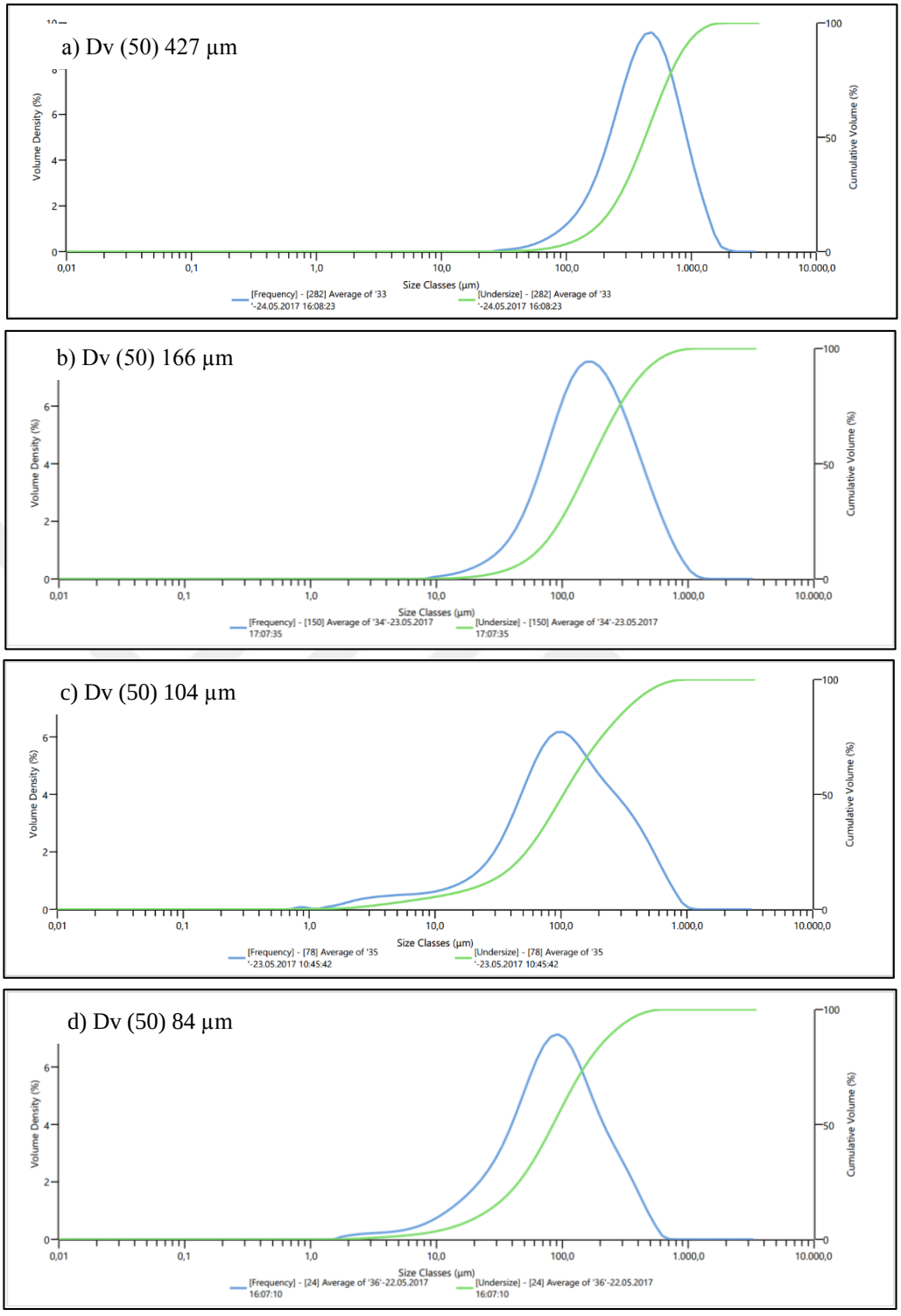


Figure 9.1. Dimensional changes of powders produced at 2 mm nozzle and 820 °C with variable pressure values, a) 5 bars, b) 15 bars, c) 25 bars, d) 35 bars.

As can be seen from Figure 9.1, the cumulative curve of the powder dimensions with the green line and the frequency values are given with the blue line. When Table 9.1 and Figure 9.1 are examined, it is seen that the powder size is significantly reduced

due to the increase in gas pressure. It is seen that the powder average size Dv (50) is 427 μm at 820 ° C atomization temperature, 2 mm nozzle diameter and 5 bar gas, by the atomization gas pressure is increased to 15 bar pressure average powder size Dv (50) value is 166 μm, 25 bar Dv (50) value of powders produced under pressure was determined as 104 μm and Dv (50) value of powders produced under pressure was determined as 84 μm. On the other hand, it has been observed that the powder size increases due to the increase in nozzle diameter. For example, when the average powder size of the powders which are produced at 790 °C atomization temperature, 35 bar gas pressure is examined (Table 9.1.) it is seen that the value is 46 μm at 2 mm nozzle diameter, 66.1 μm at 3 mm nozzle diameter, 80.2 μm at 4 mm nozzle diameter and finally 92.0 μm at 5 mm nozzle diameter. In addition, as shown in Table 9.1, the atomization temperature had a significant effect on the average size of the produced powders. For example, considering the 2 mm nozzle diameter and 35 bar atomization gas pressure; The average powder size obtained at 790 °C atomization temperature was 49 μm, 79.1 μm at 820 °C atomization temperature and 84.6 μm at 820 °C atomization temperature.

The effect of gas pressure and nozzle diameter on the size of powders produced at different atomization temperatures (790 °C, 820 °C, 850 °C) is given in Figure 9.2.

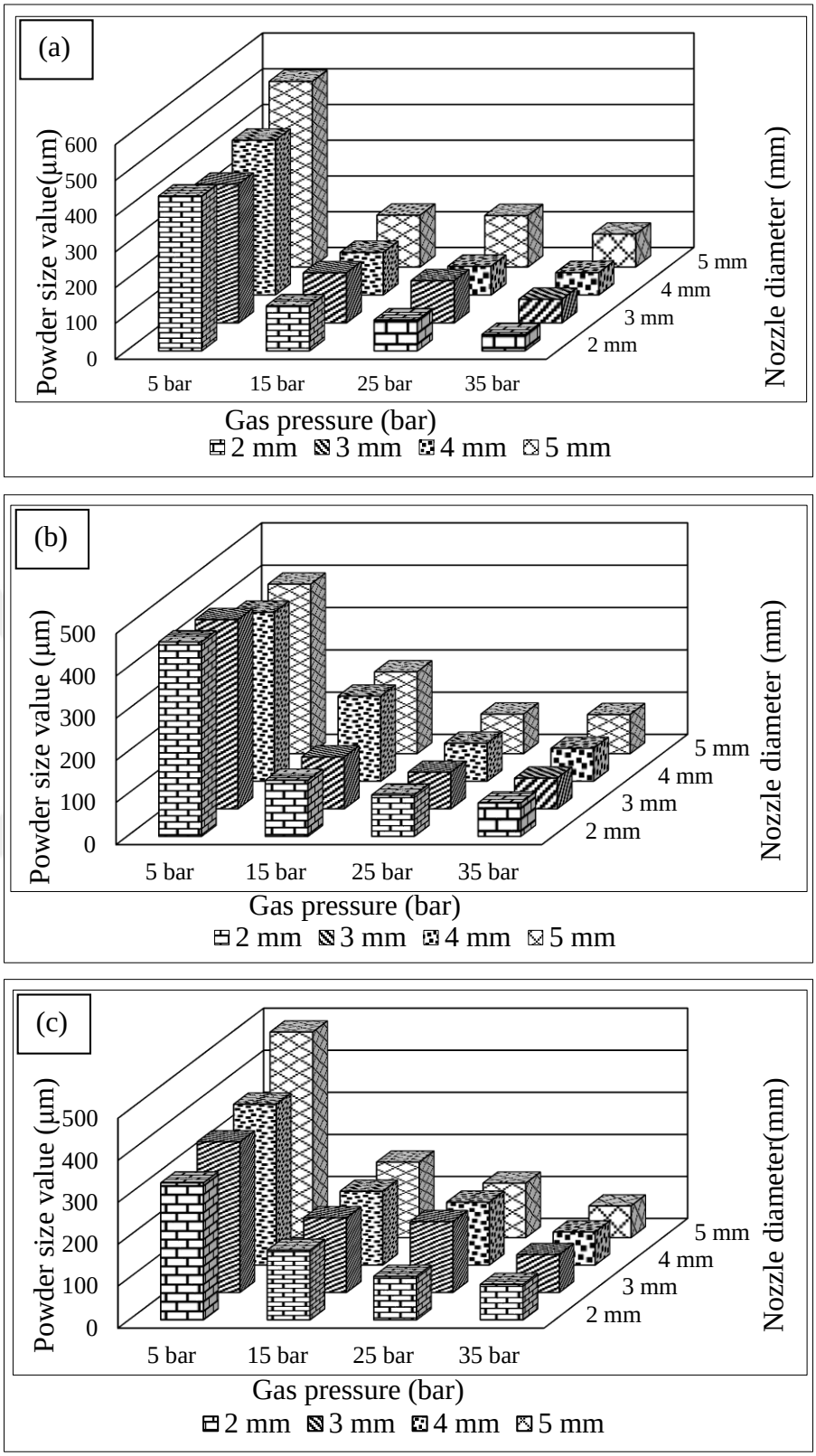


Figure 9.2. Effect of atomization gas pressure and nozzle diameter on powder size values of AZ31 powders produced at different atomization temperatures. a) 790 °C, b) 820 °C, c) 850 °C.

When the results given in Figure 9.2 are examined, it is seen that for the all temperature values the powder sizes decrease when the gas pressure is increased, and the powder sizes increase due to the increase in nozzle diameter. The reason of this; more energy is transferred to molten metal due to increased gas pressure and increased atomization effect resulted in smaller powder production. The reason for the decrease of the powder size with the decrease of the nozzle diameter is interpreted as the increase of the liquid metal flowing from the nozzle and the decrease of the energy per unit area on the molten metal.

It is known that gas pressure has a significant effect on powder size and shape in powder production by gas atomization method. In the experimental studies, the highest gas pressure value was taken as 35 bar. Above the highest pressure value, the powder production could not be performed due to the reverse effect (positive pressure) of the atomization gas on the nozzle which cause a blockage to the flow of the molten metal. Aydın and Ünal [52], in their studies on the effect of production variables on metal powder production, state that the liquid metal flow slows down if the pressure values at the end of the flow pipe are positive during the atomization process, while Gökmeşe and Bostan [141] state that the fluid flow stops in some cases. They also emphasized that the opposite direction of the flow feature. However, it has been observed that this situation does not exist below 35 bar gas pressure. In a study by Bayram et al. [142] on the effect of Pb during solidification of the AZ31 alloy, the nozzle under 30 bar gas pressure is also stressed that there is no back pressure. For example, a constant temperature of 850 °C, a nozzle diameter of 2 mm and the smallest average powder size at different gas pressures were obtained at a nozzle diameter of 2 mm and a gas pressure of 35 bar. While this value is 79.1 μm at 820 °C atomization temperature, it has the smallest value with 46 μm at 790 °C atomization temperature. In general, 10% of the powders produced for these variables are less than 21.6 μm, while 90% are less than 252 μm. It was determined that at least 10% of the produced powders consisted of powders below 10 μm. However, since these powders were sprayed into atomization towers and cyclones as well as into containers where the powders were stored, intake of these powders was not possible.

Figure 9.3 shows the effect of atomization gas pressure and nozzle diameter on specific surface areas of the produced powders at 790 °C.

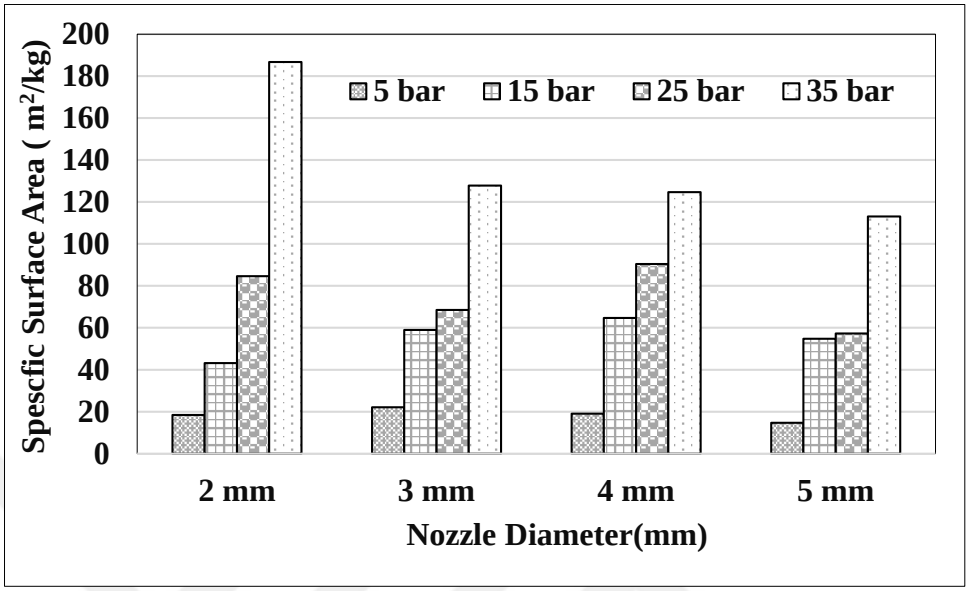


Figure 9.3. Relationship of gas pressure and nozzle diameter with specific area.

It is seen in Table 9.1 and Figure 9.3 that the specific surface areas of the produced powders increase due to the increase in gas pressure and decrease with the decrease of nozzle diameter. As is known, the specific surface areas of small powders are larger. For example, as shown in Figure 9.3, considering the atomization temperature of 770 °C and the nozzle diameter of 2 mm, the specific surface area of the powder produced at 5 bar gas pressure is 18.46 $m^2$/kg, while at 43.19 $m^2$/kg at 15 bar gas pressure and 84.58 $m^2$/kg at 25 bar gas pressure and 35 bar gas pressure is 186.70 $m^2$/kg. On the other hand, considering the atomization temperature of 790 °C and the gas pressure of 35 bar, it is seen that the specific surface areas vary significantly due to the increase in nozzle diameter. For example, with a atomization temperature of 790 °C and a gas pressure of 35 bar, the specific surface area with a 2 mm nozzle diameter was 186.7 $m^2$/kg, while the specific surface areas were 117.8 $m^2$/kg, 90.8 $m^2$/kg, respectively, when the nozzle diameter was increased to 3,4 and 5 mm, respectively and 113.1 $m^2$/kg. This results in the increase of gas pressure due to the decrease in the size of the dust and the increase in the diameter of the nozzle with the increase in the size of the powder gives the result. Aydın and Ünal [52] stated that

they encountered a similar result in their studies on “laval tipi yeni bir nozul tasarımı ile metal tozu üretimi ve üretim değişkenlerinin etkisinin incelenmesi”.

## 9.2. SEM-EDX ANALYSIS OF POWDER

As a result of the experiments carried out in the production of AZ31 powder by gas atomization method, the effect of gas pressure was clearly seen. It is also evident from the SEM images given in Figure 9.4 that the particle size of the produced powders decreases when the gas pressure increases.

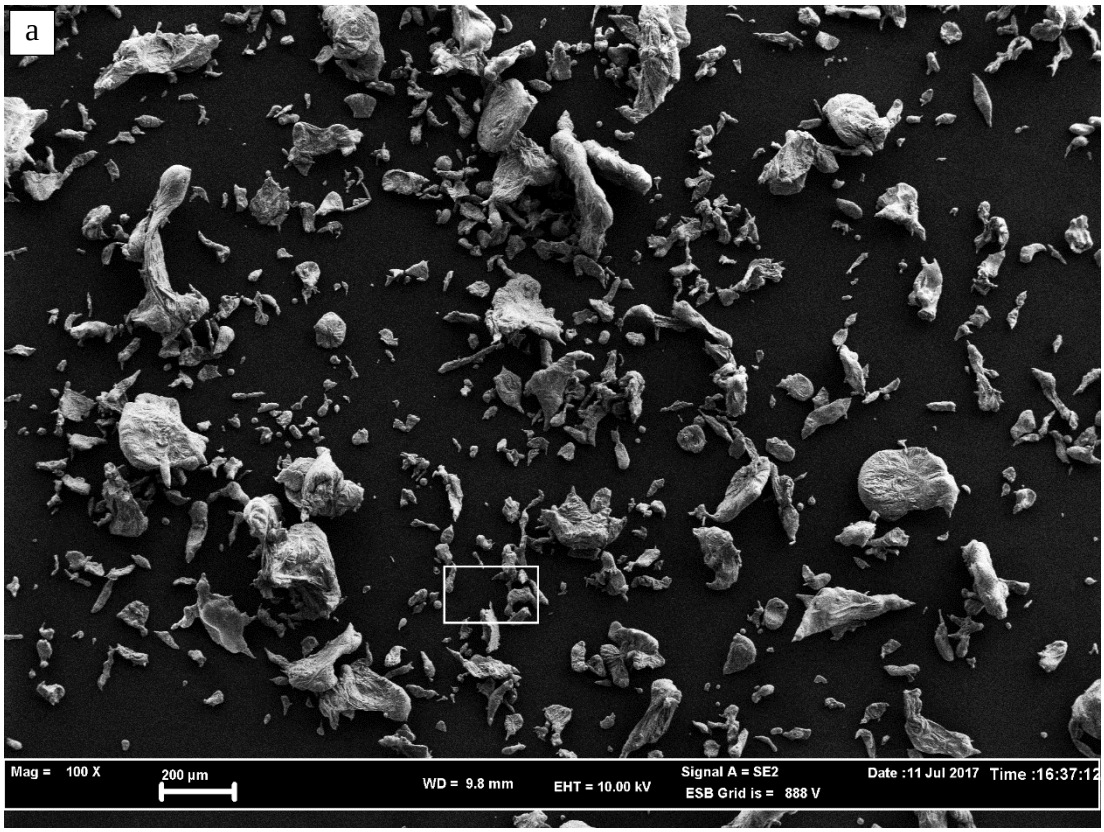

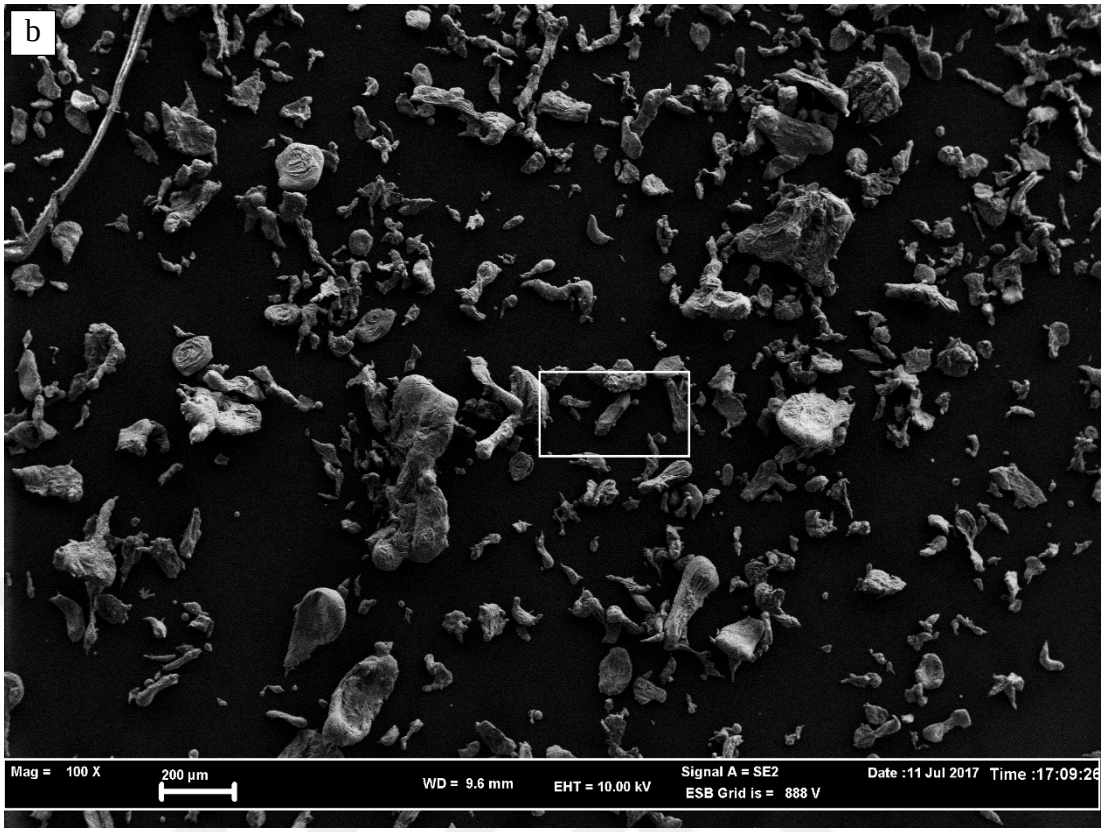
b
Mag = 100 X
200 µm
WD = 9.6 mm
EHT = 10.00 kV
Signal A = SE2
ESB Grid is = 888 V
Date :11 Jul 2017 Time :17:09:26

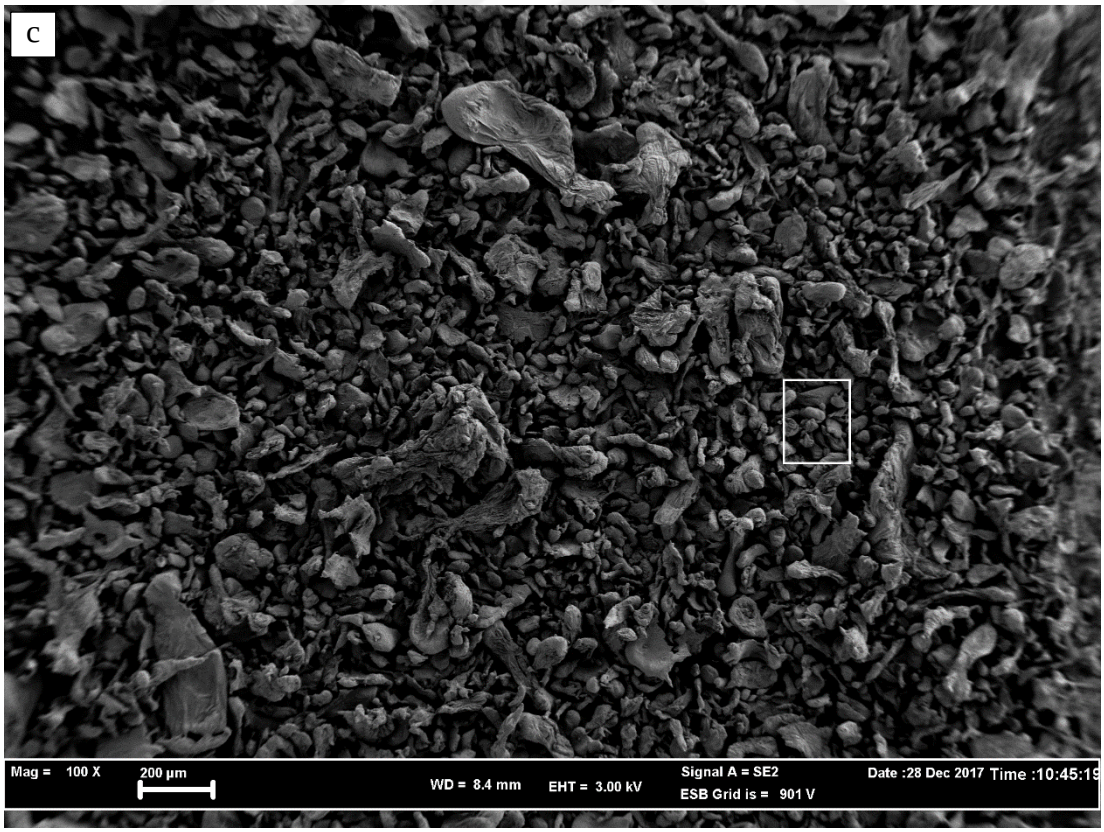
c
Mag = 100 X
200 µm
WD = 8.4 mm
EHT = 3.00 kV
Signal A = SE2
ESB Grid is = 901 V
Date :28 Dec 2017 Time :10:45:19

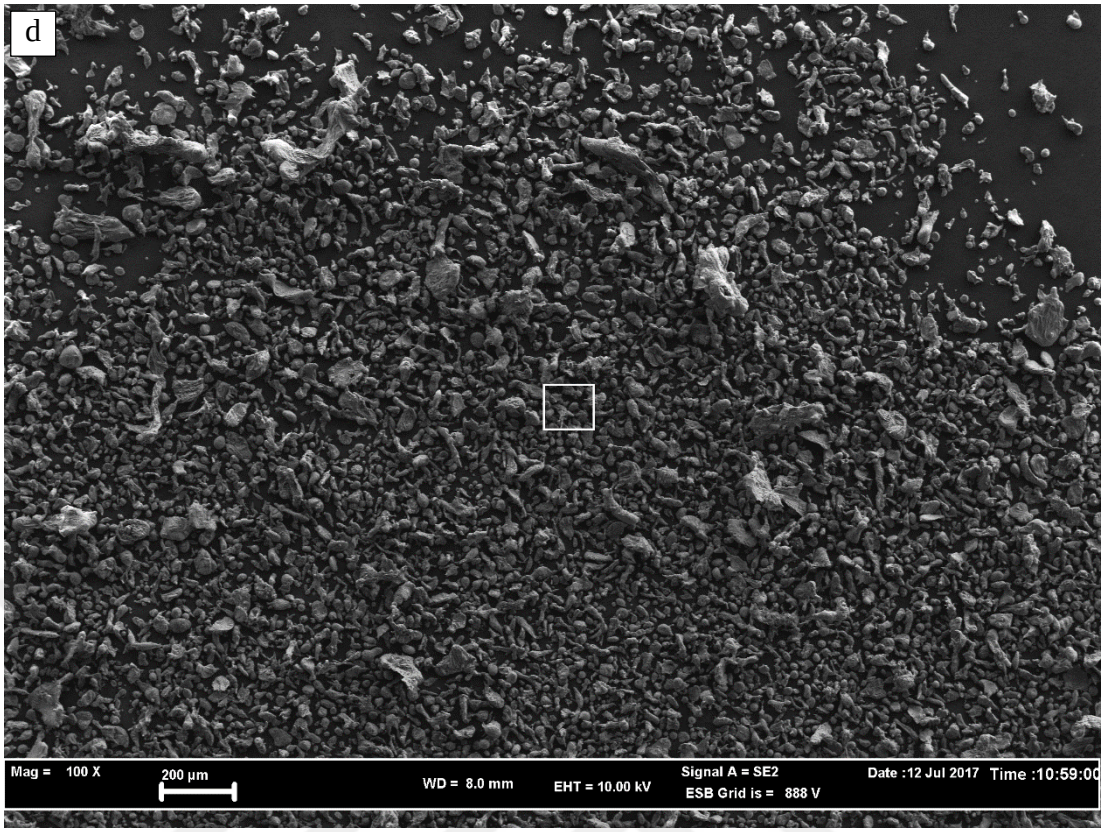


Figure 9.4. SEM images of powders produced at 2mm nozzle diameter, 790 $^{o}$C (100X) at different gas pressures (a) 5 bar, (b) 15 bar, (c) 25 bar, (d) 35 bars.

In the literature studies on this subject, it has been stated that the powder size decreases due to the increase in gas pressure [18,29,52,60,145]. Salord et al. [143] conducted experiments at 4, 9 and 14 bar gas pressures in the production of aluminum powder and determined the average powder size of the powder produced at 4 bar as 59 µm and the average powder size produced at 14 Bar as 44 µm. It is emphasized that the average powder size value is reduced in metal powder production since it provides higher energy transfer to molten metal with an increase pressure. It can be seen in Figure 9.4 that the average powder size is reduced due to the increase in gas pressure and the results obtained from this study is consistent with the literature. On the other hand, it is understood from Figure 9.5 that the powders produced are generally in the form of ligaments, droplets, rods, flakes and spheres.

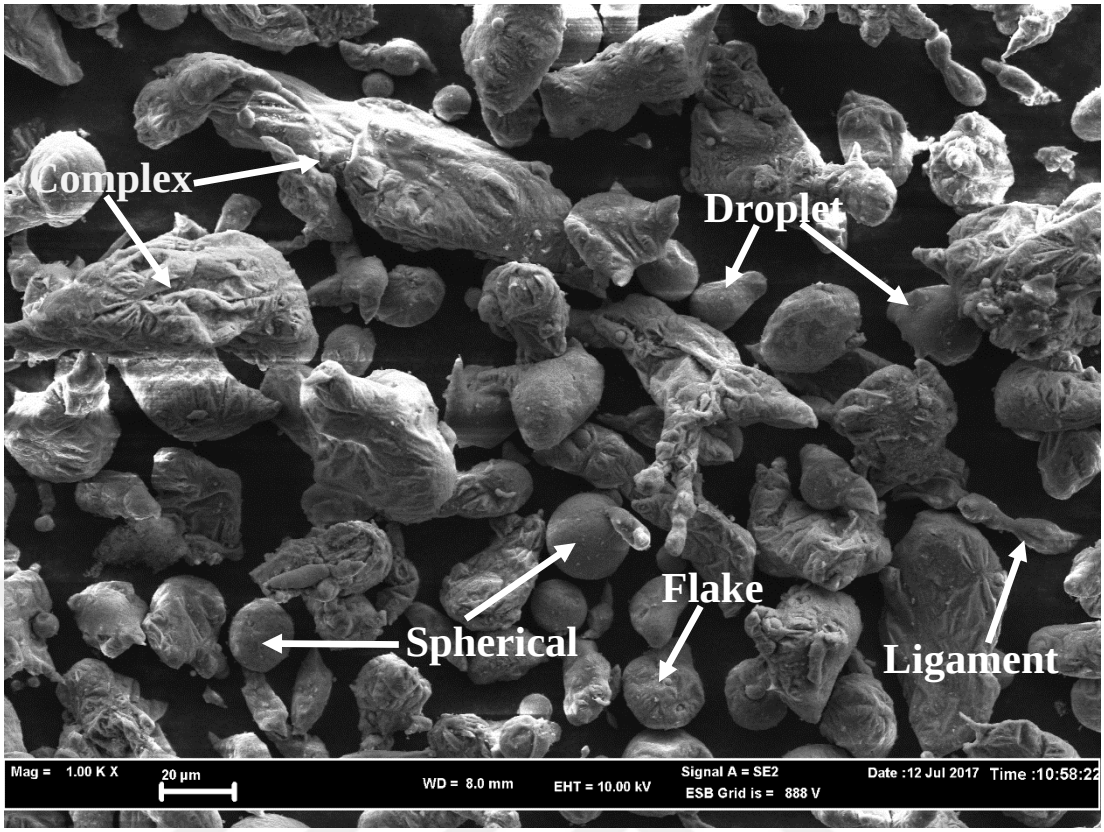


Figure 9.5. General SEM view of AZ31 powder produced at atomization temperature of 790 °C.

In the SEM images given in Figure 9.6, it is seen that the powder shape changes from ligament, rod and complex shape to flake, droplet and spherical due to the increase in gas pressure. It is seen that powder produced especially at 35 bar gas pressure and shrinks significantly and its shape is drip and spherical as it is seen in Figure 9.6. Fischmeister et al. [145] in their study on the solidification of gas atomized high-speed steels found that the most important parameter that forces a liquid droplet to globalize is surface tension. Figure 9.6a shows that a small proportion of the powders are spherical. The most important reason for this is thought to be the low atomization gas pressure and the insufficiency of the atomization tower. For the powder particles solidified by hitting the bottom of the atomization tower before they had time to sphericalize.

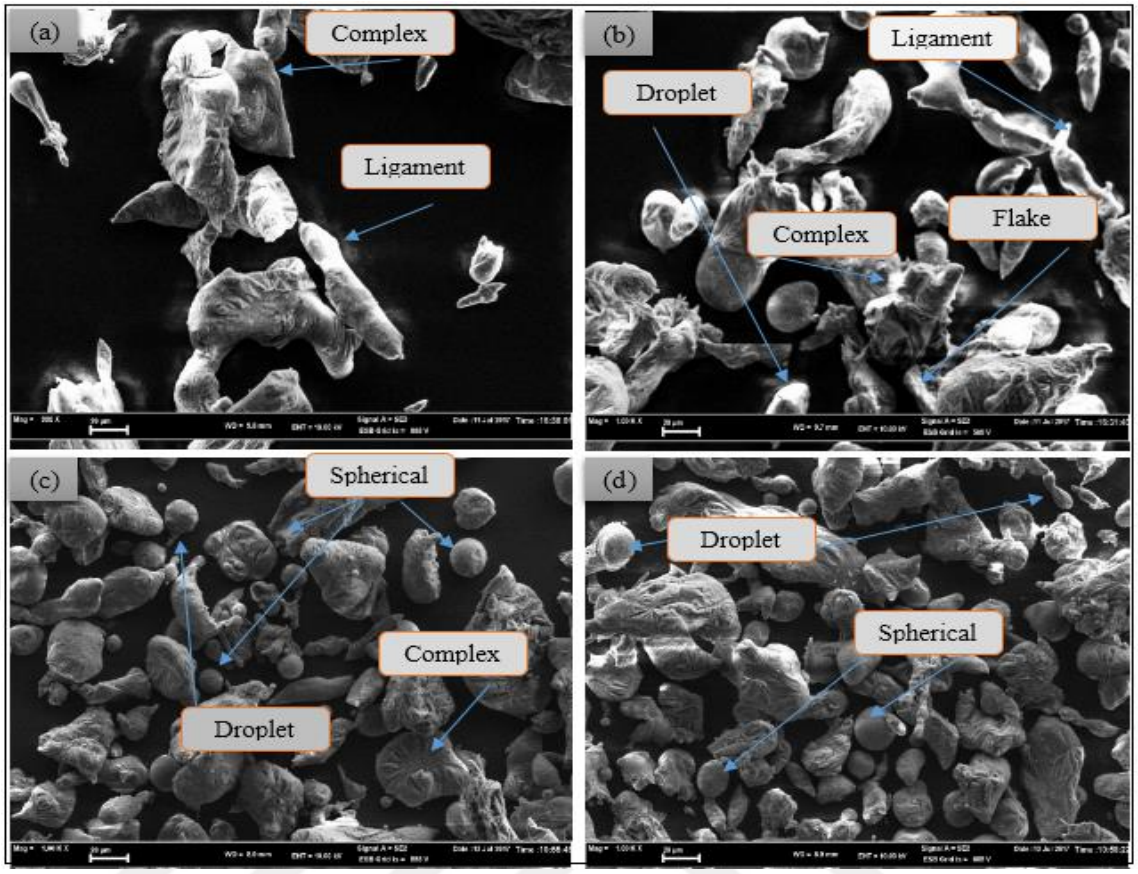


Figure 9.6. SEM images of the powders produced at 2mm, 790 ºC (1000X) at different gas pressures (a) 5 bar, b) 15 bar, c) 25 bar, d) 35 bars.

SEM images of AZ31 powders produced at atomization temperature of 820 ° C, nozzle diameter of 2 mm and atomization gas pressures of 5, 15, 25 and 35 bar are given in Figure 9.7. Figure 9.8 shows the change in shape and size of the powders produced due to the increase in nozzle diameter.

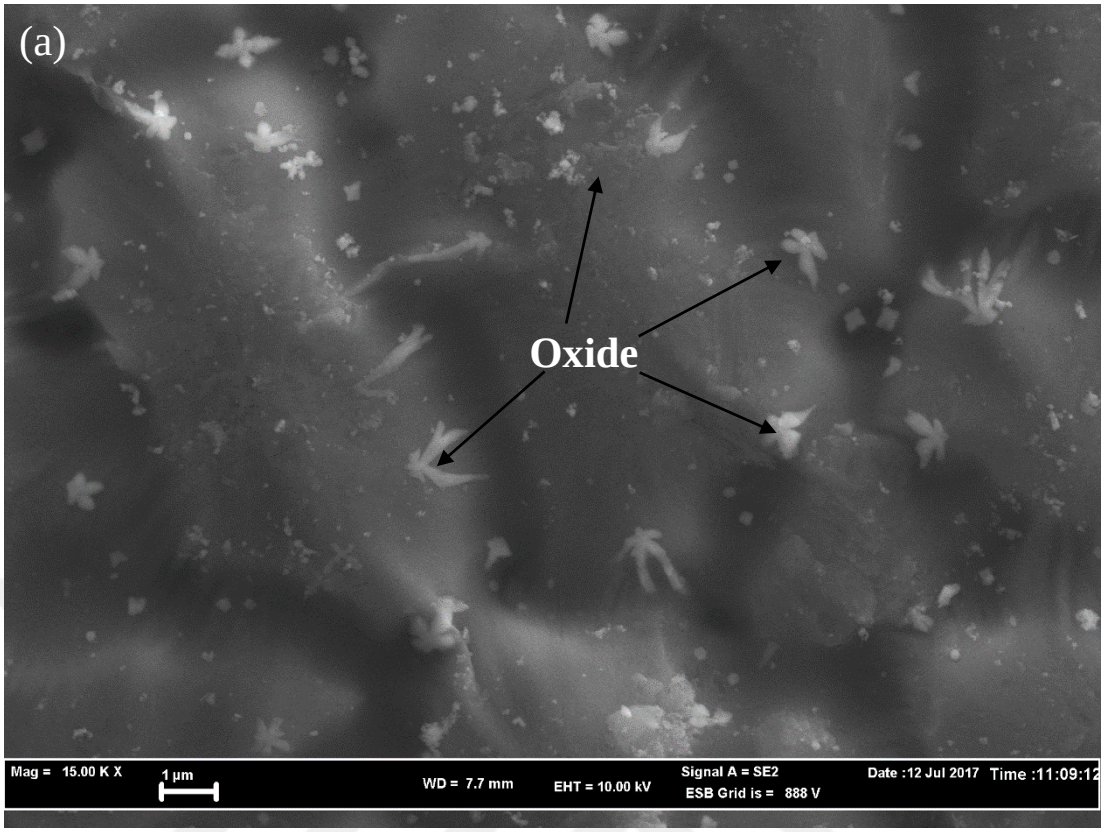
(a)
Oxide
Mag = 15.00 K X
1 µm
WD = 7.7 mm
EHT = 10.00 kV
Signal A = SE2
ESB Grid is = 888 V
Date :12 Jul 2017 Time :11:09:12

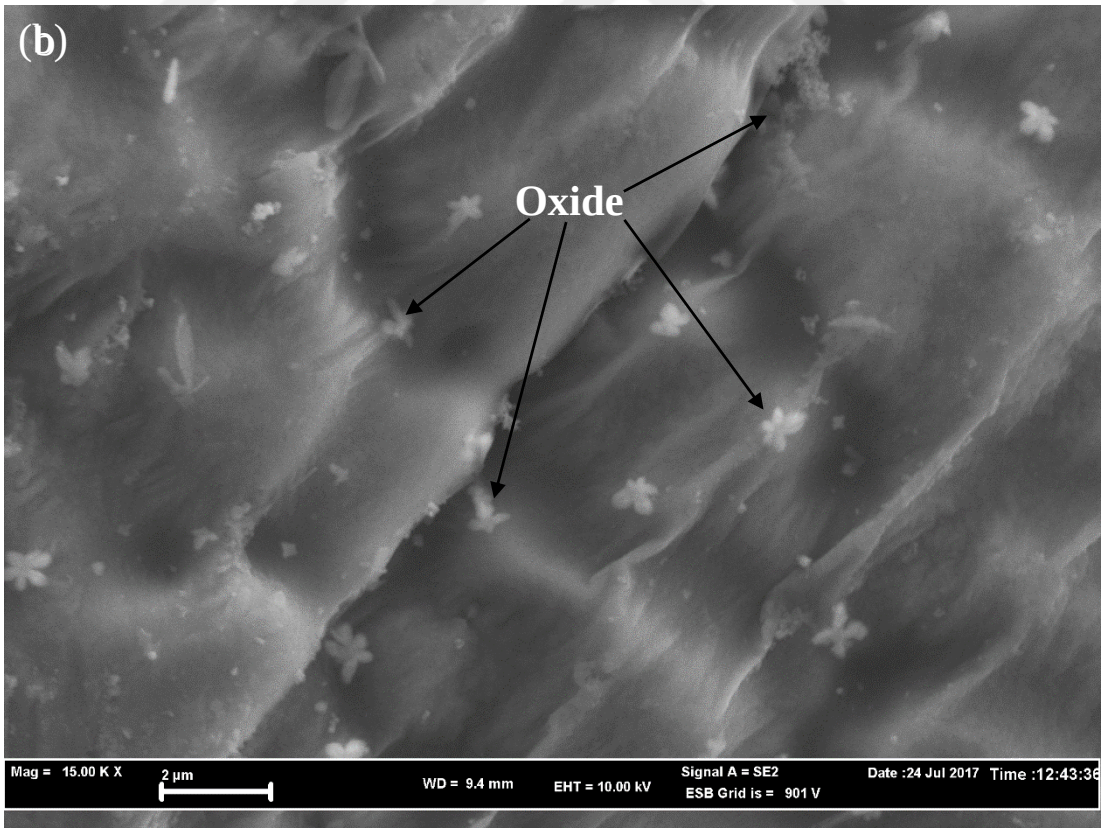
(b)
Oxide
Mag = 15.00 K X
2 µm
WD = 9.4 mm
EHT = 10.00 kV
Signal A = SE2
ESB Grid is = 901 V
Date :24 Jul 2017 Time :12:43:36

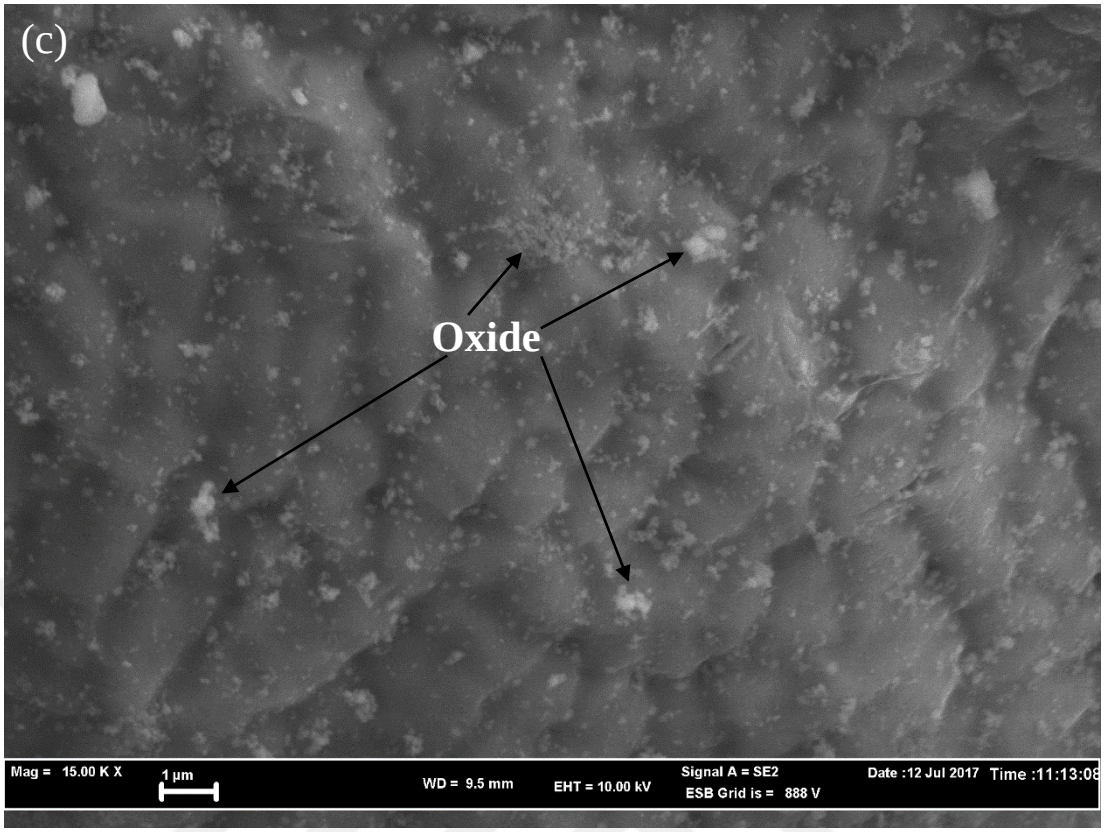


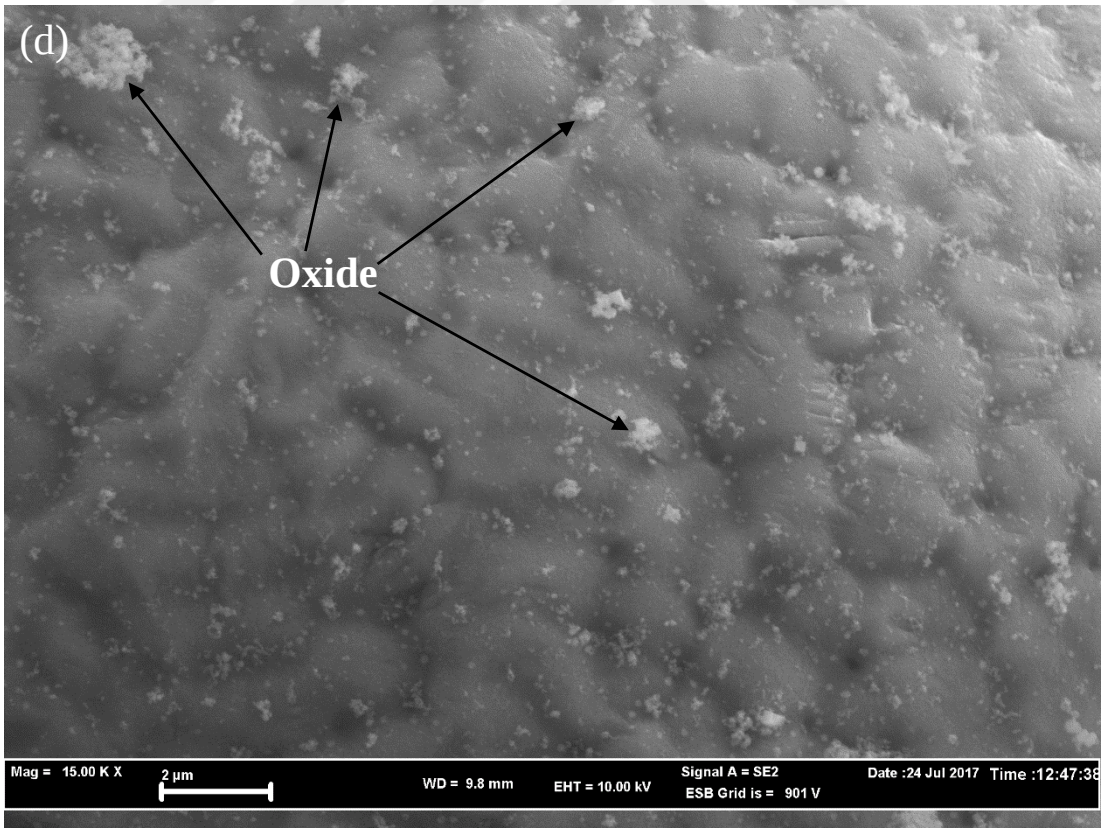


Figure 9.7. AZ31 powders' SEM images which are produced at 2 mm nozzle diameter and different gas pressures. a) 5 bar, b) 15 bar, c) 25 bar, d) 35 bar.

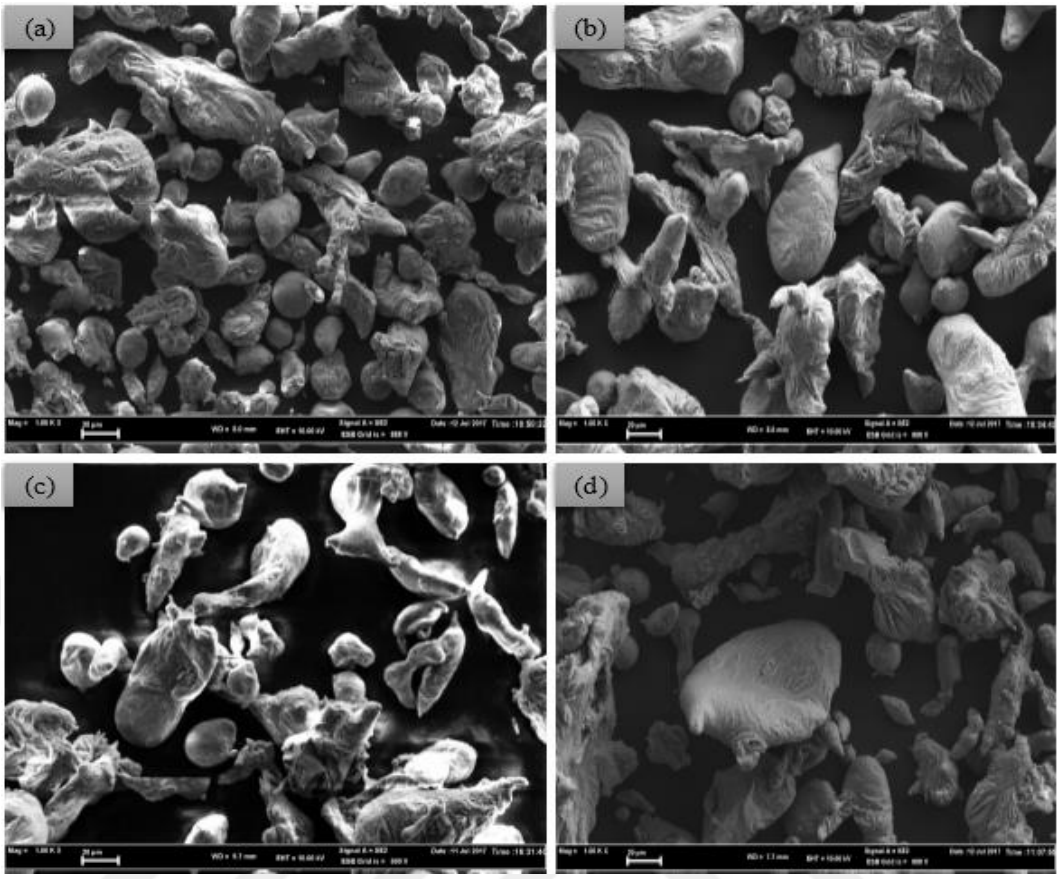


Figure 9.8. SEM images of AZ31 alloy powders produced at 790 °C, 35 bar gas pressure and different nozzle diameters. a) 2 mm, b) 3 mm, c) 4 mm, d) 5 mm.

The SEM images given in Figure 9.7 show that the snow white areas on the surfaces of the powders are oxide (visible from the EDX analysis in Figure 9.9) and the amount of oxide formed on the surface increases depending on the gas pressure. The increase in the gas pressure and the increase in the amount of oxide formed on the surface of powder is thought to be due to the fact that argon gas blown for atomization is not pure and air circulation is intense. In addition, when the surfaces are carefully examined, it can be realized that a grain of powder (as in solidification) is composed of sub-grains and that the sub-grains shrink with increasing gas pressure. The reason for this can be interpreted as the nucleation of the sub-grains due to the solidification rate, as well as the solidification of the liquid metal, depending on the cooling rate and the structure to be composed of smaller particles. On the other hand, it is understood from the SEM images that the increased gas

pressure increases the pressure on the unit surface and because of the faster cooling of the surface, a denser surface is formed.

In addition, it is known that nozzle diameter has a significant effect on powder size and shape as a production parameter in powder production by gas atomization method. It is clear from the SEM images given in Figure 9.8 that the particle size of the produced powders increases when the nozzle diameter is increased. In addition, powders produced with small nozzle diameters are mostly spherical, droplet, and flake, whereas powders produced with nozzle diameters of 4 and 5 mm generally appear to be ligaments, pulses, rods and complex shapes. The reason that the powders are coarse and complex in larger nozzle diameters is since more liquid metal per unit time passes through the nozzle and insufficient atomization of gas. In Figure 9.9, the SEM-EDX analysis of the powder produced at 850 ° C temperature, 4 mm nozzle diameter and 35 bar gas pressure is obtained from 2 different points. In the microstructure α-Mg main matrix phase, Al, Si, Zn and Oxygen are observed.

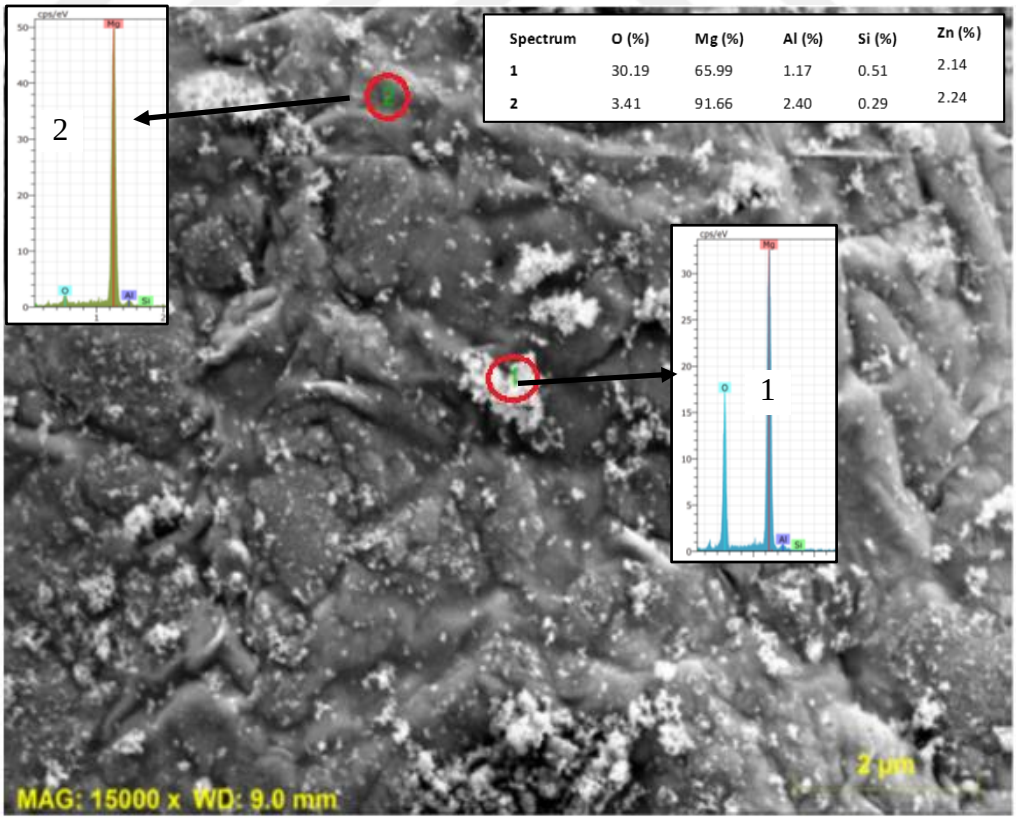


Figure 9.9. EDS analysis of AZ31 powders produced at 850 ºC, 4 mm nozzle diameter and 35 bar pressure.

### 9.3. XRD AND XRF ANALYSIS OF POWDERS

Figure 9.10 shows the XRD result of AZ31 alloy powder. When XRD result is analyzed, α (Mg main matrix) phase and β phase $Mg_{17}Al_{12}$ are seen in the structure. The precipitate of $Mg_{17}Al_{12}$ forms depending on the solidification path [146,147]. $Mg_{17}Al_{12}$ precipitates are known to provide mechanical reinforcement for the AZ31 alloy at the expense of ductility [148]. The mechanical behavior of the alloy depends on the amount, morphology and size of the precipitate. In the AZ31 alloy, strength and creep resistance decrease due to the softening of $Mg_{17}Al_{12}$ phase above 120 °C [149]. AZ31 consists of hexagonal tight package α-Mg and eutectic α + β (β phase, called body-centered cubic β-$Mg_{17}Al_{12}$ phase) phases. Precipitation of the β phase occurs in two ways as continuous and discontinuous precipitation [150,151].

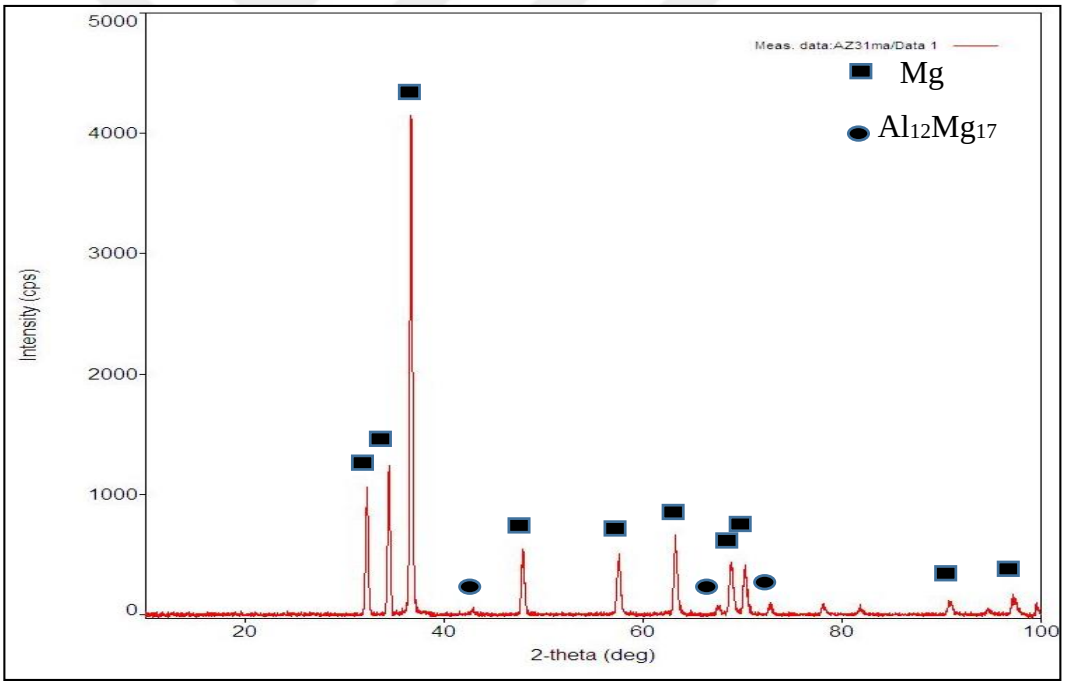


Figure 9.10. XRD pattern of AZ31.

The XRD results given in Figure 9.10 show that powders produced at different gas pressures by gas atomization have no effect on the chemical composition of the powder.

Chemical composition analysis of AZ31 material provided as ingot is given in Table 9.2. In addition, XRF chemical analysis results of AZ31 alloy powder produced by gas atomization method are given in Table 9.3.

Table 9.2. Chemical composition of AZ31 alloy.

| Material | Mg | Al | Zn | Mn |
|---|---|---|---|---|
| Content (%) | 95.7144 | 2.77 | 1.1065 | 0.4015 |

Table 9.3. Chemical (XRF) analysis of produced AZ31 powders.

| Material | Mg | Al | Zn | Mn | Si |
|---|---|---|---|---|---|
| Content (%) | 94.71 | 2.75 | 1.62 | 0.61 | 0.22 |

When the Table 9.2 and Table 9.3 were examined, it was found that the chemical composition of the AZ31 material, which was pulverized by gas atomization, was almost the same. When Table 9.2 and 9.3 are compared, it is observed that very little (up to 1%) Mg is decreased. It is understood from Figure 9.9 that the reduction in magnesium is due to oxidation during melting or atomization. Furthermore, the fact that the chemical composition is changed by atomization which shows that the production of powder by the gas atomization system is important.

## 9.4. SINTERABILITY OF PRODUCED POWDERS AND PARTS PRODUCTION

### 9.4.1. Density Analysis Before and After Sintering

The density values of the samples which are massed at different pressing pressures depending on the pressing pressure are given in Table 9.4.

Table 9.4. Before sintering Density results of AZ31 alloys.

| No | Pressing (MPa) | Weight (g) | Length (cm) | Width (cm) | Thickness (cm) | Volume ($cm^3$) | Density ($g/cm^3$) | Relative Density (%) | Average Relative Density % |
|---|---|---|---|---|---|---|---|---|---|
| 1 | 600 | 4.683 | 3.2 | 1.3 | 0.685 | 2.8496 | 1.6433 | 91.2993 | 91.123 |
| 2 | | 4.71 | 3.2 | 1.3 | 0.70 | 2.912 | 1.6174 | 89.8580 | |
| 3 | | 4.902 | 3.2 | 1.3 | 0.701 | 2.9536 | 1.6596 | 92.2038 | |
| 4 | | 4.702 | 3.2 | 1.3 | 0.69 | 2.8704 | 1.6380 | 91.0055 | 91.127 |
| 5 | | 4.669 | 3.2 | 1.3 | 0.69 | 2.8704 | 1.6266 | 90.3668 | |
| 6 | | 4.685 | 3.2 | 1.3 | 0.68 | 2.8288 | 1.6561 | 92.0099 | |
| 7 | | 4.709 | 3.2 | 1.3 | 0.7 | 2.912 | 1.6171 | 89.8389 | 91.0148 |
| 8 | | 4.683 | 3.2 | 1.3 | 0.68 | 2.8288 | 1.6554 | 91.9706 | |
| 9 | | 4.691 | 3.2 | 1.3 | 0.71 | 2.9536 | 1.5882 | 89.2350 | |

When Table 9.4 is examined, it is seen that pressing (600MPa) has no effect on the relative density of the samples. Mehmet Akkaş et al. [151, 152], in their work on the pressing and sintering of AZ91 powder produced by gas atomization, stated that the relative density values of the samples increased due to the increase of pressing pressure and sintering temperature. They stressed that the raw density of the sample at 300 MPa pressing pressure was 82.73%, whereas this value was 92.4% at 600 MPa pressing pressure. However, in this study, it was observed that there was no change in relative density of samples under pressure of 400 MPa and 600 MPa. The reason for this is thought to be caused by the reduction of Aluminum powder with a face-centered-cubic crystal lattice structure which is easier to deform in the AZ31 alloy. Therefore, Table 9.4 shows that the highest cold pressing pressure of AZ31 alloy powder is 400 MPa. The density values of 3 different pressing pressures were found to be 91 MPa on average. For this purpose, pressed samples at 600 MPa pressure will be used in all subsequent sintering and other processes.

For this purpose, powders produced at a temperature of 850 ° C and a nozzle diameter of 2 mm, pressed at 600 MPa, and the pellets massed were subjected to sintering in an atmosphere-controlled furnace at three different temperatures (500, 550 and 600 °C) for one hour.

In order to determine the ideal sintering temperature, TG-DTG analysis of AZ31 alloy powder is given in Figure 9.11 were carried out. The blue curve in the graph gives TG (Thermographic Graviometry) mass change. It has been determined from the graph that there is no change in the material heated up to 600 $^{o}$C, but the material shows an exothermic change after 604 $^{o}$C. When the DTG (Differential Thermo Gravimetric) given by the red line was examined, foaming occurred in the material after 650 $^{o}$C, so this foaming caused mass increase in the material.

For this reason, it was determined by TG-DTG analysis that the maximum sintering temperature of the materials produced at different pressures was 600 $^{o}$C. Here the blue line shows the TG, the red line shows the DTA and the green line shows the DTG analysis.

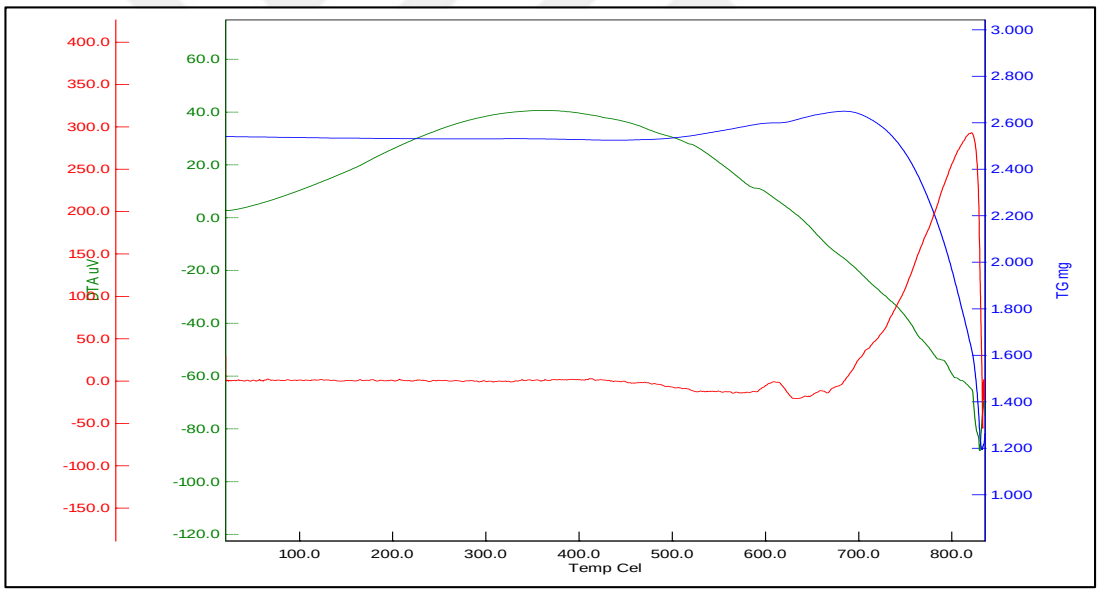


Figure 9.11. TGA-DTA analysis graph of AZ31 powder.

In order to determine the optimum sintering temperatures of the materials pressed at 600 MPa pressure, the parameters given in Table 9.5 were applied.

Table 9.5. Sintering parameters of the samples.

| Sample No | Pressing Value (MPa) | Sintering Temperature (°C) |
|---|---|---|
| 1 | 600 | 500 |
| 2 | | 550 |
| 3 | | 600 |

The samples formed into ingots were sintered at three different temperatures (500, 550, 600 ºC). The density values of sintered AZ31 alloys after sintering were determined. The density values of the samples after mass sintering are given in Table 9.6.

Table 9.6. Density results of sintered AZ31 alloys.

| No | Sintering temp (ºC) | Weight (g) | L (cm) | W (cm) | T (cm) | Volume (cm3) | Density (g/cm3) | Relative Density (%) | Average Relative Density (%) |
|---|---|---|---|---|---|---|---|---|---|
| 1 | 500 | 4.486 | 3.170 | 1.280 | 0.66 | 2.67801 | 1.6751 | 93.0622 | 93.785 |
| 2 | | 4.666 | 3.185 | 1.290 | 0.67 | 2.75279 | 1.6950 | 94.1669 | |
| 3 | | 4.580 | 3.175 | 1.290 | 0.66 | 2.70319 | 1.6942 | 94.1272 | |
| 4 | 550 | 4.198 | 3.150 | 1.260 | 0.64 | 2.54016 | 1.6526 | 91.8139 | 92.157 |
| 5 | | 4.209 | 3.150 | 1.270 | 0.63 | 2.52031 | 1.6703 | 92.7944 | |
| 6 | | 4.166 | 3.135 | 1.250 | 0.65 | 2.54718 | 1.6355 | 91.8627 | |
| 7 | 600 | 4.373 | 3.180 | 1.270 | 0.64 | 2.58470 | 1.6918 | 93.9931 | 92.241 |
| 8 | | 3.816 | 3.155 | 1.270 | 0.58 | 2.32397 | 1.6420 | 91.2230 | |
| 9 | | 4.491 | 3.190 | 1.295 | 0.66 | 2.72649 | 1.6471 | 91.5094 | |

When the density results are examined in Table 9.6, the average relative densities of the samples increased with sintering. However, it is seen that the increase in sintering temperature does not have much effect on the densities of the samples. The density values of the powders which were massed at different pressures and then sintered at different temperatures were determined. Density values before and after sintering were determined separately for each sample. The average density values for each pressure applied were calculated for the density values which are determined separately for each sample. The relative densities of the sample pressed at 600 MPa pressure before sintering are given in Figure 9.12.

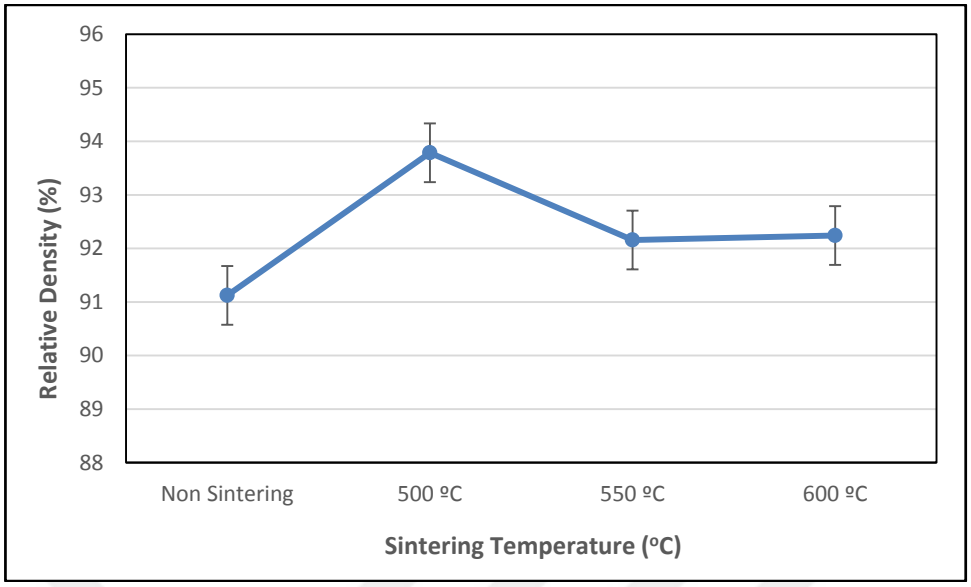


Figure 9.12. Density values of samples.

The relative density of the samples increased with sintering is shown in Table 9.6 and Figure 9.12. While the relative density of the sample at 600 MPa pressing pressure was 91.23% before sintering, the relative density value of the same sample with sintering at 500 °C was recorded as 93.785%. Sintering at 550 and 600 °C results in a slight decrease in relative density values. It is known that with sintering, the density increases due to the disappearance of small pores in the material and the grain boundaries approaching each other. However, after the sintering temperature of 500 °C, the relative density of the sample decreases. After sintering temperature of 500 °C, it will be explained the decrease in relative density from the optical microscope images after sintering given in Figure 9,13.

### 9.4.2. Optical Microscope Analysis After Sintering

The optical microscope images of AZ31 Mg alloy powders at 600 MPa pressure and sintered samples at 500, 550, and 600 ° C are given in Figure 9.13, 9.14 and 9.15.

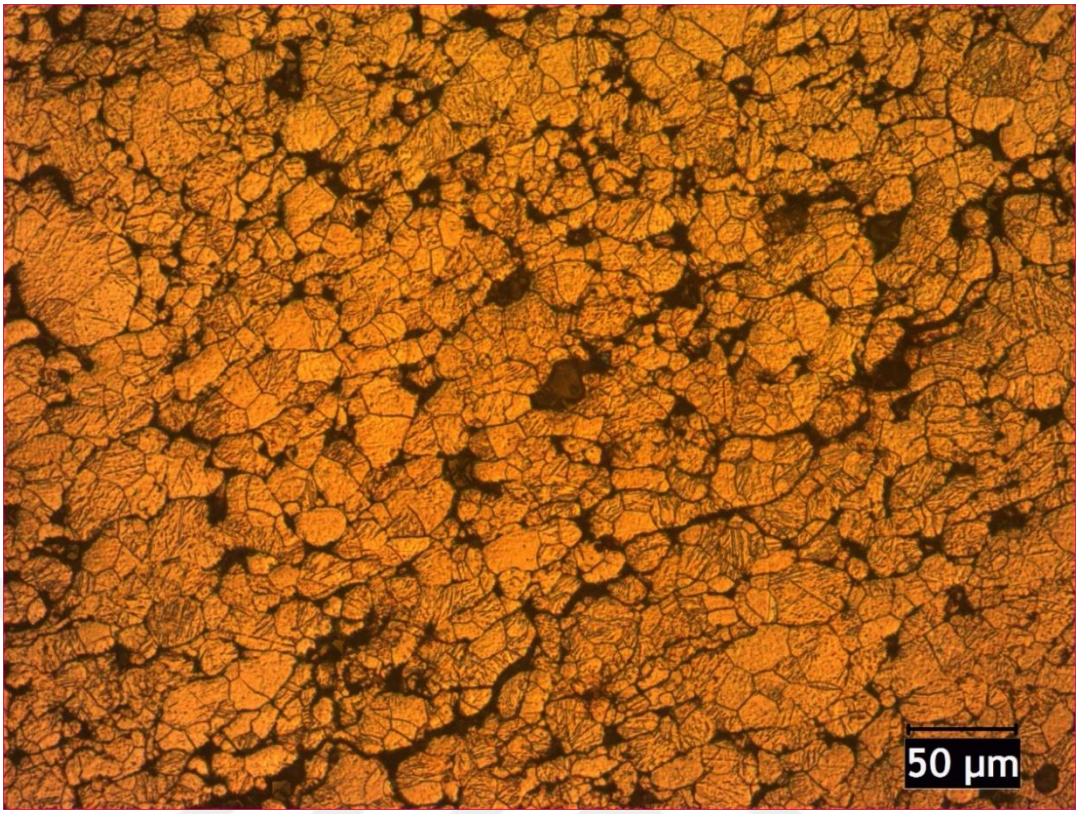


Figure 9.13. Optical microscope images after sintering at 500 °C.

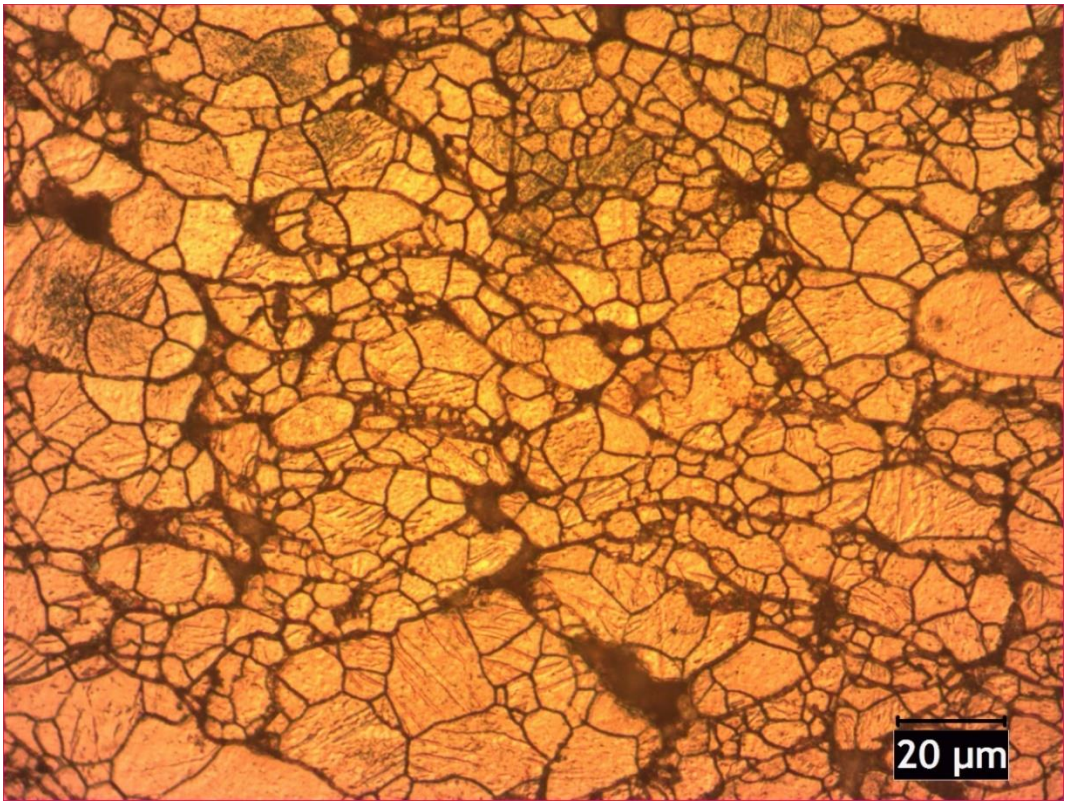


Figure 9.14. Optical microscope images after sintering at 550 °C.

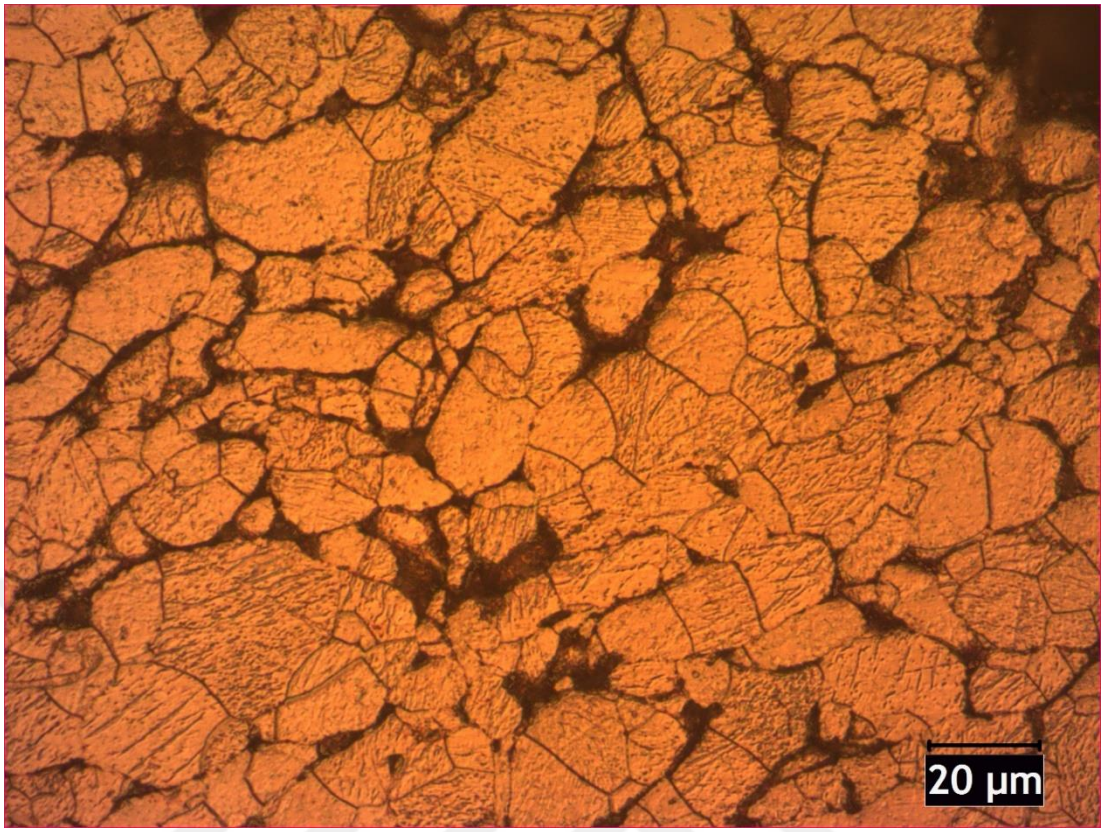


Figure 9.15. Optical microscope images after sintering at 600 °C.

From the optical images of Figures 9.13, 9.14 and 9.15, it can seen that the materials are sintered by the intergranular bond structures and the grain boundaries formed. It is known that the grain boundaries of the materials approach each other by sintering, the pores decrease and the relative density increases. However, when the optical images are examined, it is seen that due to the increase of the sintering temperature, the grains become larger with the effect of excessive sintering and small pores combine to form larger pores (Figure 9.15). The reason for the decrease in relative density with the increase of sintering temperature seen in Figure 9.12 is also considered as the reason for the increase of grain boundaries and the growth of pores mentioned above. Changes in grain boundary thickness and increase of sintering temperature of $Mg_{17}Al_{12}$ which causes pore growth are given in Figure 9.16, 9.17 and 9.18.

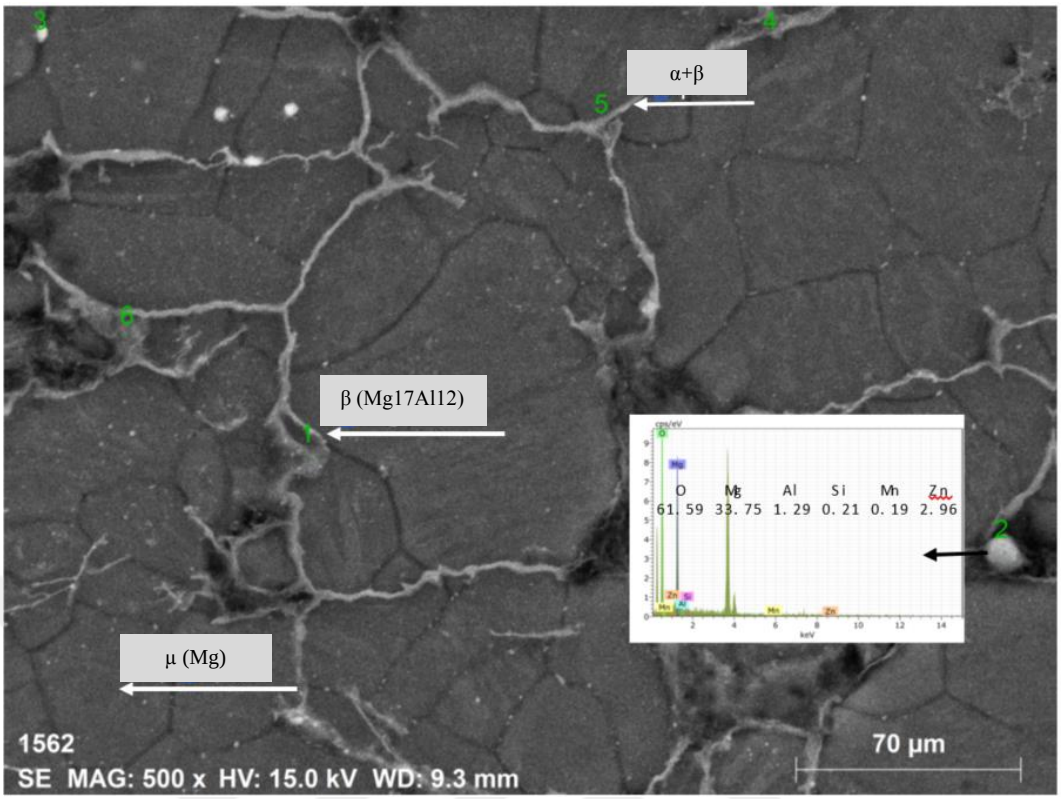


Figure 9.16. SEM images and EDX analysis after sintering at 500 °C.

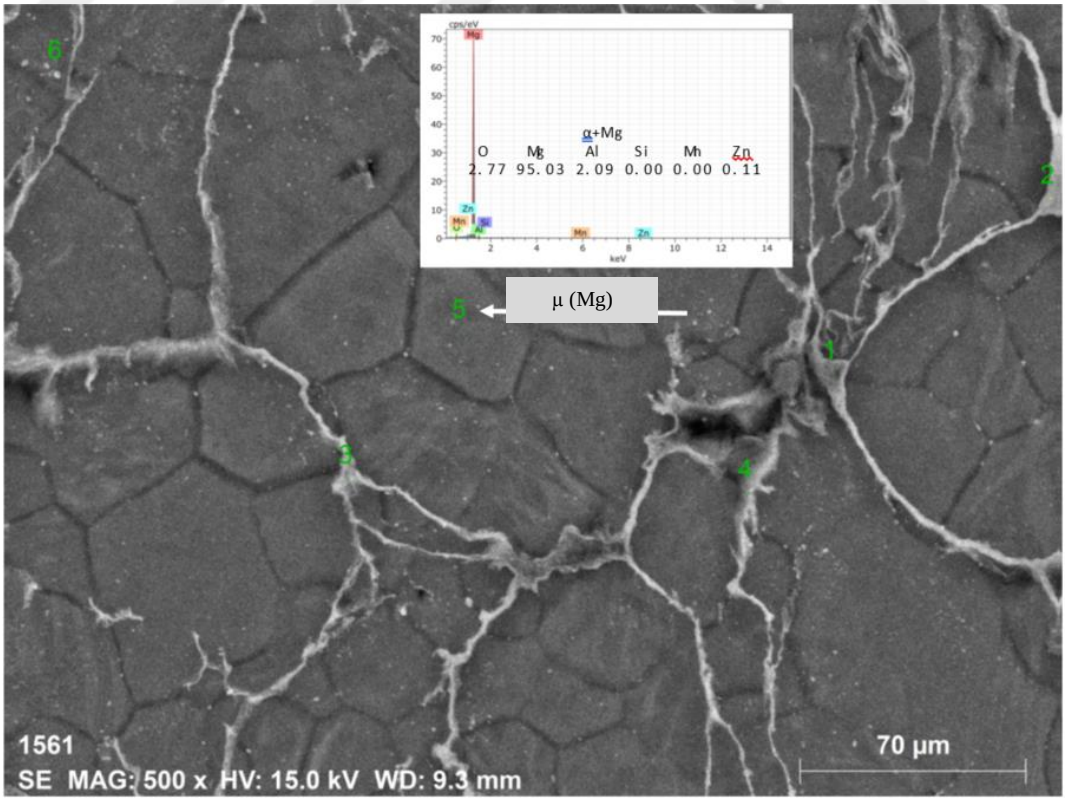


Figure 9.17. SEM images and EDX analysis after sintering at 550 °C.

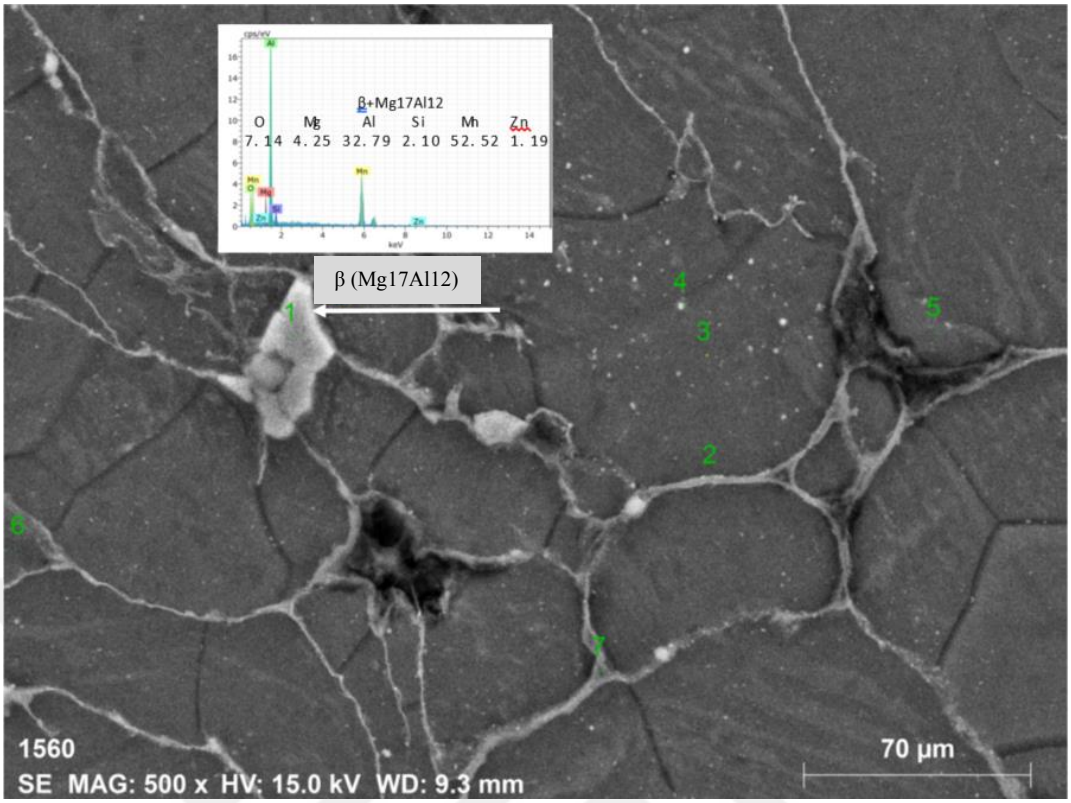


Figure 9.18. SEM images and EDX analysis after sintering at 600 °C.

When the SEM image given in Figure 9.16 is examined, it is seen that $Mg_{17}Al_{12}$ intermetallic phase is homogeneously distributed in the structure in the sintered sample at 500 °C. However, in the samples sintered at the temperatures of 550 and 600 °C, SEM images in Figures 9.17 and 9.18 show that the $Mg_{17}Al_{12}$ intermetallic phase is not homogeneously deposited at the grain boundaries and even becomes larger. The reason for the growth of the $Mg_{17}Al_{12}$ intermetallic phase and the grain boundaries is thought to be that a portion of the $Mg_{17}Al_{12}$ intermetallic phase dissolves in the α-Mg phase and that some of it grows by combining with the $Mg_{17}Al_{12}$ intermetallic phase formed at the grain boundaries. In addition, it is thought that the intermetallic phase of $Mg_{17}Al_{12}$, which increases at high sintering temperatures (500 and 600 °C), settles at the grain boundaries, preventing the grain boundaries from approaching each other and causing the pores to decrease. As a result, as shown in Figure 9.12, it has caused a decrease in density due to the increase in sintering temperature.

SEM-EDS analysis of the microstructure of the α-Mg matrix as well as along the grain boundary β ($Mg_{17}Al_{12}$) phase and a fine phase in the grain boundary α + β eutectic was observed (Figure 9.16- 9.18). On the other hand, when the EDS analysis of the point encoded by the number 2 given in the SEM image in Figure 9.16 is examined, a very intensive oxygen content is seen. Oxygen on the surface of the sintered samples is thought to occur both during powder production and during sintering.

### 9.4.3. Micro Hardness Analysis After Sintering

The micro hardness tests were performed to determine the effect of sintering temperature on the hardness of the samples produced at pressing pressures 600 MPa and different sintering temperatures (500, 550 and 600 °C). The hardness tests were performed under 500 grams force ($HV_{0.5}$) and 15 seconds retention time. The hardness values were determined by calculating the average of 3 hardness values of each sample. Hardness results are given in Table 9.7.

Table 9.7. Hardness values after sintering.

| Pressure (MPa) | Sintering Temp (°C) | 1.Measurement (HV0.5) | 2.Measurement (HV0.5) | 3.Measurement (HV0.5) | Average Value (HV0,5) |
|---|---|---|---|---|---|
| 600 | 500 | 54.9 | 55.4 | 54.3 | 54.86 |
| | 550 | 54.2 | 53.5 | 55.3 | 54.33 |
| | 600 | 54.1 | 53.4 | 53.9 | 53.80 |

When the hardness results given in Table 9.7 are examined, it is seen that the hardness values of the samples decrease due to the increase in the sintering temperature. The highest hardness value was 54.86 $HV_{0,5}$ at same 600 MPa pressing pressure and 500 °C sintering temperature. At the same 600 MPa pressing pressure, 600 °C sintering temperature the lowest hardness value was measured as 53.8 $HV_{0,5}$.

The decrease in the hardness values due to the increase in the sintering temperature can be explained by the SEM images in Figure 9.16-18. When the surface images of

the sintered samples in Figure 9.16-18 are examined, it is seen that the $Mg_{17}Al_{12}$ precipitates are distributed to the whole surface homogeneously in the sample produced at 500 °C, whereas in the sample produced at 600 °C $Mg_{17}Al_{12}$ is located at the grain boundaries. Hence, as the hardness test measurements of the samples are made homogeneously from all surfaces decrease due to the increased sintering temperature [18].

### 9.4.4. Three Point Bending Tests

The 3-point bending tests were performed to determine the effect of sintering temperature on the bending of the samples produced at pressing pressures 600 MPa and different sintering temperatures (500, 550 and 600 °C) (Figure 9.19-9.21). The bending measurements were taken under 1mm/min loading speed.

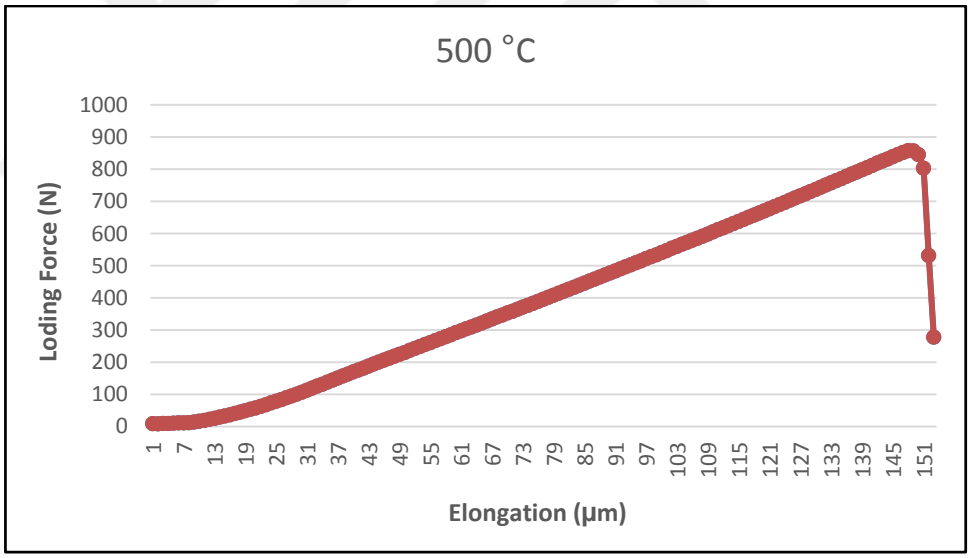


Figure 9.19. Three-point bending test sample at 500 °C sintering.

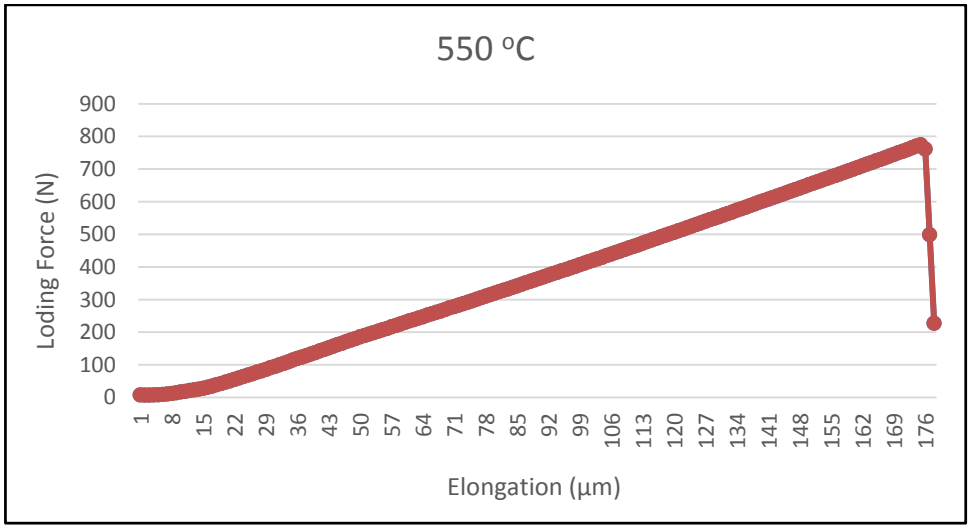


Figure 9.20. Three-point bending test sample at 550 °C sintering.

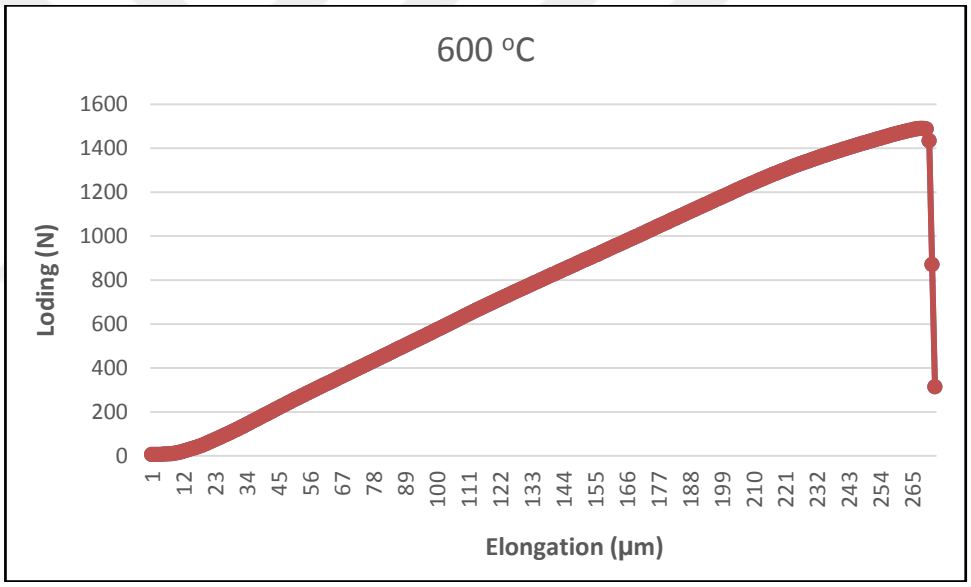


Figure 9.21. Three-point bending test samples at 600 °C sintering.

Figure 9.19-21 shows the three-point bending test results of sintered samples at 500 ºC, 550 ºC and 600 ºC sintering temperatures. Three-point bending results are shown as the change in fracture elongation according to the applied load. When the three-point bending results are examined in Figure 9.19-21, it is seen that the bending elongation of the material applied to the breaking point changes linearly. All specimens have significant bending fracture. Furthermore, it is seen that the fracture elongation of the samples increases due to the increase of sintering temperature (500-600 ºC). The fracture elongation of the sintered sample at 500 ºC was 151 µm, while

the fracture elongation of the sintered sample at 600 ºC was 265 µm. On the other hand, Figures 9.19-21 show that, depending on the sintering temperature, the maximum load required for rupture of the sample increases. The maximum load required to break the sintered sample at 500 ºC was 800 N, while the maximum load required to break the sintered sample at 600 ºC was 1500 N.

In fact, for AZ31, a magnesium alloy, the main strength enhancing phase is the $Mg_{17}Al_{12}$ intermetallic phase. In addition, the intermetallic phase of $Mg_{17}Al_{12}$ has a softer structure [130]. It is thought that the bending elongation of the samples increases as a result of the increase of the intermetallic phase of $Mg_{17}Al_{12}$ and the grain coarseness with increasing sintering temperature. In addition, the sintering temperature of the intermetallic phase of α + β and β ($Mg_{17}Al_{12}$) formed by sintering and the formation of a tight bond at the α Mg interface increased the bending strength of the samples.

# PART 10

# GENERAL RESULTS AND RECOMMENDATIONS

## 10.1. GENERAL RESULTS

In this study, the characterization of AZ31 powder produced by the gas atomization method under different parameters are carried out, the results obtained from this study are summarized as below.

1. Gas atomization unit was designed and manufactured in Karabük University, Technology Faculty, Manufacturing Engineering Department.

2. In this gas atomization unit designed and manufactured, the production of magnesium alloy AZ31 powder was carried out by gas atomization method which is widely used in the production of powders.

3. It is understood that the temperature of the liquid metal in the production of powder by gas atomization method has little effect on the size, distribution, shape and surface appearance of the powders.

4. When the nozzle diameter was decreased and gas pressure was increased, it was observed that the powder size decreased and the powder shape changed from complex, ligament, pulse and rod-like structure to dripping and spherical. In addition, since the pressure increase provides for transferring more energy to the melt, the powders produced have a smaller average powder size. In the production of gas atomized magnesium alloy AZ31 powder, the smallest powder size was measured as 46 μm under condition of 790 °C, 2 mm nozzle diameter and at 35 bar pressure.

5. During the atomization, different formations of satellites were observed on the surfaces due to the clashes between droplets and powders. Furthermore, it was observed that the surfaces of the powder vary depending on the gas pressure and they have dendritic and cellular shapes.

6. At the end of XRF, it was seen that the chemical composition of AZ31 powder and ingot material has almost same proportion of elements.

7. As a result of XRD analysis, micro phase α (Mg main matrix) phase β (Mg17Al12) was observed.

8. Sintered samples at three different temperatures (500, 550 and 600 °C) were examined and decrease of their relative density after sintering was seen. The sample having the highest relative density value after sintering process was measured as 93.785 % which was compressed at 600 MPa pressure and sintered at 500 °C.

9. After sintering, XRD analysis results showed that α-Mg, β ($Mg_{17}Al_{12}$) and α + β phases were present in the structure. However, XRD analysis before sintering clearly showed Mg peaks, while the XRD analysis after sintering showed a slight decrease in the degree of Mg peaks. In addition, it was seen in XRD analysis that the $Mg1_7Al_{12}$ phase became clearer to observe due to the increased the sintering temperature. After sintering, it was determined that the decrease in Mg phase was caused by precipitation in the material.

10. In the SEM images, the ductile fractures of the sintered materials were observed at high sintering temperatures. At lower sintering temperature values fracture were observed at grain boundaries. It is believed that internal energies increase the deformation of particles and increase their size during sintering.

11. The hardness values of the samples decreased due to the increase in sintering temperature. The decrease in these hardness values is thought to be caused by the formation of a brittle structure due to sintering temperature and rapid

solidification during atomization. In the samples sintered at low temperatures, $Mg_{17}Al_{12}$ was distributed to the entire surface homogeneously, whereas in the sample produced at 600 °C, Mg17Al12 was deposited on the grain boundaries. Hence, as the hardness measurements of the samples were made homogeneously from all surfaces, the hardness measurement results decreased due to the increased sintering temperature. The highest hardness values of the massed samples were measured at 54.86 HV0, 5 at 600 MPa pressing pressure and 500 °C sintering temperature.

12. As a result of the bending test analysis, the highest value of the bending force was observed in the sample which was sintered at 600 °C.

## 10.2. RECOMMENDATIONS

In line with the studies conducted, it is possible to carry out the following studies regarding the powder production of AZ31 magnesium alloy;

1. The design and manufacture of the gas atomization unit can be improved by eliminating the deficiencies of the gas atomization unit by more technique.

2. Powder production can be carried out using different types of magnesium alloys.

3. Different types of nozzles and materials designs can be compared to produce AZ31 alloy powders and differences that may occur in powder production can be compared.

4. In order to improve the properties of Mg and its alloys by means of powder metallurgy, strengthening mechanism can be provided by adding various elemental powders into the powders produced.

## REFERENCES


1. Mordike, B.L., Ebert, T., "Magnesium Properties Applications Potential", ***Mat. Sci. Eng. A,*** 302: 37-45 (2001).

2. Benedyk J.J., "Magnesium Challenges Aluminum Dominance as the Light Metal of Choice in Automotive Markets", ***Light Metal Age-The International Magazine of Light Metal Industry***, (2004).

3. "American Society for Testing and Materials-ASM, Metal Handbook, Forming and Forging 9th Edition", 791-804 (1988).

4. Kaya, A. A., Özdoğru, E.F., Abanoz, D., Yiğit, S., Yücel, O., "Otomotivde Magnezyum Alaşım Uygulamaları", OTEKON'02, ***Otomotiv Teknolojileri Kongresi***, Bursa, (2002).

5. Duygulu, Ö., Oktay, G., Kaya, A.A., "The Use of Magnesium Alloys in Automotive Industry", ***OTEKON'06, Otomotiv Teknolojileri Kongresi***, Bursa, (2006).

6. Kaya, A.A., Pekgüleryüz, M., Türkoğlu, S., Özdoğru, E.F., "Ağırlık Tasarrufu Amacıyla Otomobil Motor Bölmesinde Magnezyum Alaşımlarının Kullanımı", ***OTEKON'04, Otomotiv Teknolojileri Kongresi***, Bursa, (2004).

7. Fredrich, H., S. Schumann, "Research for a New Age of Magnesium in the Automotive Industry", ***J. Mat. Proc. Tech.,*** 117: 276-28, (2001).

8. Furuya, H., Kogiso, N., Matunaga, S., Senda, K., "Applications of Magnesium Alloys for Aerospace Structure Systems", ***Materials Science Forum***, 341-348, 350-351, (2001).

9. Froes, F.H., Eliezer, D., Aghion, E., "The Science, Technology, and Applications of Magnesium", ***J. Mat. Proc. Tech.,*** 50 (9): 30-34, (1998).

10. Chaffin, G.N., J.E., Jacoby, "Guidelines for Aluminum Sow Casting and Charging", ***The Aluminum Association, Washington***, D.C., (1998).

11. Gray, J.E., Luan, B., "Protective Coatings on Magnesium and its Alloys—A Critical Review", ***J. Alloys Compd.***, 336: 88-113, (2002).

12. Kaya, R.A., Çavuşoğlu, H., Tanık, C., Kaya, A. A., Duygulu, Ö, Mutlu, Z., Zengin, E., Aydın Y., "The Effects of Magnesium Particles on Posterolateral Spinal Fusion: An Experimental in Vivo Study in a Sheep Model", ***J.Neurosurg***-Spine, 6: 141-149, (2007).

13. Duygulu, O., Kaya, R.A., Oktay, G. and Kaya, A.A., "Investigation on the Potential of Magnesium Alloy AZ31 as a Bone Implant", ***Materials Science Forum***, 546-549: 421-424, (2007).

14. Duygulu, O., Kaya, R.A., Oktay, G., Berk, C., and Kaya, A.A., "Can Magnesium Alloys be Used as Implants?- SEM Examinations from an in Vivo Study", ***16th International Microscopy Conference***, Sopporo, Japan, (2006).

15. Kaya, A.A., "Future of Magnesium: Applications in Transportation and Bone Surgery", ***10th Int. Symposium on Advanced Materials (ISAM-2007)***, Islamabad, Pakistan, (2007).

16. Kaya, A.A., Kaya, R.A., Witte F., and Duygulu, Ö., "Useful Corrosion-Potential of Magnesium Alloys as Implants", ***International Corrosion Engineering Conference***, Seoul, Korea, (2007).

17. İnternet: ÜNAL, R., "Gaz Atomizasyonu" ***http://rahmiunal.net/toz/3.gaz%20atomizasyonu.pdf.***

18. Ünal, R. "Gaz atomizasyonu ile metal tozu üretimi değişkenlerinin araştırılması." ***Yüksek Lisans Tezi, Gazi Üniversitesi***, Ankara (1995).

19. Uslan, İ. ve Küçükarslan S., "Kalay tozu üretimine gaz atomizasyonu parametrelerinin etkisinin incelenmesi", ***Gazi Üniv. Müh. Mim. Fak. Der.,*** Cilt 25, No (1): 1-8 (2010).

20. Gokmese, H., Ozdemir, M. and Bostan, B., "The Characterization and Production by Gas Atomization Method of Pre-alloyed AA 2014 Powder Metal Aluminum", ***International Journal of Scientific and Technological Research***, 1 (1) 26-38 (2015).

21. İnternet: "Makine Teknolojileri Elektronik Dergisi 2007" (1) 69-76", ***http://www.teknolojikarastirmalar.com/pdf/tr/01_040107_8_aydin_tr.pdf***, (2007).

22. Rudajevova, A., Staněk, M., & Lukáč, P., "Determination of thermal diffusivity and thermal conductivity of Mg–Al alloys". ***Materials Science and Engineering***: A, 341(1), 152-157, (2003).

23. CAO, F. H., LIN, L. Y., ZHANG, Z., ZHANG, J. Q., & CAO, C. N., "Environmental friendly plasma electrolytic oxidation of AM60 magnesium alloy and its corrosion resistance". ***Transactions of Nonferrous, Metals Society of China***, 18(2), 240-247 (2008).

24. Li, Y. G., Wei, Y. H., Hou, L. F., & Han, P. J., "Atmospheric corrosion of AM60 Mg alloys in an industrial city environment". ***Corrosion Science***, 69: 67-76 (2013).

25. Kondoh, K., Hamada, E. S. A., Imai, H., Umeda, J., & Jones, T., "Microstructures and mechanical responses of powder metallurgy non-combustive magnesium extruded alloy by rapid solidification process in mass production". ***Materials & Design***, 31(3): 1540-1546, (2010).

26. Lagutkin, S., Achelis, L., Sheikhaliev, S., Uhlenwinkel, V. and Srivastava, V., "Atomization process for metal powder", ***Materials Science and Engineering***, 383 (A): 1–6 (2004).

27. Neikov, O.D., Vasilieva, G.I. Sameljuk, A.V. and Krajnikov, A.V., "Water atomised aluminium alloy powders", ***Materials Science and Engineering***, 383 (A): 7–13 (2004).

28. Liu, X., Xie, H., Wang, L., Luo, J. and Cai, Y., "Production of Fe-Si-Al-Ni-Ti soft magnetic alloy powder by inert-gas atomization", ***Chinese Materials Conference***, 27: 1426-1433 (2012).

29. Kim, T.S. and Chae, H.J. "Consolidation of gas atomized mg alloy powders", ***Rev.Adv.Mater.Sci***., 18: 769-772 (2008).

30. Karagöz, Ş., Yamanoğlu, R., ve Atapek, Ş.H., "Metalik toz işleme teknolojisi ve prosesleme kademeleri açısından parametrik ilişkiler", ***Eskişehir Osmangazi Üniversitesi Mühendislik Mimarlık Fakültesi Dergisi***, Cilt:XXII, Sayı:3, 77-87 (2009).

31. Öztürk, S., Arslan, F., ve Öztürk, B., "Su soğutmalı döner disk atomizasyonuyla üretilen AA 2014 alaşımı tozlarının soğuma hızına atomizasyon parametrelerinin etkisi", ***Toz Metalurjisi Konferansı***, İzmir, 44-52 (2002).

32. Bao, C.M., Dahlborga, U., Adkins, N. and Calvo-Dahlborg, M., "Structural characterisation of Al–Ni powders produced by gas atomisation", ***Journal of Alloys and Compounds***, 481: 199–206 (2009).

33. Zdujic, M., and Uskokovic, D., "Production of atomized metal and alloy powders by the rotating electrode process", ***Powder Metallurgy and Metal Ceramics***, 29.9: 673-683 (1990).

34. Ünal, R., "The influence of the pressure formation at the tip of the melt delivery tube on tin powder size and gas/melt ratio in gas atomization method", ***Journal of Materials Processing Technology***, 180: 291–295 (2006).

35. Sofuoğlu, A., "Investıgation of the production parameters of gas atomised aluminium and tin powders: experimental and numerical study***", International Symposium on Computing in Science & Engineering. Proceedings, GEDIZ University, Engineering and Architecture Faculty,*** p. 86. (2013).

36. Duygulu, Ö., Yücel, O. ve Kaya A.A., "Magnezyum levha alaşımlarının üretimi ve geliştirilmesi", ***itüdergisi/d***, Cilt:9, Sayı:4, 133-138 (2011).

37. Hou, L., Li, B., Wu, R., Cui, L., Ji, P., Long, R., ... & Sun, B., "Microstructure and mechanical properties at elevated temperature of Mg-Al-Ni alloys prepared through powder metallurgy". ***Journal of Materials Science & Technology,*** 27:367-382 (2017).

38. Vahidgolpayegani, Alireza, et al. "Production methods and characterization of porous Mg and Mg alloys for biomedical applications." ***Metallic Foam Bone***. 25-82 (2017).

39. Oğuz, Ş., Öztürk, Z., Uzun, E., Kurt, A. ve Boz, M., "Gaz atomizasyonu yöntemi ile kalay tozu üretiminde gaz basıncının toz boyutu ve şekline etkisi", ***6th International Advanced Technologies Symposium*** (IATS'11), Elâzığ, 565-568 (2011).

40. Öztürk, F. ve Kaçar, İ., "Magnezyum alaşımları ve kullanım alanlarının incelenmesi", ***Niğde Üniversitesi Mühendislik Bilimleri Dergisi***, Cilt 1 Sayı 1: 12-20 (2012).

41. Boz, M., Kurt A., "The Effect Of Al2O3 On The Frictıon Performance Of Automotive Brake Frictıon Materials", ***Trıbology International***, 40: 1161-1169 (2007).

42. Ünlü, B.S., Kurgan, N., Yılmaz, S.S., "Toz Metal Çeliklerin Mikroyapı Ve Mekanik Özellikleri", ***Mühendis ve Makine***, 50(588): 11-12 (2008)

43. Yalçın, B., "Toz Metalurjisi Yöntemiyle İmal Edilen Titanyum Alaşımı İmplantların Temel Özelliklerinin Araştırılması", ***Doktora Tezi, Süleyman Demirel Üniversitesi Fen Bilimleri Enstitüsü***, Isparta, 6-25 (2007)

44. Özay, Ç., Hasçalık, A., "T/M Yöntemi İle Üretilen Cu-C-Al2SiO5 Kompozitinde C Oranının Abrasiv Aşınma Dayanımına Etkisi", ***Doğu Anadolu Bölgesi Araştırmaları***; 150-154 (2004)

45. Boz, M. ve Kurt, A., "Toz metal fren balata malzemelerinin sürtünme-aşınma performansı üzerine çinkonun etkisi." ***Gazi Üniversitesi Mühendislik-Mimarlık Fakültesi Dergisi***, 21.1 (2006).

46. İnternet: Metal Powder Injection Molding › Chair of Materials Science and Engineering for Metals, ***https://www.wtm.tf.fau.eu/forschung/hochtemperaturwerkstoffe/prozesstechnik/metal-powder-injection-molding/***

47. Ersümer, A., 'Toz Metalürjisi', ***İ.T.Ü. Makine Fakültesi***, İstanbul (1970).

48. Demirkesen, E., "Kompozit Malzemeler Ders Notları", ***İstanbul Teknik Üniversitesi*** (2003).

49. Sarıtaş, S., Türker M., Durlu, N., "Toz Metalurjisi ve Parçacıklı Malzeme İşlemleri", ***Türk Toz Metalurjisi Derneği Yayınları***, Ankara, (2007).

50. Sarıtaş, S., and Doğan, C., "Metal powder production by centrifugal atomization", ***Int. J. Powder Metallurgy***, 30, 419 – 427 (1994).

51. Clyne, T.W., Metal Matrix Composites: Matrices and Processing, in Encyclopaedia of Materials: Science and Technology, Ed. ***Mortensen, A., Elsevier*** 785-801 (2001)

52. Aydın, M. ve Ünal, R., "Laval tipi yeni bir nozul tasarımı ile metal tozu üretimi ve üretim değişkenlerinin etkisinin incelenmesi", ***Makine Teknolojileri Elektronik Dergisi***, (1): 69-76 (2007).

53. Yıldız, E.S., "Gaz Atomizasyonu İle Metal Tozu Üretiminde Nozul Geometrisinin Toz Boyutuna Etkisinin Araştırılması", Yüksek Lisans Tezi, ***Dumlupınar Üniversitesi Fen Bilimleri Enstitüsü***, Kütahya, 5-14 (2007)

54. İnternet: ÜNAL, R., "Kişisel web sayfası", ***https://rahmiunal.net/toz/tozuretimi/powder_product.html.***

55. German, R.M., ***Powder metallurgy science,2nd edition, Metal Powder Industries Federation,*** USA 567-572 (1994).

56. Sarıtaş, S., ***Toz metalurjisi, Makine müh. el kitabı***, MMO, 2. Baskı, I.Cilt: 421-427 1994.

57. Turan, H., "Gaz atomizasyonu ile metal tozu üretimi", Yüksek Lisans Tezi, ***Gazi Üniversitesi***, Ankara (1993).

58. İnternet: "Türk Toz", ***http://www.turktoz.gazi.edu.tr.***

59. İnternet: "Mühendis Beyinler", ***https://www.muhendisbeyinler.net/elektroliz-nedir/***

60. Uslan, İ. ve Küçükarslan S., "Kalay tozu üretimine gaz atomizasyonu parametrelerinin etkisinin incelenmesi" ***Gazi Üniv. Müh. Mim. Fak. Der***., Cilt 25, No (1): 1-8 (2010).

61. İnternet: "Toz Üretimi", ***http://mf.dumlupinar.edu.tr/~runal/toz/tozuretimi/powder_product.html***, (2008).

62. Graf, W., Potschke, J., Sibum, H., and Weiglin, W., "Production of Gas-Atomized Metal Powders." ***Metall***, 45(4), 348-354 (1991).

63. German, R. M. “Powder Metallurgy&Particule Metarials Procsessin” Çeviri Editörleri, ***Süleyman SARITAŞ, Mehmet TÜRKER, Nuri DURLU, Türk Toz Metalurjisi Derneği***, 398-405 (2007).

64. Kurt, A., “Toz Metal Bronz Yatak Malzemelerin Özellikleri”, Yüksek Lisans Tezi, ***Gazi Üniversitesi Fen Bilimleri Enstitüsü*** , Ankara, 1-2 (1992)

65. Singh, S.N. and Ojha, S.N., “Microstructural investigation on rapidly solidified cast iron powders”, ***Int.J. Rapit Solidification***, 7, 201 – 217 (1992).

66. Baksan, B., Gürler, R., “Toz Metalurjisinin Savunma Sanayiinde Uygulanması”, Doktora Tezi, ***Osmangazi Üniversitesi, Metalurji Enstitüsü***, Eskişehir (2003).

67. Gerking, L., “Powder from metal and ceramic melts by laminar gas streams at supersonic speeds”, ***Powder Metallurgy Int***., 25(2), 59 – 65 (1993).

68. Yaşa, A., “Düz Dişlilerin Modellenmesi Ve Mekanik Özelliklerinin Karşılaştırılması”, ***Celal Bayar Ünv.*** Yüksek Lisans Tezi, 14-30 (2008).

69. Ünal R. ve Aydın, M., “Hesaplamalı akışkanlar dinamiği (CFD) yöntemi ile gaz atomizasyon nozulu modellenmesi”, TÜBİTAK Destekli Proje, ***Dumlupınar Üniv. Mühendislik Fak. Makina Mühendisliği Bl***, Kütahya, Türkiye (2008).

70. Hohmann, M. Jonsson, S., “New concepts for inter gas atomization Plants”, ***Metal Powder Report***, 47 – 50 (1990).

71. Lawley, A., Atomization: “The production of metal powders, Metal Powder Industries Federation”, ***Princeton***, New Jersey, USA (1992).

72. Dombrowski, N., and Johns, W.R., “The aerodynamic instability and disintegration of viscous liqiud sheets”, ***Chemical Engineering Science***, 18, 203 – 214 (1963).

73. Neikov, O. D., Murashova, I. B., Yefimov, N. A., & Naboychenko, S. “Handbook of non-ferrous metal powders”: ***technologies and applications. Elsevier*** (2009).

74. Yule, A.J., and Dunkley, J.J., “Atomization of melts”, ***Oxford Univ. Press***, New York, USA (1994).

75. Matei, G., Matei, D., Moraru, V., “Studies on the metal and alloys atomization methods”, ***1. Ulusal Toz Metalurjisi Konferansı***, 67-89 (1996).

76. Mates, S.P., Settles, G.S., “A study of Liquid Atomization using Close-Coupled Nozzles”, ***Atomization and Sprays***, Vol 15 (No. 1), 19-60 (2005).

77. Aksel, M. H., Eralp, O. C., "Gas Dynamics", ***Prentice Hall International Ltd.***, UK (1994).
78. Uslan, İ., "Gaz atomize aluminyum tozlarının özelliklerine üretim değişkenlerinin etkisinin araştırılması", Doktora tezi, ***Gazi Üniversitesi***, Ankara (1999).

79. Cui, C., Cao, F., and Li, Q., "Formation mechanism of the pressure zone at the tip of the melt delivery tube during the spray forming peocess", ***Journal of Materials Processing Technology***, 1377, 5 – 9 (2002).

80. Le, T., & Henein, H. "Effect of nozzle geometry and position on gas atomization". ***Metal Powder Report***, 6(52), 35 (1997).

81. Erdoğan, M., "Malzeme Bilimi ve Mühendislik Malzemeleri", ***Nobel Yayınevi***, 2, Ankara, 36-45 (1999).

82. Hanyaloğlu, S.C., M Colm, I.J., "Alüminyum Nitrür / Nikel-Alüminyum kompozitleri toz metalurjisi metoduyla üretimi", ***Uluslararası Katılımlı 2. Toz Metalurjisi Konferansı***, ODTÜ-1999, Ankara, 653-659 (1999).

83. İnternet: "Bulk Density", ***http://sc02.alicdn.com/kf/HTB1qBEcLpXXXXacXpXXq6xXFXXXi/Bulk-Density-Apparatus-Powder-Apparent-Density-Meter.jpg***

84. Göktaş, A.A., "AI2O3-B4C kompozit seramiklerin sinterlenmesi ve karakterizasyonu", ***8.Uluslar arası Metalurji ve Malzeme Kongresi***, İstanbul, 1317-1321 (1995).

85. İnternet: "TOZ MALZEME TEKNOLOJİSİ-2", ***http://content.lms.sabis.sakarya.edu.tr/Uploads/48939/27932/toz_malz_tek_2.pdf***

86. İnternet: ÜNAL, R., "Kişisel web sayfası", ***http://rahmiunal.net/toz/tozuretimi/powder_product.html***

87. Özgün, Ö., "Toz metalurjisi ile üretilen alaşımlı çeliklerin mikroyapı ve mekanik özellikleri", ***(Master's thesis)***, (2007).

88. Upadhyaya G. S., "Powder Metallurgy Technology", ***Cambridge Ambridge International Science Publishing***, Hindistan, 31 (2002).

89. İnternet: "Turbula," ***http://www.eskens.com/wp-content/uploads/2014/05/TURBULA-MASCHINEN-T50A.jpg***

90. Koch, C.C., "Milling of brittle and ductile materials". In ASM Handbook, ***ASM International Publishers***, 53 – 66 (1998).

91. Kurt, A., "Toz Metal Bronz Yatak Malzemelerin Özellikleri", Yüksek Lisans Tezi, ***Gazi Üniversitesi Fen Bilimleri Enstitüsü***, Ankara (1992).

92. İnternet: "Yalıtımlı Alüminyum", ***https://www.yalitimli-aluminyum.com/wp-content/uploads/ekstruzyon.png*** (2009).

93. Ekşi, A. ve Kurt, A.O., "Metal ve seramik tozlarının bilgisayar kontrollü tek eksenli kalıpta preslenmesi", ***Uluslararası Katılımlı 2. Ulusal Toz Metalürjisi Konferansı, ODTÜ***, Ankara, 557-563 (1999).

94. Bahçeci, E., "Al matrisli Si3N4 takviyeli kompozit malzeme üretimi ve işlenebilirliğinin karakterizasyonu", ***Gazi Üniversitesi Fen Bilimleri Enstitüsü,*** Ankara, 18-20 (2006).

95. Matik, U., "Akımsız nikel kaplamalarda ısıl işlemin sertlik ve aşınma özelliklerine etkisi", Doktora Tezi, ***Gazi Üniversitesi Fen Bilimleri Enstitüsü,*** Ankara, 1-50 (2010).

96. Ünlü, M. D., "SiC Esaslı Seramiklerin Spark Plazma Sinterleme(SPS) Yöntemi ile Üretimi ve Karakterizasyonu", (Doktora tezi) ***Istanbul Technical University*** (2014).

97. Boz, M., "Toz Metalurjisi İle Üretilmiş Bronz Esaslı Fren Balata Malzemelerinin Sürtünme-Aşınma Davranışlarının İncelenmesi", Yüksek Lisans Tezi, ***Gazi Üniversitesi Fen Bilimleri Enstitüsü***, Ankara (1999).

98. German R.M., "Liquid Phase Sintering", ***Plenum Press***, New York, 1-3 (1985).

99. Avedesian, M.M., "Baker, H., Grades and alloys", in: ASM Speciality Handbook: ***Magnesium and Magnesium Alloys, International ASM***, pp. 12e25 (1999).

100. Cho, K., Sano, T., Doherty, K., Yen, C., Gazonas, G., Montgomery, J., Moy, P., Davis, B. And DeLorne, R., "Magnesium Technology and Manufacturing for Ultra Lightweight Armored Ground Vehicles", ***Army Research Laboratory*** (ARL), (2009).

101. Kang, S. J. L., "Sintering: Densification, Grain Growth and Microstructure", ***Butterworth-Heinemann***, 3-5 (2004).

102. Deng, K.K., Li, J.C., Nie, K.B., "Wang, X.J. and Fan, J.F. High temperature damping behavior of as-deformed Mg matrix influenced by micron and submicron SiCp", ***Mater. Sci. Eng***. A 624, 62e70 (2015).

103. Mordike, B.L. and Luka, P., "Chapter 3-Physical metallurgy, in: Magnesium Technology", ***Springer***, 63 (2006).

104. F. Czerwinski, “Controlling the ignition and flammability of magnesium for aerospace applications”, ***Corros. Sci***. 86, 1e16 (2014).

105. Yıldırım, M., and Özyürek, D., "The effects of Mg amount on the microstructure and mechanical properties of Al–Si–Mg alloys", ***Materials & Design*** 51, 767-774 (2013).

106. Neite, G., Kubota, K., Higashi, K. and Hehmann, F., “Chapter 4-MagnesiumBased alloys”, in: R.W. Cahn, P. Haasen, E.J. Kramer (Eds.), ***Structure and Properties of Nonferrous Alloys***, vol. 8, 113-212 (1996).

107. Qian, M. and Das, A., “Grain refinement of magnesium alloys by zirconium: Formation of equiaxed grains”, ***Scripta materialia***, 54(5), 881-886 (2006).

108. Vinotha, D., et al. "Grain refining mechanisms in magnesium alloys—An overview." ***Transactions of the Indian Institute of Metals***, 62.6, 521-532 (2009).

109. İnternet:Tms, ***http://www.tms.org/Communities/FTAttachments/Material%20Properties%20of%20Magnesium.pdf*** (2010).

110. StJohn, D.H., Qian, M., Easton, M.A., Cao, P. and Hildebrand, Z., “Metall”. ***Mater. Trans***. A, 36A, 1669 (2005).

111. Ersümer, A., “Toz Metalürjisi”, ***İ.T.Ü. Makine Fakültesi***, İstanbul (1970).

112. Kulekci, M. K., “Magnesium and its alloys applications in automotive industry”, ***International Journal of Advanced Manufacturing Technology***, 39, 851-865 (2008).

113. Colombié, M., “Chapitre 13-Magnésium et alliages de magnésium. Matériaux Métalliques”, ***Dunod***, Paris, 679-726 (2000).

114. Cizek, L., Greger, M., Pawlica, L., Dobrzanski, L.A. and Tanski, T., “Study of selected properties of magnesium alloy AZ91 after heat treatment and forming”, ***J. Mater. Process. Technol***., 157-158, 466-471 (2004).

115. Mordike, B. L., Ebert, T., “Magnesium properties-applications-potential”, ***Materials Science and Engineering,*** A 302, 37-45 (2001).

116. ASM Handbook, Properties and Selection: “Nonferrous Alloys and Special-Purpose Materials”, ***2, ASM International, Materials Park***, USA (1990).

117. İnternet: AKDOĞAN, A.A., “Malzeme II ders notları” ***http://www.yildiz.edu.tr./~akdoğan/lessons/malzeme***

118. Beffort, O. and Hausmann, C., “Das leichtmetal magnesium und seine egierungen’’, ***EPMA Mg Seminar***, Thun, 15-22 (1999).

119. Barber, L.P., "Characterization of the solidification behavior and resultant microstructures of magnesium-aluminum alloys", A Thesis of Master, ***Worcester Polytechnic Institute***, Worcester, 10-46 (2004).

120. Zhang, Z., "Development of magnesium-based alloys for elevated temperature applications", ***PhD Thesis, Faculte Des Sciences Et De Genie Universite***, Quebec-Canada, 2-75 (2000).

121. Gaines, L., Cuenca, R., Stodolsky, F. and Wu, S., "Potential automotive uses of wrought magnesium alloys", ***Automotive Technology Development,*** Detroit, Michigan, 1-7 (1996).

122. Polmear I.J., "Magnesium alloys", Light Alloys, ***Metallurgy and Materials Science Series,*** New York, 169-210 (1989).

123. Bolstad, J., "Magnesium alloy development for intelligent magnesium Designs", ***SinoMaG seminar***, Beijing-China, 8-14 (2000).

124. Kondori, B., and Mahmudi, R., "Effect of Ca additions on the microstructure, thermal stability and mechanical properties of a cast AM60 magnesium alloy", ***Materials Science and Engineering A***, 527: 2014-2021 (2010).

125. Sevik, H., Açıkgöz, S., and Can Kurnaz, S., "The effect of tin addition on the microstructure and mechanical properties of squeeze cast AM60 alloy", ***Journal of Alloys and Compounds*** 508, 110-114 (2010).

126. Erçayan, Y., İrizalp, S. G., Saklakoğlu, N., "A380 Alasımında Yarı-Katı Şekillendirmenin Kompozit Yapılara Etkisinin İncelenmesi". ***I. Ulusal Ege Kompozit Malzemeler Sempozyumu***, İzmir (2011).

127. Johansson, S., "Magnesium Alloys", ***Summary of chapter 1-7 in light alloys by I.J. Polmear, Engineering Materials***, 5: 17-20 (2002).

128. Schwam, D., Wallace, J.F., Zhu, Y. and Viswanathan, S. and Iskander, S., "Enhancements in magnesium die casting ımpact properties, final report", ***Case Western Reserve University***, DOE-FC07-98ID13611, Ohio, 5-22 (2000).

129. Vogel, M., "Mikrostruktur und kriechverhalten von magnesium-druckgusslegierungen im system Mg-Zn-Al-Ca", ***Ph.D. Thesis, Max-Planck-Institut für Metallforschung***, Stutgart, 6-20 (2002).

130. İnternet: "Preporties of mg alloys", ***http://mg.tripod.com/asm_prop.htm.***

131. Mendis, C.L., "Chapter 4-Understanding precipitation processes in magnesium alloy"s, ***in: Fundamentals of Magnesium Alloy Metallurgy***, Publishing W: 125-151 (2013).

132. Gökçe, A., Fındık, F. ve Kurt, A. O., "Alüminyum ve Alaşımlarının Toz Metalurjisi İşlemleri", ***Engineer***, 58(686), 21-47 (2017).

133. Tzamtzis, S., "Solidification Behaviour and Mechanical Properties of Cast Mgalloys and Al-based Particulate Metal Matrix Composites Under Intensive Shearing", ***PhD thesis, Brunel University, Brunel Centre for Advanced Solidification Technology*** (2011).

134. Dahle, A.K., Lee, Y.C., Nave, M.D., Schaffer, P.L. and St.John, D.H., "Development of as the cast microstructure in magnesium-aluminium alloys", ***Journal of Light Metals***, 1: 61-72 (2001).

135. Bilgin, M., Karabulut, Ş., ve Özdemir, A., "Alüminyum Magnezyum Alaşımlarının Sürtünme Karıştırma Kaynağı İle Kaynak Edilebilirliğinin Değerlendirilmesi", ***Gazi Üniversitesi Fen Bilimleri Dergisi Part C: Tasarım Ve Teknoloji***, 5(2): 191-209 (2017).

136. Trajonova, Z., and Lukac, P., "Compressive deformation behaviour of magnesium alloys". ***Achievements in Mechanical and Materials Engineering***, 681-684 (2005).

137. Friedrich, H. and Schumann, S., Research for a ''new age of magnesium'' in the automative industry", ***Journal of Materials Processing Technology***, 117, 3, 276-281 (2001).

138. Schunmann, S., "The paths and strategies for increase magnesium application in vehicles", ***Material Science Forum***, 488/489, 1-8 (2005).

139. Ostrovsky, I. and Henn, Y., "Present State and Future of Magnesium Application in Aerospace Industry", ***International Conference "New Challenges in Aeronautics" ASTEC'07***, Moscow (2007).

140. Phillips Plastics Corporation, ***New Technologies for Modernizing and Improving Ground Soldier Equipment***, (2009)

141. Gökmeşe, H. and Bostan B., "Fabrication and characterization of nanoparticle MgO/B4C composite by mechanochemical method", ***Proceedings of the Institution of Mechanical Engineers, Part E: Journal of Process Mechanical Engineering 0954408916629106***, (2016).

142. Bayram, J., "Pressure Characteristics at The Pour- Tube Orifice in Ultrasonic Gas Atomization", ***Materials Science And Engineering***, 98: 65-69 (1988).

143. Kim, T. S. and Chae, H. J., "Consolidation of gas atomized mg alloy powders", ***Rev.Adv. Mater.Sci***., 18: 769-772 (2008).

144. Salord, F., Gaussorgues, P., Marti-Flich, J., Sirodot, M., Allimant, C., Lyonnet, D. and Robert, D., "Nosocomial maxillary sinusitis during mechanical ventilation: a prospective comparison of orotracheal versus the nasotracheal route for intubation", ***Intensive care medicine***, 16(6), 390-393 (1990).

145. Clyne, T. W., Ricks, R. A. and Goodhew, P. J., “The production of rapidly – solidified aluminium powder by ultrasonic gas atomization. Part I: Heat and fluid flow”, ***Int.J. Rapid solidification***, 1, 59 – 80 (1984).

146. Aller, A. J. and Losada, A., “Characteristics of atomized powders”, ***Powder Metallurgy Int.,*** 21(5), 15 –19 (1985).

147. Grant, N. J., "Recent trends and developments with rapidly solidified materials", ***Metallurgical and Materials Transactions*** A 23.4, 1083-1093 (1992).

148. Daloz, D. and Michot, G., “Influence of the consolidation step on the mechanical properties of rapidly solidified Mg-Al-Zn alloys”, ***Int. J. Rapid Solidif***., 9, 289e304 (1996).

149. Rajan, T. P. D., Jayakumar, E. and Pai. B. C., "Developments in solidification processing of functionally graded aluminium alloys and composites by centrifugal casting technique", ***Transactions of the Indian Institute of Metals*** 65.6, 531-537 (2012).

150. Pai, B. C., Pillai, U. T. S., Manikandan, P. and Srinivasan, A., “Modification of AZ91 Mg alloys for high temperature applications”, ***Transactions of the Indian Institute of Metals***, 65(6), 601-606 (2012).

151. Akkaş, M., “Gaz Atomizasyon Yöntemi İle Az91 Tozu Üretimi Ve Karakterizasyonu”, Doktora Tezi, ***Karabük Üniversitesi Fen Bilimleri Enstitüsü***, Karabük, 30-40 (2017).

152. Akkaş, M., Çetin, T. and Boz, M., “The Effect Of Gas Pressure On Powder Size And Morphology In The Production Of AZ91 Powder By Gas Atomization Method”, ***Arch. Metall. Mater.*** 63 (4): 1587-1594 (2018).

## RESUME

Kamal Mohammad AKRA was born in Zawia, Libya in 1965 and he graduated first and elementary education in this city. He completed high school education in Zawia High School, after that, he started BSc Mechanical Engineering program in Hoon Technical College, Department of Mechanical Engineering in 1984. Then in 2004 he started M. Sc. Education in Industrial Engineering in The Academy of Janzour and then he started to work as a lecturer at Zawia University in 2010.

## CONTACT INFORMATION

Address: Zawia University
Engineering Faculty
ZAWIA – LIBYA

E- mail: kamalakra55@gmail.com